3-21-2023

Movement, Behavior, and Trophic Ecology of a Pelagic Predator Guild in the Eastern Tropical Pacific Ocean

Ryan Keith Logan
Guy Harvey Research Institute

Dissertation of
Ryan Keith Logan

Submitted in Partial Fulfillment of the Requirements for the Degree of

Doctor of Philosophy
Oceanography/Marine Biology

Nova Southeastern University
Halmos College of Arts and Sciences

March 2023

Approved:
Dissertation Committee

Committee Chair: Mahmood Shivji, Ph.D.

Committee Member: Bradley Wetherbee, Ph.D.

Committee Member: Christopher Lowe, Ph.D.

Committee Member: Jeremy Vaudo, Ph.D.

NOVA SOUTHEASTERN UNIVERSITY

HALMOS COLLEGE OF ARTS AND SCIENCES

MOVEMENT, BEHAVIOR, AND TROPHIC ECOLOGY OF A PELAGIC PREDATOR GUILD IN THE EASTERN TROPICAL PACIFIC OCEAN

By

Ryan Keith Logan

Submitted to the Faculty of
Halmos College of Arts and Sciences
in partial fulfillment of the requirements for
the degree of Doctor of Philosophy with a specialty in:

Oceanography and Marine Biology

Nova Southeastern University

March 2023

ABSTRACT

Pelagic apex predators exert strong influences on ecological communities, and often support valuable commercial or recreational fisheries worldwide. Yet, due to their relative rarity and pelagic lifestyle, many such species, like billfishes, have proven particularly difficult to study at resolutions necessary to define dynamics of recovery from fishery interaction, physical interaction with environmental features and prey exploitation, and competitive interactions among other billfish species. This leads to a paucity of knowledge on billfish ecology and habitat use, and hinders management and conservation efforts. With the ever-improving and miniaturization of technology and expanding oceanographic datasets, the ability to define and quantify these interactions of fish to each other and their environment has never been greater. In this dissertation, I developed a novel tag and deployment method to characterize the recovery dynamics of blue marlin (*Makaira nigricans*) and sailfish (*Istiophorus platypterus*) after catch and release in a typical recreational fishery. I also utilized these tags to document fine-scale movement and foraging behavior of these two species in the vertically compressed eastern tropical Pacific, where a large naturally occurring oxygen minimum zone exists. This oceanographic feature compresses the prey of these predators to a narrow range during the day, and I hypothesize that the billfishes are using this to their advantage to increase foraging opportunities. Indeed, animal-borne video and associated high-resolution movements data documented a sailfish exploiting the hypoxic boundary, initiating a pursuit of its prey at depth, chasing the prey to the surface, and capturing it after a pursuit at the surface. Using physiological and bioenergetic modeling, I estimated the net energetic gain over the 24 hour period the event took place. In the final chapter, I used a multidisciplinary approach to investigate the competitive interactions and mechanisms of niche partitioning employed by blue marlin, sailfish, and black marlin (*Istiompax indica*) in the vertically compressed environment. This work demonstrated a seasonal response in vertical habitat use, alleviating competition and allowing these sympatric predators to coexist. Together, these works provide unparalleled insights into the fish-fishery interaction, biology, physiology, and ecology of these top pelagic predators, and provide necessary information for ecosystem function and management.

Keywords: biologging, billfish, marlin, sailfish, recovery period, hunting behavior, oxygen minimum zone, habitat compression, pelagic predator, niche partitioning

ACKNOWLEDGMENTS

Thank you to my advisor Dr. Mahmood Shivji for providing me with the opportunity to pursue a doctoral degree in his lab, and for sending me off to remote locations fulfilling some bucket list trips for me. The environment he provided allowed me the freedom to create my own path and pursue new frontiers in the field, and tackle challenging questions with untested methods. Thank you to my committee members Dr. Bradley Wetherbee, Dr. Chris Lowe, and Dr. Jeremy Vaudo, for graciously volunteering their time, knowledge, and expertise to this work, and all of their valuable feedback along the way.

I am very grateful to Dr. Guy Harvey, Jessica Harvey, and everyone at the Guy Harvey Foundation. It was Guy's passion for the ocean, and especially billfish, that got this project off the ground, and for that I am eternally grateful. Guy and Jessica's help in the field catching and tagging these fish was instrumental in completing all of the fieldwork, provided me with some lifelong memories, and some incredible underwater footage of these elusive fish thanks to Jess's amazing camera work and long breath holds.

I must also give my sincerest thanks to everyone at my new 'home-away-from-home', Tropic Star Loge. Richard and Mallory White, Ursula Marais, Kyla McCafferty, Ross Alford, Paola Martinez, Hayden Houser and Nelis Theron, your help and friendship made all those trips to the jungle feel like time spent with family, rather than work. A very special thank you to the captains and mates of the lodge, without whom, this work could not have been accomplished. This research is the product of a significant amount of time at sea, often just me, the captain and mate for 8 hours a day. These guys have dedicated their lives to fishing and know marlin fishing better than anyone on the planet. Thank you, Candelo, Gavilan, Jacob, Flacco, Mario, Jose, Lorenzo, Walter, Luis, Fidel, Armando, Adolfo, Vicente, and twice as many mates, for teaching me everything there is to know about catching marlin, and for being unbelievably helpful in whatever task the crazy scientist wanted to do next.

After roughly 6 years living in Miami, I have met many amazing people. Thank you to all of my NSU lab mates and other graduate students, both past and present, and my lab mate in-laws at FIU. We have shared many great times together that I will not soon forget, with many more great times still to be had.

Finally, thank you to all of my family, my grandfather who never missed an opportunity to say how proud of me he was, and especially my mom, Karen, who fostered my love of animals and the ocean from an early age, and supported my passion and pursuit of marine biology. Thank you to my brother Kyle, and my dad Bruce, who are no longer here to celebrate with me. It was my dad who instilled a love of fishing in me, and Kyle who I emulated growing up, so there is no doubt that the two of them shaped me into who I am today and my pursuit of fish ecology and conservation. Lastly, thank you to my fiancé, Sarah, for all of her love and support throughout this journey. Living on two PhD salaries in Miami has its challenges, mixed in with a global pandemic, but I could not imagine going through this process with anyone else. Thank you to my soon-to-be family, Frank, Robbie and Frankie, and the rest of the Luongos for all of their love and support over the past 5 years.

Funding for this dissertation was provided by the Guy Harvey Foundation, Guardians of the Eastern Tropical Pacific Seascape donor group, Ron Vergnolle, the Gallo-Dubois Scholarship, Fish Florida Scholarship, Batchelor Foundation Scholarship, and Nova Southeastern University Halmos College of Arts and Sciences. In kind logistical support in the field was provided by Tropic Star Lodge. For all of your support, large and small, thank you.

Contents

ABSTRACT 2

ACKNOWLEDGMENTS 3

CHAPTER I 7

INTRODUCTION 7

CHAPTER II 13

HIGH-RESOLUTION POST-RELEASE BEHAVIOR AND RECOVERY PERIODS OF TWO HIGHLY PRIZED RECREATIONAL SPORTFISH: THE BLUE MARLIN AND SAILFISH 13

ABSTRACT 14

INTRODUCTION 15

METHODS 17

RESULTS 22

DISCUSSION 34

CONCLUSIONS 38

LITERATURE CITED 39

CHAPTER III 45

PATROLLING THE BORDER: BILLFISH EXPLOIT THE HYPOXIC BOUNDARY CREATED BY THE WORLD'S LARGEST OXYGEN MINIMUM ZONE 45

ABSTRACT 46

INTRODUCTION 47

METHODS 48

RESULTS 51

DISCUSSION 60

CONCLUSIONS 64

CHAPTER IV 65

HUNTING BEHAVIOR OF A SOLITARY SAILFISH *ISTIOPHORUS PLATYPTERUS* AND ESTIMATED ENERGY GAIN AFTER PREY CAPTURE 65

ABSTRACT 66

INTRODUCTION 67

METHODS 68

RESULTS AND DISCUSSION 70

CONCLUSIONS 80

LITERATURE CITED 81

CHAPTER V 86

SEASONALLY MEDIATED NICHE PARTITIONING IN A VERTICALLY COMPRESSED PELAGIC PREDATOR GUILD 86
ABSTRACT 87
INTRODUCTION 88
METHODS 90
RESULTS 94
DISCUSSION 104
CHAPTER VI 110
CONCLUSION 110
APPENDIX A: CHAPTER II SUPPLEMENTAL INFORMATION 115
SUPPLEMENTAL TABLES 115
APPENDIX B: CHAPTER III SUPPLEMENTAL INFORMATION 116
SUPPLEMENTAL TABLES 116
SUPPLEMENTAL FIGURES 118
APPENDIX C: CHAPTER IV SUPPLEMENTAL INFORMATION 120
SUPPLEMENTAL METHODS 120
SUPPLEMENTAL TABLES 124
SUPPLEMENTAL FIGURES 125
APPENDIX D: CHAPTER V SUPPLEMENTAL INFORMATION 129
SUPPLEMENTAL TABLES 129
SUPPLEMENTAL FIGURES 130
LITERATURE CITED 133

CHAPTER I

INTRODUCTION

Movements, behavior, and trophic interactions are fundamental components of the ecology of all vertebrate life on earth. Knowledge of where animals go, what they do and what they eat provides insights into virtually every aspect of a species' biology, including fitness and evolution, population and community structure, role within the ecosystem, responses to environmental change and potential for anthropogenic interaction (Swingland and Greenwood, 1983; Nathan et al., 2008; Hazen et al., 2013; Queiroz et al., 2016; Hooten et al., 2017). Yet, much of our understanding of large predatory fish movements remains restricted to broad-scale migrations and summarized behavior obtained from relatively low-resolution telemetry instruments. Recent technological advances (smaller tag size, increased battery life, remote sensing improvements) allow individual animal movements to be tracked for longer periods of time at increased resolutions, while simultaneously collecting important information about the ambient environment, allowing scientists to infer behaviors within a movement trajectory and contextualize them within the environment (Block, 2005; Payne et al., 2014; Whitford and Klimley, 2019).

Furthermore, recently developed high-resolution acceleration biologging tags are used to study the fine-scale swimming kinematics of fish not under direct observation by recording acceleration multiple times per second along three dimensions: the longitudinal body axis (surge), the dorsoventral axis (heave), and transversely across the animal's body (sway) (Yoda et al., 1999). Accelerometer tags have been applied to a variety of aquatic species to quantify a range of fine-scale behaviors, energetics and post-release recovery periods (Myers and Hays, 2006; Whitney et al., 2010; Gleiss et al., 2011; Logan et al., 2022). By incorporating other instruments with accelerometers, one can obtain additional fine-scale behavioral data: tri-axial magnetometers are added to enable calculation of the animal's heading (Williams et al., 2017a; Andrzejaczek et al., 2019) and tri-axial gyroscopes to measure angular velocity of the animals' movements and turning. Combining these kinematic sensors with physical sensors (e.g., depth, temperature, oxygen) can help to provide a near complete picture of the animals' movements and behavior in relation to environmental cues.

While understanding movements and behavior of individual species can be important for directed management measures, ecosystem conservation efforts generally provide the best results when focused on ecological communities (Hazen et al., 2018). Because monitoring fish movements, behavior, and trophic interactions in the marine environment is expensive and

logistically difficult, ecosystem conservation may be more practically achieved by focusing efforts on sentinel species, such as large predatory fishes, that have a disproportionally large impact on the ecosystem and are more vulnerable to human extirpation (Myers and Worm, 2003; Sergio et al., 2008; Hazen et al., 2019; Juan-Jordá et al., 2022).

Large predatory fishes (e.g., tunas, billfishes, sharks) play critical roles as top consumers by regulating the structure, function, and stability of oceanic ecosystems (Scheffer et al., 2005; Baum and Worm, 2009; Ferretti et al., 2010; Heithaus et al., 2012). However, many marine predator populations have been significantly overharvested due to 1) a disproportionate impact of fisheries on large-bodied fishes, 2) the rapid expansion of global industrialized fishing fleets to satisfy demand for their products, and 3) bycatch (Jackson et al., 2001; Sibert et al., 2006; Collette et al., 2011; Dulvy et al., 2014; Byrne et al., 2017; Pacoureau et al., 2021). As a result of these fishery impacts, many predatory fish populations have seen their populations depleted by as much as 50-90% (Hilborn et al., 2003; Myers and Worm, 2003; Sibert et al., 2006). Additional anthropogenic stressors, such as rising temperatures associated with climate change, can alter population dynamics within marine communities by causing shifts in both horizontal and vertical distributions of species, creating new ecological and anthropogenic interactions with unknown long term consequences (Stramma et al., 2012; Hazen et al., 2013; Pinsky et al., 2013; Poloczanska et al., 2013).

Among all the ecosystems in the world's oceans, the pelagic environment is a particularly harsh one. Often described as the oceanic equivalent of a desert, the pelagic environment is the largest environment on earth, covering more than 70% of its surface. In general, pelagic waters contain exceptionally low vertebrate abundance, with sporadic biological hotspots that are dynamic in both space and time. As such, the predators that reside in the pelagic realm are highly migratory and must cover vast expanses of water in search of suitable habitat, food, and reproductive opportunities. Because many of these predators spend most, if not all, of their life in the open ocean and are not amenable to captivity, they are particularly difficult to study and observe. As such, basic information about life history, population size and demographics, behavior, habitat use, and consumption estimates severely lag behind that of their more coastal and terrestrial counterparts. Similarly, because of their wandering nature, pelagic predators must contend with several fisheries of varying gear types and fishing pressures within different countries' waters and areas beyond national jurisdiction (i.e., the high seas). Therefore, the lack

of information about pelagic predators movements, behavior and habitat use, and trophic interactions, particularly in relation to one another, hampers our ability to manage their populations as anthropogenic stressors only continue to increase (Dulvy et al., 2008).

Of particular importance to this dissertation is the role that the physical environment and oceanographic features play in structuring the pelagic ecosystem. In the Eastern Tropical Pacific, prevailing winds promote upwelling, bringing nutrient rich waters to the surface leading to high rates of surface productivity, which results in a continuous rain of biological material that decomposes while sinking. Concomitantly, stagnant deep-water masses reduce water column mixing and turnover, and a sharp and permanent pycnocline prevents oxygenated surface waters from mixing downward. The combination of these oceanographic features contribute to a large naturally occurring hypoxic zone that extends from ~20°N to ~15°S in the eastern Pacific, and can be several hundred meters thick (Prince and Goodyear, 2006; Karstensen et al., 2008; Stramma et al., 2012; Fiedler and Lavín, 2017). As a result, the water column in this region features a narrow, productive surface layer of uniform temperature and oxygen saturation, and a strong and shallow thermocline coexistent with the upper boundary of the oxygen minimum layer (i.e. oxycline), beyond which lies the world's largest oxygen minimum zone (OMZ). These oceanographic features cause a marked compression of preferred temperature and dissolved oxygen concentrations, restricting deep water habitat use for gill-breathing animals with high metabolic rates, a phenomenon known as hypoxia-based habitat compression (Prince and Goodyear, 2006; Prince et al., 2010; Stramma et al., 2012). Therefore, much of the pelagic ecosystem in the ETP is vertically compressed to highly productive surface waters, supporting some of the largest commercial fisheries catches in the world (e.g., Peruvian anchoveta, yellowfin tuna).

Furthermore, some of these pelagic predators, such as the billfishes, are also considered highly prized sportfish by the recreational fishing community, with fishers traveling great distances and spending millions of dollars annually for the opportunity to catch them. These activities contribute significantly to the economy of fishing destinations and grow in popularity every year (Holland et al., 1998; Rollins and Hospital, 2019). Due to the economic impact of the recreational fishing sector, the countries home to these fishing destinations have a vested economic interest in conserving billfish stocks. As such, many countries have banned the landing, sale, or export of billfish products in commercial fisheries and imposed mandatory catch

and release practices for recreational anglers as conservation strategies. At the same time, many recreational anglers have become more conscientious of fish populations and have overwhelmingly shifted to catch and release as a widespread practice. As a result, a growing proportion of billfish populations are subjected to the stresses associated with catch and release. Yet, very little information is known about how billfish respond to this stress and how long it takes them to recover from catch and release fishing.

With the overall goal to aid conservation and management of billfish and their pelagic communities, this dissertation seeks to increase our knowledge of the ecology of three commercially, artisanally and recreationally exploited billfishes (blue marlin - *Makaira nigricans*, black marlin - *Istiompax indica*, and sailfish - *Istiophorus platypterus*) in the Eastern Tropical Pacific. To accomplish the research described in Chapters II, III and IV, I designed a novel biologging tag package and deployment method for marlin and sailfish to obtain high-resolution kinematic and environmental data for the first time on billfish. In Chapter II, blue marlin and sailfish were instrumented with the biologging tag after being fought for varying amounts of time by a typical recreational angler and released. Using the high resolution kinematic and environmental data, I analyzed the typical behavioral response, habitats utilized, and the amount of time it takes for the average blue marlin or sailfish to recover from the metabolically intense capture event. In Chapter III, I discard the time period prior to when each fish recovered (as determined by Chapter II) and examine blue marlin and sailfish diving fine-scale behavior and interaction with a vertical habitat front at a resolution that has never been done for these species. Based on the behaviors exhibited in this Chapter, I proposed a hypothesis about how these species may be using this vertical habitat front to enhance foraging opportunities. I then provide support for this hypothesis in Chapter IV, where I analyzed a foraging attempt captured on video from the point of view of an individual sailfish. From this foraging attempt, I estimated a likely metabolic rate of the sailfish using a proxy species and modeled its energetic expenditure over the course of the day to determine how profitable that prey fish might have been, and to estimate a daily intake requirement. Finally, in Chapter V I compiled a robust dataset to investigate how the billfish predator guild in the vertically compressed ETP are partitioning the available resources. Leveraging long-term satellite tracking tags and stable isotope analysis, I assessed the amount of 3D habitat overlap, trophic overlap, and estimate the most dominant prey sources for each of the three species. Overall, in this

dissertation I employ an interdisciplinary approach and a novel suite of tagging technology to overcome the logistical challenges associated with studying fine-scale habitat use and ecology of large pelagic fishes. In doing so, I significantly enhance our knowledge and understanding of billfish movements, behavior, and trophic ecology, and ultimately hope these data are useful for proper billfish and ecosystem management in the face of a rapidly changing ocean environment.

CHAPTER II

HIGH-RESOLUTION POST-RELEASE BEHAVIOR AND RECOVERY PERIODS OF TWO HIGHLY PRIZED RECREATIONAL SPORTFISH: THE BLUE MARLIN AND SAILFISH

This chapter was originally published as Logan R.K., Vaudo J.J., Lowe C.G., Wetherbee B.M., Shivji M.S. (2022) High-resolution post-release behaviour and recovery periods of two highly prized recreational sportfish: the blue marlin and sailfish. *ICES Journal of Marine Science* 79(7): 2055-2068. doi.10.1093/icesjms/fsac137

Abstract

High recreational catch rates of istiophorid billfishes in the eastern tropical Pacific (ETP) have led to substantial eco-tourism derived economic benefits for the countries in the region, prompting many countries to mandate catch-and-release practices for recreational anglers. Previous estimates of billfish post-release behaviors and recovery periods after these physiologically stressful capture events, however, vary widely depending on the type of tag used. Using high-resolution, multi-sensor biologging tags, we provide a fine-scale, detailed view of the behavior and recovery periods of blue marlin (*Makaira nigricans*; n = 9) and sailfish (*Istiophorus platypterus*, Istiophoridae; n = 9) caught in a typical recreational fishery in the eastern tropical Pacific (ETP). Angling times ranged from 4–90 min, and fish were monitored for periods of 6–70 h after release. Blue marlin showed a characteristic long, deep dive immediately after release, with significantly greater duration associated with longer fight times, a behavior not typical for sailfish. Diving depths were, however, much shallower than those previously reported for both species due to the shallow thermocline and oxycline present in the ETP. Data from 40 derived metrics from acceleration (i.e., tailbeat period, amplitude, pitch, etc.) and physical parameters (i.e., depth, speed, temperature, oxygen saturation, etc.) used to quantify a recovery period suggest blue marlin and sailfish recover 9.0 ± 3.2 and 4.9 ± 2.8 h after release, respectively. Our high-resolution assessment of post-release behavior suggests that these billfish are capable of rapid physiological recovery after capture in recreational fisheries, and that catch-and-release practices like those used here can be an effective approach to conserve and sustain billfish populations in the ETP. Predicted climate change caused shallowing of the oxygen minimum zone, however, would increase the vertical habitat compression present in this region, potentially prolonging or inhibiting recovery.

Introduction

Recreational billfish fisheries have increased in popularity around the globe since the 1930's and provide considerable economic benefits via eco-tourism. Among avid offshore anglers, the eastern tropical Pacific (ETP) is widely considered to be one of the world's best fishing locations for istiophorid billfish (e.g., blue marlin *Makaira nigricans,* black marlin *Istiompax indica* and sailfish *Istiophorus platypterus;* Istiophoridae). Many countries in the ETP either mandate or have programs in place to encourage catch-and-release practices for istiophorid billfish. Fortunately, data collected using acoustic tags and pop-up satellite tags document low rates of immediate and post-release mortality (mean 13.5%; 95% CI: 10.3-17.6%) for billfish (Musyl et al., 2015). Capture on recreational gear, however, specifically subjects billfishes to exhaustive stress and exercise, the effects of which are exacerbated by direct injuries caused by the hook, contact with fishing vessel, and air exposure (e.g., Prince et al., 2002; Graves and Horodysky, 2008; Schlenker et al., 2016). These factors can subsequently result in physiological and behavioral responses that can negatively affect fish health, growth, reproduction, and escape response, and may ultimately influence stock dynamics (Lewin et al., 2006; Cooke and Schramm, 2007; Donaldson et al., 2008). Therefore, efforts focused on determining recovery periods and minimizing stress will inform the global recreational fishing industry for these two billfishes and add to basic biological data on billfish behavior.

Fish stress and recovery time are not traditionally sought-after metrics for fisheries managers, but this could be due, in part, to the lack of availability of these numbers. In ecology, it is widely recognized that organismal physiology plays a role in population level demographics (Bergman et al., 2019). As such, there is a growing push to integrate fish physiology with fishery science, which intersect at the behavior of individuals within a population (Horodysky et al., 2015; Killen et al., 2016a; McKenzie et al., 2016; Lennox et al., 2017). For example, armed with species-specific knowledge of behavioral traits and physiological tolerances after release from a fishing event, managers may be able to predict rates of post-release mortality based on environmental conditions (Horodysky et al., 2015). Therefore, post-release behavior and recovery time can shed light on the underlying physiological state of the individual and is an important component of assessing the success of catch-and-release as a management practice for billfish.

Post-release behavior and recovery times have previously been estimated for istiophorid billfish, including blue marlin and sailfish using acoustic telemetry and pop-up satellite archival tags (PSATs) (Jolley Jr and Irby Jr, 1979; Holland et al., 1990; Block et al., 1992a; Hoolihan et al., 2011a). Estimated recovery times have varied widely between studies, however, which may ultimately be due to differences in methodology and resolution of tag data. For example, blue marlin post-release recovery period estimates range from 4–6 hours using active acoustic tracking (Holland et al., 1990; Block et al., 1992a) to 40 days using PSATs (Hoolihan et al., 2011a). Recovery period estimates appear correlated with tag type, suggesting data resolution is important and coarse-scale data typically produced by PSATs in past studies has not been detailed enough to accurately measure and define recovery period (Musyl et al., 2015). Additionally, previous studies of post-release recovery time have relied on changes in fish depth or speed of a tracking vessel (a proxy for animal speed) as an indicator of recovery (Jolley Jr and Irby Jr, 1979; Holland et al., 1990; Block et al., 1992a; Hoolihan et al., 2011a; Musyl et al., 2015). Yet, pelagic fishes' depth use can be plastic depending on environmental conditions (Vaudo et al., 2016; Carlisle et al., 2017; Vaudo et al., 2018), thus complicating determination of post-release recovery among studies. In addition, fish depth and heading metrics provide no information of body kinematics or swimming performance, which are known to be impacted by recreational fishing and that provide much more detailed estimates of recovery behavior than depth information alone (Gleiss et al., 2013; Whitney et al., 2016).

Tri-axial accelerometry can be used to study the fine-scale swimming kinematics of fishes not under direct observation by recording acceleration multiple times per second along three dimensions: the longitudinal body axis (surge), the dorso-ventral axis (heave) and transversely across the animal's body (sway) (Yoda et al., 1999; Wilson et al., 2008). Accelerometers have been applied to a variety of aquatic species to quantify a range of fine-scale behaviors (e.g. routine and burst swimming, resting, foraging and mating), energetics and post-release recovery period (Myers and Hays, 2006; Whitney et al., 2010; Gleiss et al., 2011; Watanabe and Takahashi, 2013; Whitney et al., 2016). More recently, other instruments have been incorporated with accelerometers to obtain additional fine-scale behavioral data: tri-axial magnetometers are added to enable calculation of the animal's heading (Williams et al., 2017a; Andrzejaczek et al., 2019) and tri-axial gyroscopes to measure angular velocity of the animals' movements and turning. These can be combined with pressure (i.e., depth) and temperature

sensors that gather data traditionally collected by other tag types to give a more complete picture of the animals' movements in relation to environmental cues.

The ETP is home to a unique combination of oceanographic features that contribute to a large, naturally occurring, hypoxic zone near the surface that can be several hundred meters thick (Prince and Goodyear, 2006; Karstensen et al., 2008; Stramma et al., 2012; Fiedler and Lavín, 2017). As a result, the water column features a narrow, productive surface layer of uniform temperature and oxygen saturation with a shallow, strong thermocline concomitant with the upper boundary of the oxygen minimum layer (i.e., oxycline). Together, these features cause vertical habitat compression, and are believed to increase the catchability of epipelagic fishes, such as billfishes, in surface-based fisheries (Evans et al., 1981; Prince and Goodyear, 2006; Prince et al., 2010; Stramma et al., 2012).

Low temperatures and dissolved oxygen concentrations have large negative physiological impacts on fish, including cardiac function and output (Brill et al., 1998; Brown et al., 2004; Pörtner and Knust, 2007). A fish's ability to survive and recover from a metabolically intense event such as capture and release would therefore be reduced or prolonged in low temperatures and/or dissolved oxygen concentrations. Due to the oceanographic conditions in the ETP and the high-metabolic rate of regionally endothermic billfish caught and released in this region (Block, 1986; Idrisi et al., 2003; Wegner et al., 2010), these fish may be susceptible to extreme stress and may require prolonged recovery periods, putting these fish at greater risk of post-release mortality compared to other popular fishing destinations worldwide without a similarly shallow thermocline and oxycline. As such, billfish recovery behavior in the ETP may provide a glimpse into the future of recreational billfish fisheries worldwide, as hypoxia-based habitat compression becomes widespread and oxygen minimum zones become increasingly shallow (Laffoley and Baxter, 2019; Leung et al., 2019). Due to the lack of agreement of recovery times between previous studies and the importance of quantifying recreational fishery impact, we use a high-resolution biologging tag to determine the post-release recovery behavior and period of blue marlin and sailfish in a catch-and-release fishery in the vertically compressed habitat of the ETP.

Methods

Tagging

We caught ten blue marlin and nine sailfish off the Pacific coast of southeast Panama via rod-and-reel and trolling high-speed lures or natural bait from September to November 2019.

Each fish was brought alongside the vessel, assessed for physical trauma associated with hooking, and its weight estimated by an experienced captain. We attached a custom-designed biologging tag package to the dorsal musculature, just below the largest dorsal spine with two umbrella dart anchors. Once both anchors were securely imbedded in the muscle, the tag was firmly cinched against the fish's body using two galvanic timed releases (International Fishing Devices Inc., Northland, New Zealand) and a zip tie. The shape of the biologging tag was designed to be as hydrodynamic as possible, while also providing the necessary flotation for recovery. The tag consisted of an acceleration data logger (complete with tri-axial accelerometer, tri-axial magnetometer and tri-axial gyroscope recording at 50 or 100 Hz), depth, temperature, and light sensors, and a small turbine-based fluid speed sensor all recording at 1 Hz (OpenTag 3.0, Loggerhead Instruments, Sarasota, FL). The speed sensor was secured to the acceleration data logger and oriented such that the sensitive direction corresponds with the forward direction of movement (Gabaldon et al., 2019). A small (12 mm diameter x 20 mm long) oxygen sensor (Micro Probe; OxyGuard, Farum, Denmark) that recorded dissolved oxygen concentration (% saturation) of the water at 1 Hz was also incorporated into the acceleration data logger (for details of the oxygen probe, see Coffey and Holland, 2015). The sensor has a manufacturer specified measuring range of 0–200% with accuracy within ±1 % of the measured value. Finally, the tag package also contained a miniaturized video camera (68 mm × 21 mm × 22 mm; Little Leonardo, Tokyo, Japan) and a Smart Position and Temperature tag (SPOT-363A; Wildlife Computers, Redland WA) to aid in package recovery. The tag body was constructed of a high-density mixture of microballoons and resin to achieve desired buoyancy (Whitmore et al., 2016). Tag package dimensions were 18 x 7 cm, increasing to 18 x 10.5 cm at the widest point with a weight of 335 g in air (see Appendix A; supplemental figure S1). Upon dissolution of the galvanic timed releases (selected for 1, 2 or 3 days after tagging), the tag package released from the fish, floated to the surface, and began transmitting its location via the SPOT tag and was tracked and retrieved at sea using a UHF handheld receiver (AOR AR8200, USA).

Data processing

Depth

We smoothed depth data to a 10-s running mean to reduce small scale changes in vertical movements and examine localized trends in diving activity. Depth was then split into three swimming phases ('ascent', 'descent' and 'level') using vertical velocity (VV), calculated as the

difference between successive points of the smoothed depth data at 1 s intervals. Ascents and descents were categorized as periods where VV exceeded a magnitude of 0.05 ms^{-1} for more than 10 s; periods where this threshold was not exceeded were considered level swimming (Whitney et al., 2016; Andrzejaczek et al., 2019). Each period of ascent, descent or level swimming was analyzed as an individual event, allowing for calculation of the average VV of each phase, and the number and duration of ascent, descent, or level swimming phases as it related to time since fish release.

Speed

We calibrated the turbine with water velocity by placing the completed tag package into a 90-L Loligo swim tunnel respirometer with a flowmeter. Calibration resulted in a measured linear relationship of $ms^{-1} = 0.022 * \text{rotations } s^{-1} + 0.25$ ($R^2 = 0.99$, $p < 0.0001$). It was found that the turbine requires a minimum flow speed of ~ 0.25 ms^{-1} to turn, therefore, after the calibration step any calculated speed of $\leq$ 0.25 ms^{-1} was set to zero. In addition, speed could not be estimated for some deployments because the tag attachment angle prevented water from consistently moving over the speed sensor in the desired orientation, so speed data were removed for those fish.

Oxygen

Not all tags used in this study had oxygen sensors incorporated into the acceleration data logger. As a result, four blue marlin and four sailfish did not have accompanying oxygen data. To assign oxygen data to all fish, we created *in situ* percent dissolved oxygen and depth profiles from each fish carrying an oxygen sensor, and the mean percent oxygen saturation was calculated at 0.5-m depth intervals. Because all tag deployments occurred over the same spatial and temporal scale, and % oxygen saturation variability was low across depths and deployments (average standard deviation = 4.35%), the mean percent oxygen values were assigned to the corresponding depths of fish without oxygen readings.

Tri-axial sensors

We analyzed acceleration, gyroscopic and magnetometer data using Igor Pro v. 8.0.4.2 (Wavemetrics, Inc. Lake Oswego, OR, USA) with the Ethographer extension (Sakamoto et al., 2009), R (R Core Team, 2019) or a combination of the two. We calculated the static component of the acceleration, which indicates body position from changes due to gravity, using a 3-s box smoothing window on the raw acceleration data (Shepard et al., 2008). Tag attachment angle on

each fish was corrected by rotating the raw acceleration data so that the X and Y axis had a mean of 0. Body pitch (angle) was then calculated from the surge axis (anterior-posterior) of the static component. The static component of each axis was then subtracted from their respective raw acceleration value to isolate the dynamic component, which represents the movement due to the fish. From this dynamic component, ODBA (overall dynamic body acceleration) was calculated by summing the absolute value of the dynamic acceleration from all three axes (Wilson et al., 2006). Because it has been shown to produce the clearest tailbeat signal (Andrzejaczek et al., 2019), we used the sway (lateral) axis of the angular velocity data (i.e. gyroscope) to calculate the tailbeat amplitude (TBA) and tailbeat period (TBP) using a continuous wavelet transformation with Ethographer (Sakamoto et al., 2009). As such, all further mention of 'tailbeat' is indicative of the lateral sway of angular velocity. Finally, a compass heading was calculated from the magnetometer data using the *magHead* function in the gRumble R package (https://github.com/MBayOtolith/gRumble).

Recovery behavior

It has been previously observed that blue marlin in other geographic regions dive to the upper layers of the thermocline upon release and remain there for an extended period (Holland et al., 1990; Block et al., 1992a). To quantify this initial dive behavior and determine how fight time may have affected the dive, we regressed the duration of the initial dive (min) against the fight time (min). Dive duration was calculated as the time elapsed from the first dive below 10 m lasting at least 20 sec, until the fish returned to 10 m. Each variable was natural log transformed prior to regression so that the residuals of the model approximated a normal distribution.

We used heading data to calculate the circular mean and standard deviation of movement for each fish over the duration of the tracking period, as well as the mean resultant length, $\bar{R}$, as a measure of the concentration of unimodal circular data in 15 min time windows using the circular R package (Pewsey et al., 2013; Cremers and Klugkist, 2018). When $\bar{R}$ is close to or equal to one, values in that time window are closely clustered around the mean direction and are highly directional, and as $\bar{R}$ approaches zero, values are spread more evenly between 0 and 360˚, indicative of a tortuous path. The circular mean and standard deviation were compared within species using a Watson-Williams test, and between species using a Watson's two sample test of homogeneity, with significance determined at the $p < 0.05$ level. $\bar{R}$ was used as a continuous

time series variable to determine if path tortuosity changed over the course of the tracking period using the methods outlined below.

Recovery period

We summarized metrics of depth, speed, static and dynamic components of acceleration, angular velocity and heading hourly and evaluated them for the presence of a recovery period. To investigate relationships between behavioral metrics and hour post-release, several models were built using the nlme (Pinheiro et al., 2007) and mgcv (Wood, 2015) R packages. All statistical analyses treated individual as a random effect. First, each metric was regressed against hour post-release using linear mixed models (LMMs). Each of these models was compared to a null model that did not include hour post-release. Model comparison was performed using Akaike Information Criterion (AIC). Candidate models were deemed significantly better than the null if $\Delta AIC < 10$. This threshold was used following Whitney et al. (2016), as it is highly conservative to limit type I error during repeated analyses. Many of the metrics displayed nonlinear relationships, thus, were subsequently fitted using generalized additive mixed models (GAMMs) with a smoother around hour post release. GAMMs were compared to LMMs and deemed significantly better than the LMM if $\Delta AIC < 10$. Due to the relatively rapid recovery of sailfish across all metrics examined, LMMs did not sufficiently capture the short recovery period. As such, only GAMMs were used to investigate the relationships between each behavioral metric and hour post-release for sailfish. An increased threshold of $\Delta AIC < 20$ was used to determine significance against the null model to remain consistent across species, where blue marlin GAMMs had to be 10 less than LMMs which had to be 10 less than the null. Many of the metrics examined appeared to follow an asymptotic relationship with time since release. Therefore, if a metric was deemed to have a significant change over time using the previously described methods, the metric was then fit with an asymptotic regression nonlinear mixed model (NLMM). Models were run for each metric with random term structures that incorporated individual variability into the asymptote, the initial value at time zero (hour 0 post release), and the rate constant that controls the speed at which the metric reached the asymptote. This procedure allowed for flexibility in determining how the individual fish recovered, accounting for variability within the population and different sized fish with varying fight times.

For metrics that displayed a recovery period, we calculated time to recovery as the time at which the metric had changed by 90% of the difference between the initial post-release value (hour 0)

and the recovered value (the asymptote). Finally, to test if fight time or fish size were significant predictors of recovery time across all metrics, estimated recovery times from all metrics were compared to fight time and estimated weight in a Generalized Linear Model (GLM; each species analyzed separately), where the recovery times were the response variable and fight time, estimated weight, and the interaction between fight time and estimated weight were used as predictor variables.

Results

Recovery behavior

Data were recovered from nine blue marlin and nine sailfish (n = 18) after deployments ranging from 6.1 to 70.5 h (mean ± SD; 36.2 ± 19.2 h). Analyses were limited to the first 36 h of each deployment to keep sample size high through the models, culminating in a total of 293 h of blue marlin and 233 h of sailfish depth, temperature, and inertial measurement data. Despite some animals moving up to 47 km (28 ± 13 km) from their point of capture, 100% of tag packages deployed were successfully recovered. Blue marlin tended to move further from the point of capture (38 ± 7 km) than sailfish (18 ± 9 km), even with similar deployment durations (Figure 2-1A; Table 2-1), and all fish remained within the region defined by hypoxia-based habitat compression throughout the duration of their tracks (Figure 2-1).

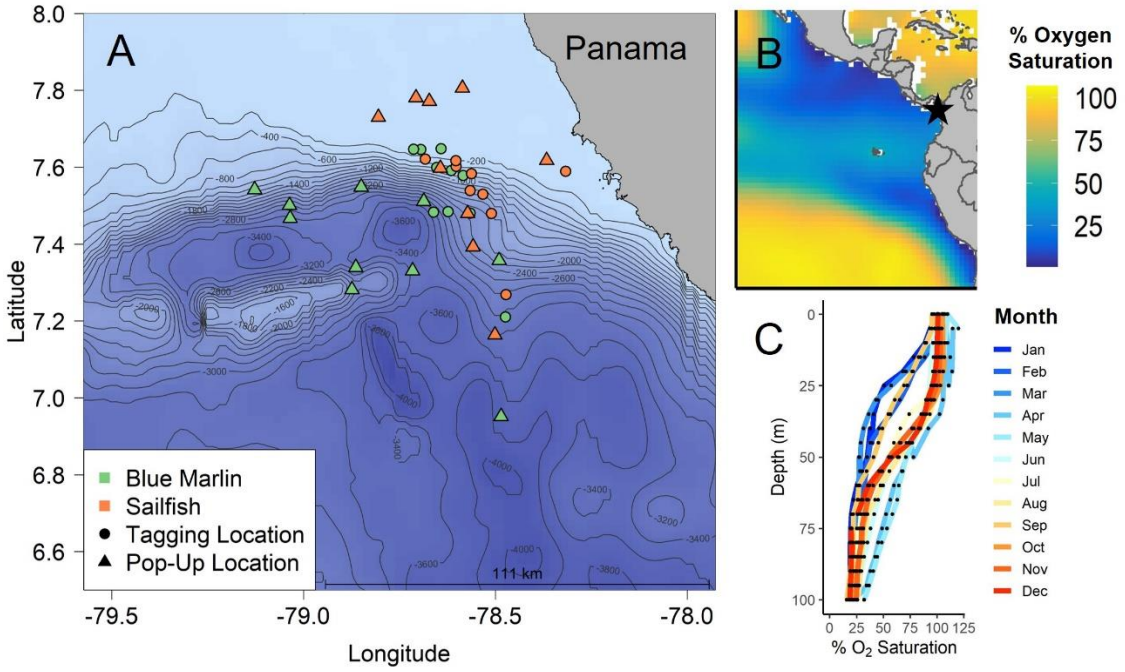

Figure 2-1. A) Tagging and tag pop-up locations for blue marlin and sailfish off the coast of southeast Panama, with bathymetric contour intervals of 200 m, B) 1° grid cell annual mean percent oxygen saturation at 100 m with the study site indicated by a black star, and C) the monthly mean percent oxygen saturation at 5 m depth intervals within the study site (black star). Data for B and C were obtained from NOAAs National Centers for Environmental Information World Ocean Atlas 2018.

After being released blue marlin typically exhibited a long dive (Figure 2-2) varying in duration from 14 to 383 min (mean 153 ± 120 min). The length of this initial dive increased with fight time ($\log(y) = 1.02*\log(x) + 0.47$, $r^2 = 0.68$, $p = 0.006$; Figure 2-3). Among all blue marlin, regardless of dive duration, depth of the initial dive was consistent across individuals (29.5 ± 6 m; Figure 2-2). While some vertical activity was apparent in sailfish after release, they did not exhibit a similar characteristically long dive immediately after release (Figure 2-2). There was considerable individual variability in sailfish vertical movements after release however (Figure 2-2). Sailfish 1 and 2, for example, display very limited diving behavior compared to the others and the reasons for this are not clear. After sailfish 9, sailfish 1 and 2 have the shortest tag attachment durations which could be a contributing factor.

Table 2-1. Tagging summary of the fish used in recovery behavior and recovery period analysis.

Tagging date (d/m/Y)	Estimated weight (kg)	Fight time (min)	Deployment duration (h)	Displacement distance (km)
Blue Marlin				
22/09/2019	160	80	14.8	30
24/09/2019	205	90	34	45
3/10/2019	115	12	35.9	45
3/10/2019	90	8	36.4	47
5/10/2019	90	26	35.9	42
9/10/2019	115	40	32	31
21/10/2019	115	13	32.7	42
25/10/2019	180	73	67	32
30/10/2019	70	61	70.5	29
Blue marlin mean ± SD	125 ± 45	44.8 ± 30.1	39.9 ± 16.7	38 ± 7
Sailfish				
19/09/2019	50	8	16.8	18
23/09/2019	30	10	13.4	20
9/10/2019	25	8	33.5	21
14/10/2019	45	6	36.8	21
15/10/2019	45	10	60.2	7
18/10/2019	45	6	67.2	34
27/10/2019	35	4	38.7	12
31/10/2019	45	14	18.9	20
4/11/2019	35	5	6.1	6
Sailfish mean ± SD	40 ± 10	7.9 ± 2.9	32.4 ± 19.8	18 ± 9

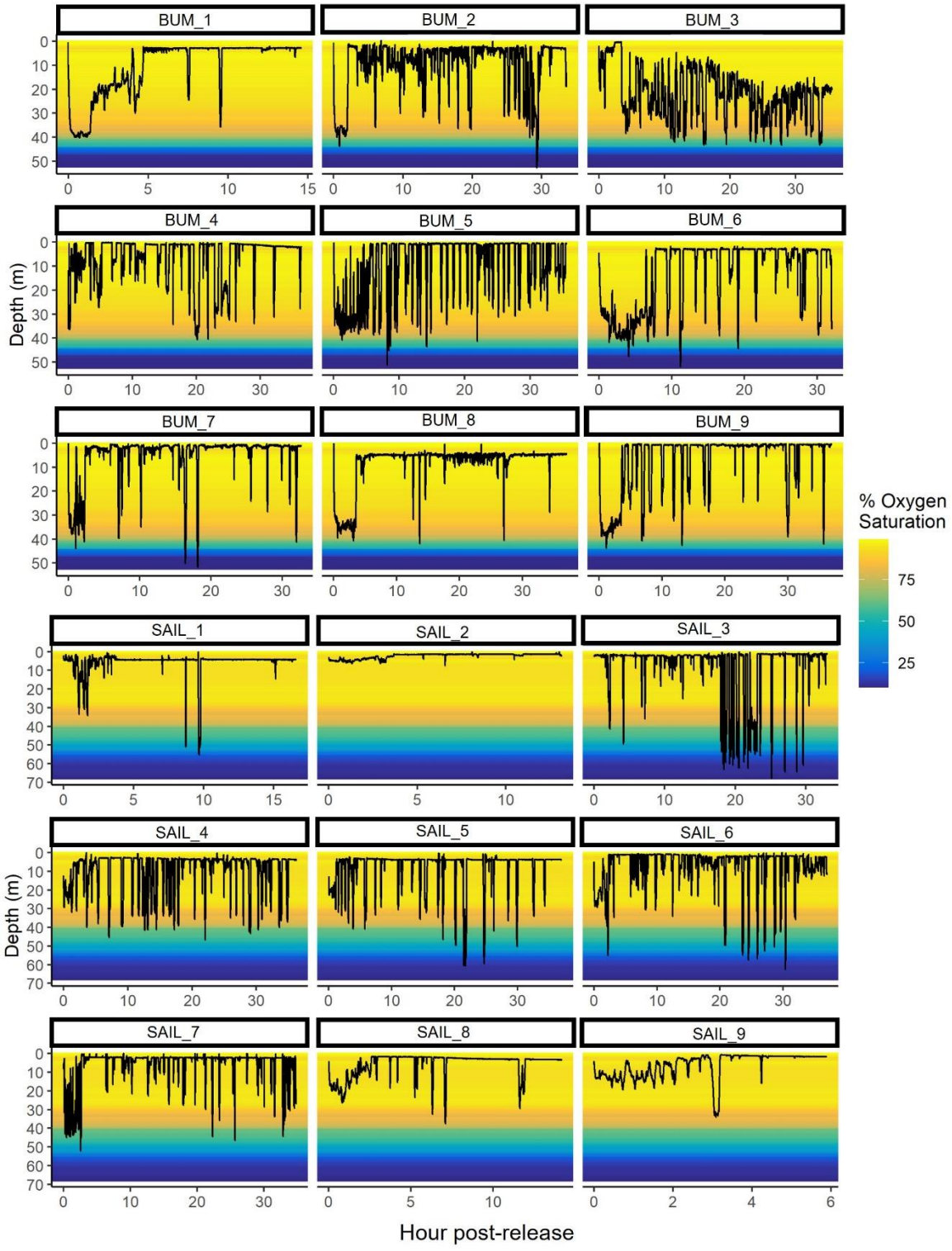

Figure 2-2. Depth profiles for each fish overlaid on mean percent oxygen saturation level at 0.5 m depth intervals obtained from animal borne oxygen sensors. Note x-axes differ based on the individual deployment duration, and y-axes differ by species.

The circular mean heading (degrees) was significantly different among individual blue marlin (Watson Williams test; $F_{(8,1059388)} = 145800$, $p < 0.001$) and sailfish ($F_{(8,820181)} = 127340$, $p < 0.001$). The mean overall heading between species though was not significantly different (Watson's Two-Sample Test of Homogeneity $T = 0.03$, $p = 0.19$). The overall circular mean ± SD heading from the point of capture for all blue marlin combined was 260 ± 70° (clockwise range 172 - 342°), while the mean heading for all sailfish was 249 ± 98° (clockwise range 19 – 320°), indicating the mean direction of travel for both species was west southwest from the point of release.

Recovery period

Sailfish #9 was omitted from recovery period analyses because of its short track duration (6 h). Immediately after release, marlin and sailfish typically displayed rapid, high amplitude tailbeats with elevated speed, and had a deeper average depth compared to the rest of the track. During this initial period after release, they actively swam during descents, periods of level swimming, and ascents. Average depth became shallower, and speed decreased as tailbeats became slower and less forceful with time.

Nonlinear relationships with time since release were found for 14 and 13 of the 40 metrics calculated for blue marlin and sailfish, respectively (Table 2-2). The categories of data that indicated a recovery period were depth, diving behavior, TBP, TBA, ODBA, swim speed, tortuosity, and percent dissolved oxygen content of the water. Metrics derived from vertical velocity, pitch and temperature use did not display a change over time.

Table 2-2. Swimming behavior metrics calculated from acceleration data-loggers for each hour after release and evaluated for indication of a recovery period in blue marlin and sailfish. Model fit (ΔAIC) is shown for linear and additive models with hour post release relative to the null model. Metrics with significant change over time in both the linear and additive models for blue marlin and additive models for sailfish are marked in bold (refer to methods for description of significance and the omission of sailfish linear models).

		Blue marlin		Sailfish
Variable	Description	Linear ΔAIC	Additive ΔAIC	Additive ΔAIC
Depth-Avg	Average depth (m)	**-36.8**	**-108.5**	**-25**
Depth-Min	Average minimum depth (m)	3.7	-19.9	**-26.9**
Depth-Max	Average maximum depth (m)	**-13.7**	**-12.3**	-11.2
Depth-Avg Ascent	Average depth during all ascents (m)	-9.5	-32.1	-5.3
Depth-Avg Descent	Average depth during all descents (m)	-1.8	-10.5	-0.7

Depth-Avg Level	Average depth during all level swimming (m)	**-42.6**	**-122.5**	**-36.8**
Diving Ratio	Amount of time spent moving vertically (s)	8.2	-9.4	-8.8
Dive Duration-Avg	Average length of dives (s)	**-25.4**	**-49.9**	**-21.1**
Dive Depth-Avg	Average depth of individual dives (m)	1.9	1.3	-5.4
VV-Avg	Average absolute value of ascending or descending swimming (ms^{-1})	11.1	-10.5	-9.3
VV-Min	Minimum VV (the fastest ascent) (ms^{-1})	8.1	-7.7	-14.2
VV-Max	Maximum VV (ms^{-1})	10.8	-3.1	-5.8
VV-Avg Ascent	Average VV during ascents (ms^{-1})	10.7	-13.3	-7.2
VV-Avg Descent	Average VV during descents (ms^{-1})	10.7	-9.3	-6.6
TBP-Avg	Average tailbeat period (s)	**-65.1**	**-149.1**	**-114.4**
TBP-Avg Ascent	Average tailbeat period during ascents (s)	**-13.1**	**-26.8**	**-73.5**
TBP-Avg Descent	Average tailbeat period during descents (s)	12.1	-5	**-23.4**
TBP-Avg Level	Average tailbeat period during level swimming (s)	**-66.4**	**-165.9**	**-119.1**
TBA-Avg	Average tailbeat amplitude ($°s^{-1}$)	**-34.4**	**-126.7**	**-123.2**
TBA-Avg Ascent	Average tailbeat amplitude during ascents ($°s^{-1}$)	10.8	-16.8	-16.2
TBA-Avg Descent	Average tailbeat amplitude during descents ($°s^{-1}$)	**-14.9**	**-36.1**	**-26.4**
TBA-Avg Level	Average tailbeat amplitude during level swimming ($°s^{-1}$)	**-39.3**	**-141.2**	**-146.8**
ODBA-Avg	Average ODBA (g)	19.3	-34.9	**-44.8**
ODBA-Max	Maximum ODBA (g)	11.2	-3.4	-1.2
ODBA-Avg Ascent	Average ODBA of ascents (g)	16.9	-7.3	-19.7
ODBA-Avg Descent	Average ODBA of descents (g)	15.8	-7.9	-6.4
ODBA-Avg Level	Average OBDA of level swimming (g)	19.2	-35.1	**-49**
Swim Speed-Avg	Average swim speed (ms^{-1})	**-10.9**	**-39.9**	-19.8
Swim Speed-Avg Ascent	Average swim speed during ascents (ms^{-1})	10.1	-7.3	-0.3
Swim Speed-Avg Descent	Average swim speed during descents (ms^{-1})	9.9	-1.9	-12.2
Swim Speed-Avg Level	Average swim speed of level swimming (ms^{-1})	**-11.8**	**-39.5**	-18
Tortuosity-Avg	Average hourly tortuosity of 15 min intervals (R)	**-27.5**	**-68.8**	-2.5
Tortuosity-Avg Level	Average hourly tortuosity of 15 min intervals of level swimming (R)	6.6	-39.6	-3.1
Pitch-Avg Ascent	Average pitch during ascents (°)	5.9	4.8	-11.9
Pitch-Avg Descent	Average pitch during descents (°)	5.2	5.4	8.7
Pitch-Avg Level	Average pitch during level swimming (°)	4.6	-1.2	-7.6
Oxygen-Avg	Average dissolved oxygen concentration encountered (% O_2 saturation)	**-14.9**	**-54.5**	-17.9
Oxygen-Min	Minimum dissolved oxygen concentration encountered (% O_2 saturation)	-1.8	0	-11
Temperature- Avg	Average temperature encountered (°C)	3.7	-8.9	-3.8
Temperature-Min	Minimum temperature encountered (°C)	10	2.3	-19.7

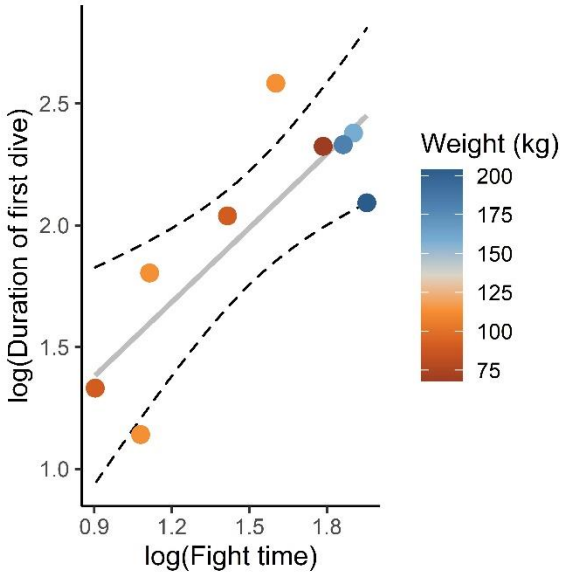

Figure 2-3. Relationship of initial dive duration with the duration of fight time for blue marlin, color coded by the estimated weight of the individual. Both variables were log transformed so residuals approximated a normal distribution. Line of best fit log(y) = 1.02*log(x) + 0.47, r^2 = 0.68, p = 0.006. Dashed lines indicate standard errors.

Depth use and diving activity

During the first hour after release, blue marlin and sailfish on average used deeper depths, which became shallower until 90% of the asymptote was reached at 6.7 and 3.8 h, respectively (Table 2-2; Figure 2-4A, D). After this period, predicted depth values were similar between blue marlin (6.9 m) and sailfish (5.8 m) with average decreases of 78 and 65%, respectively (Table 2-3). Average maximum depth was also greatest for blue marlin in the first hour after release but did not stabilize until 8.2 h after release. For sailfish, average minimum depth decreased from 5.4 to 1.9 m (63%) after 2.5 h (Table 2-3). Like the average overall depth, average depth of level swimming decreased (became shallower) by 81 and 72% for blue marlin and sailfish, respectively.

While sailfish did not exhibit a characteristically long dive immediately after release like blue marlin, their average dive duration decreased by 87% after 1.1 hours post-release when 90% of the asymptote was reached. Blue marlin average dive duration immediately after release was nearly 2.5x that of sailfish and decreased by 98% after 90% of the asymptote was reached at 2.4 h after release (Table 2-3).

Tailbeat period and amplitude

Immediately after release, both blue marlin and sailfish exhibited rapid tailbeats, which slowed with time after release (Figure 2-4B, E; Figure 2-5). Blue marlin and sailfish TBP (the time to complete one full tailbeat) increased (i.e., slowed down) by 26% and 93% when 90% of the asymptote had been reached at 10.2 and 5.7 h, respectively (Table 2-3), with similar results for TBP of level swimming periods in both species (Table 2-3). Compared to the overall TBP, the average TBP of ascents reached 90% of the asymptote much faster for blue marlin (4.7 h) than sailfish (8.2 h).

Tailbeat amplitude, a proxy measure of how forceful each tailbeat is, decreased during descents, periods of level swimming, and overall for both blue marlin and sailfish as fish recovered. TBA of level swimming periods displayed the greatest change over time for both species, decreasing by 61 and 80% for blue marlin and sailfish after 90% of the asymptote was reached at 9.7 and 4.4 h, respectively (Table 2-3; Figure 2-4C, F).

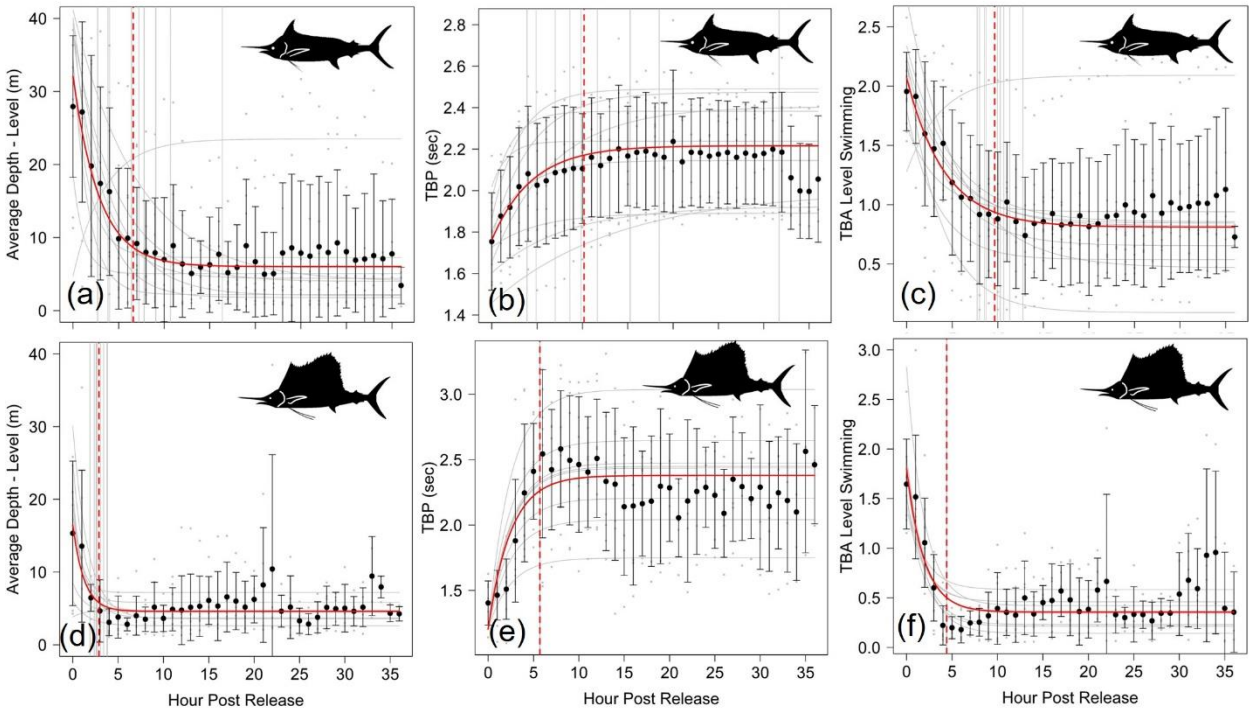

Figure 2-4. Example recovery periods of blue marlin (A-C) and sailfish (D-F) after being caught and released by recreational fishing gear in southwest Panama. Shown are the hourly means of (A, D) average depth during level swimming, (B, E) overall tailbeat period and (C, F) tailbeat amplitude during level swimming. Gray lines and dots represent individual hourly means and regressions, with black dots and standard deviation bars representing means across individuals. The solid red line is the combined regression, with the vertical red dashed line denoting the point at which this metric reached its 90% threshold and the fish was considered to be recovered for that metric.

Overall dynamic body acceleration (ODBA)

Only sailfish showed a significant decrease in ODBA as fish recovered. The overall average ODBA and the average level phase ODBA showed nearly identical decreases of 43 and 42% after release, yet 90% of the asymptote was reached two hours earlier for overall average ODBA than for the average level phase ODBA (Table 2-3).

Swimming speed and tortuosity

The overall average swimming speed and average level phase swimming speed decreased by 41 and 39% for blue marlin after 90% of the asymptote was reached at 11.4 and 11.6 h. Sailfish swimming speed did not significantly change over time (Table 2-3).

While the metric of path tortuosity ($\bar{R}$) only showed a change over time for blue marlin, this metric had the longest overall time to reach 90% of the asymptote (14.1 h) of any metric for

this species. The value of 0.99 immediately after release indicates blue marlin heading is highly directional and unimodal, whereas after 90% of the asymptote had been reached, their heading is less directional (0.63), indicative of a more tortuous path (Table 2-3).

Dissolved oxygen

Blue marlin used water with higher average percent oxygen saturation after 90% of the asymptote was reached 7.4 h after release, with an increase of 9% from 86% to 94% O_2 saturation (Table 2-3).

Table 2-3. Metrics that indicated a significant change over time indicative of a recovery period. Percent change represents the percent increase (positive) or percent decrease (negative) of the value at hour 0 compared to the recovered value. Values come from the line of best fit from the nonlinear mixed models. Grey shading indicates the metric was only significant for the other species. See Table 2 for descriptions of each metric.

	Blue marlin				Sailfish			
Metric	Hour 0 value	90% asymptote value	% change	Hour recovered	Hour 0 value	90% asymptote value	% change	Hour recovered
Depth-Avg	31.4	7	-78	6.7	16.6	5.8	-65	3.8
Depth-Max	38.5	21	-45	8.2				
Depth-Min					5.4	2	-64	2.6
Depth-Avg Level	32	6	-81	6.6	16.5	4.6	-72	2.9
Dive duration-Avg	150.5	3	-98	2.4	57.1	7.4	-87	1.1
TBP-Avg	1.8	2.2	26	10.2	1.2	2.3	93	5.7
TBP-Avg Ascent	1.5	1.8	21	4.7	1.3	1.6	24	8.2
TBP-Avg Descent					1.5	1.8	24	11.9
TBP -Avg Level	1.8	2.2	27	11.9	1.2	2.4	103	5.8
TBA-Avg	2.1	0.9	-58	9.8	1.8	0.4	-76	4.5
TBA-Avg Descent	1.2	1.1	-33	11	1.7	1.1	-39	2.9
TBA-Avg Level	2.1	0.8	-61	9.7	1.8	0.4	-80	4.4
ODBA-Avg					0.04	0.03	-43	4
ODBA-Avg Level					0.04	0.03	-42	6
Speed-Avg	0.8	0.5	-41	11.4				
Speed-Avg Level	0.8	0.5	-39	11.6				
Oxygen-Avg	86	94	9	7.4				
Tortuosity-Avg	0.9	0.6	-36	14.1				
				9.0 ± 3.2				4.9 ± 2.8

Recovery periods

By incorporating individual as a random effect in the NLMMs, the overall recovery period for each fish could be calculated, resulting in an individual mean recovery period of 9.8 ± 6.7 h for blue marlin and 5.1 ± 3.2 h for sailfish. The recovery periods across all metrics were variable by species, with a range of 1.2 – 31.3 h for blue marlin and 0.3 – 16.8 h after release for sailfish. When all significant metrics were incorporated and averaged for each species, the mean recovery period for this study population of blue marlin was 9.0 ± 3.2 h, and 4.9 ± 2.8 h for sailfish. For blue marlin, dive duration produced the shortest estimated times to recovery (2.4 h), while tortuosity and swimming speed displayed the longest times to recovery (14 and 11.6 h, respectively). Like blue marlin, sailfish dive duration produced the shortest estimated times to recovery (1.1 h), while TBP of ascents and overall average TBP displayed the longest time to recovery (11.9 and 8.2 h, respectively).

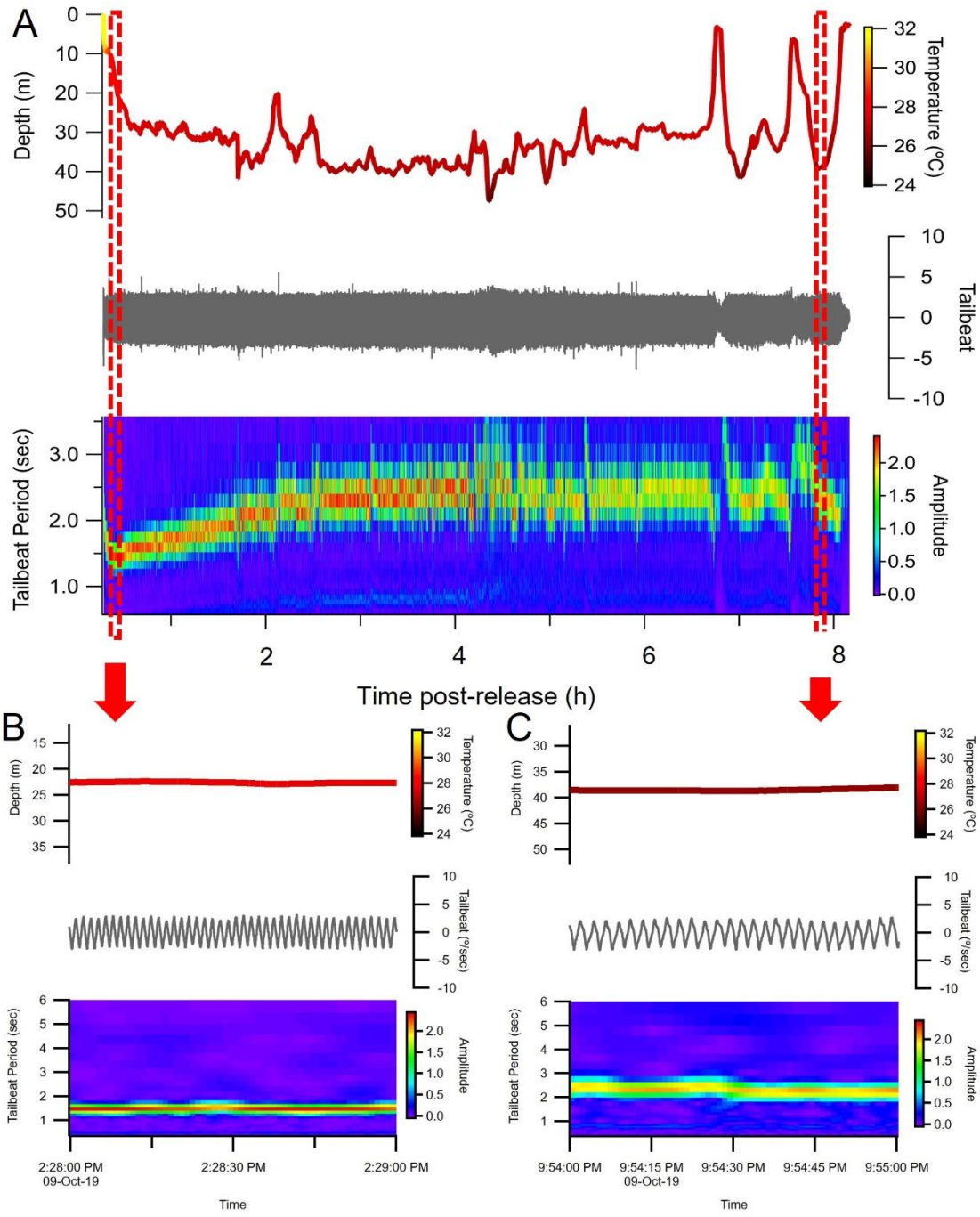

Figure 2-5. Recovery dive of a blue marlin. Depth, sway angular velocity (tailbeats; °rotation s^{-1}) and the output of the wavelet transformation of tailbeats during the initial dive of blue marlin #6 after release. (A) The fish rapidly descends after being released to a mean depth of 33.5 ± 5.2 m and remains near this depth in a constant temperature during this initial dive period of nearly eight hours, with constant tailbeat activity. The wavelet transformation reflects a gradual increase in tailbeat period of the fish (i.e., tailbeats become slower) to an asymptote while the average amplitude of tailbeats decreases. (B) Immediately upon release, tailbeats are rapid (dominant period of ~1.4 s) with low variability in period and amplitude whereas (C) near the end of this

initial dive period (nearly 8 h after release), tailbeat period is slower with more variability (dominant period of ~2.1 – 2.5 s). Note scale of x axis in A is ~ 8 h, versus 1 min in B and C.

Fight time and fish size

As previously discussed, dive duration of the initial dive after release significantly increased with increasing fight time for blue marlin (Figure 2-3). After averaging the recovery periods from all metrics, however, neither the length of the fight nor the estimated weight of the fish (or the interaction between them) were significant predictors of time to recovery for blue marlin (GLM; fight time, $p = 0.14$; estimated fish weight, $p = 0.29$; fight time*weight, $p = 0.17$), or sailfish (fight time, $p = 0.20$; estimate fish weight, $p = 0.21$; fight time*weight, $p = 0.18$).

Discussion

Our study shows that multi-sensor biologging tags may be used to determine fine-scale habitat use, swimming behavior and recovery periods from fishery interaction for large, wide-ranging pelagic predators. Understanding this type of information is important in assessing how these highly sought-after sportfish may be impacted by recreational fishing activity via sublethal behavioral modifications. This type of information additionally has the potential to allow fisheries managers to determine if and how different handling and fishing practices may reduce animal stress and recovery time.

Recovery behavior

Immediately upon release, blue marlin often exhibit a stereotypic recovery behavior, where they descend to the upper layers of the thermocline and remain there for an extended period of time, previously described as roughly 4 – 6 h (Holland et al., 1990; Block et al., 1992a; Block et al., 1992b). During this time, it has also been observed that blue marlin swim at elevated speeds (via speed of a tracking vessel or through direct measurement; Holland et al., 1990, Block et al. 1992b, respectively). This initial dive may be an attempt to seek cooler waters in response to elevated muscle temperature. For example, Block et al. (1992a) found that after only a 15-min fight on rod and reel, epaxial musculature of a blue marlin was 2.1° C greater than ambient water immediately after release, but that muscle temperature equilibrated to ambient temperature 5 h after release. In addition, increased time at depth after release has been related to increases of $[Ca^{2+}]$ in the blood of white marlin after capture and tagging (Schlenker et al., 2016). Furthermore, increased fight time in istiophorid billfish is associated with concentrations of other blood plasma ions and metabolites related to stress (i.e., sodium, chloride, glucose,

cortisol, and lactate) (Dobson et al., 1986; Davie, 1990; Schlenker et al., 2016). Because istiophorids are obligate ram ventilators, elevated swimming speed after release is thought to aid in repayment of the severe anaerobic debt incurred during the fight, without being high enough to incur new debt (Holland et al., 1990), and would serve to meet the higher oxygen demand required to metabolize accumulated lactate (Block et al., 1992a). Alternatively, elevated swim speed may simply be a flight response to an unknown stressful event. Indeed, both elevated swim speed and use of deeper water were also generally observed here for blue marlin following release; however, the average depth at which these dives occurred was much shallower (30-40 m) compared to previous studies in Hawaii (70-100 m) (Holland et al., 1990; Block et al., 1992a). This difference is likely due to the shallow thermocline of the ETP, in addition to the concomitant oxycline limiting these fish to shallower water (Prince et al., 2006; Figures 2-1 & 2-2). Importantly, we were also able to determine that the length of the initial dive increased with fight time. While the sailfish studied here did not exhibit a pronounced long duration dive after release, they did use deeper average depths compared to the rest of their track after release and did exhibit elevated speeds immediately after release.

Fortuitously, the tag of blue marlin 4 was angled down toward the gills allowing the video camera to record the left gill operculum of the fish. Immediately after release, the gill operculum was constantly flared open for roughly 3 h, after which the fish began actively pumping the operculum at a rate of roughly 1 pump sec^{-1} during routine swimming, regardless of depth. Sharksuckers (*Echeneis naucrates*) transition from buccal pumping to ram ventilation depending on the travelling speed of their host, and it was found that oxygen consumption increased between 3.7 and 5.7% when shifting from ram gill ventilation to active branchial pumping (Steffensen and Lomholt, 1983). While blue marlin are known to be obligate ram ventilators, it is possible that they may increase oxygen uptake, or flush accumulated metabolites and CO_2 from the gills more readily via opercular pumping at low swimming speeds.

Since the thermocline and oxycline often occur at similar depths in the ETP, it is difficult to discern the relative influence of the two variables on billfish depth use after release. But given that they do co-occur, these fish are still able to dive to cooler waters to thermoregulate, while also remaining in sufficiently oxygenated water to ram ventilate. Climate change, however, is predicted to lead to oceanographic changes in this region, such as warming and acidification of surface waters, increased stratification, and upwelling of hypoxic waters into the surface layer

(Fiedler and Lavín, 2017). Further, hypoxia-based habitat compression is predicted to become widespread as global climate change intensifies and oxygen minimum zones are expected to become shallower (Laffoley and Baxter, 2019; Leung et al., 2019). In the ETP and other regions where the oxygen minimum zone is already shallow, this will cause the oxygen minimum zone to shoal above the thermocline, potentially prolonging or inhibiting recovery of marlin as they seek cooler water temperatures at depth.

Another feature common among fine-scale post-release movement studies of istiophorid billfishes is the tendency of the fish to move away from the coast after release. This directional movement has been observed in active acoustic tracking studies of blue marlin (Holland et al., 1990; Block et al., 1992a), striped marlin (Brill et al., 1993) and sailfish (Jolley Jr and Irby Jr, 1979). Although we found substantial individual variability in mean direction of travel for the duration of the track in both blue marlin and sailfish, the overall mean resultant length for each species indicated a west-southwest mean direction of travel, opposite that of the Panamanian coast nearest the tagging locations. This offshore movement has been suggested as a response to tagging, but may also reflect use of local currents to aid in recovery (Brill et al., 1993; Pepperell and Davis, 1999). Prevailing currents in the region during the study were predominantly north-northwest nearshore, becoming more easterly further offshore (R. Logan pers. obs.; Fiedler and Lavín, 2017). Given that the mean direction of travel for blue marlin and sailfish was west-southwest, it is possible they were swimming into the current to aid in oxygen debt recovery, or aid in predator detection via olfaction while in a more vulnerable swimming state. Interestingly, due to the high-resolution magnetometer heading data obtained, we were able to detect a significant increase in path tortuosity after blue marlin had recovered, suggesting they were less inclined to stay swimming into the current.

Recovery period

In addition to gathering information on depth, heading and temperature use to determine a post-release recovery period, we found that swimming kinematics (particularly tailbeat period and tailbeat amplitude) follow a predictable response among individuals indicating a recovery period. Combining all significant metrics reveals a recovery period of ~9 h for blue marlin, and ~5 h for sailfish. These measurements are similar to that of Holland et al. (1990), Block et al. (1992a) and Block et al. (1992b) for blue marlin, where depth, heading and speed information were used to estimate a recovery period of roughly 4–6 h. In addition, Jolley Jr and Irby Jr

(1979) suggest that sailfish acoustically tracked along southeast Florida appeared to recover within 1 – 3 h following release as indicated by inshore movement and an increase in activity (i.e., changes in vessel tracking speed and heading). Additionally, using acceleration data loggers similar to those described here, Atlantic bluefin tuna (*Thunnus thynnus*) displayed increased speed and tailbeat activity for approximately 6 h after release from recreational angling (Gleiss et al., 2019).

Due to the need to affix acceleration data loggers with two points of attachment on bony fish to obtain accurate tailbeat signatures, most effort to date using acceleration data loggers in marine fishes has been focused on elasmobranchs, whose rigid dorsal fin makes tag attachment more straightforward. Estimated recovery periods of elasmobranchs using these methods range from 4 to ~11 h (Whitney et al., 2016; Andrzejaczek et al., 2019). Similar to Whitney et al. (2016), metrics derived from tailbeat activity here (tailbeat period and amplitude) often displayed a more consistent period of recovery among individuals than those derived from depth. In contrast to blacktip sharks (Whitney et al., 2016), recovery periods derived from tailbeat activity in blue marlin and sailfish were longer than those derived from depth, indicating that depth information alone does not fully encompass swimming behavior, and may not be sufficient to accurately describe a recovery period for pelagic fish where seafloor depth is deeper than maximum diving depth.

While our methodology and results increase the knowledge base of sublethal stress impacting post-release behavior in istiophorid billfishes, caution is warranted in interpreting these data. Due to the nature of the high-resolution data being collected and needing to physically recover the tag package, the amount of time a tag can be attached to an individual is limited, particularly for highly migratory pelagic species such as blue marlin and sailfish. As such, it is possible that the short duration deployments reported here may not have extended beyond the true recovery periods, and what we determined to be recovered behavior may not be representative of normal behavior. Using a majority of Argos transmitted summary depth-temperature profiles (PDT), Hoolihan et al. (2011a) found that blue marlin and sailfish displayed post-release behavior modification for an average of 8.2 ± 8.5 and 3.5 ± 5.8 days after release, respectively. Interestingly, larger blue marlin ($\geq$ 90 kg; like 89% of the blue marlin tagged in this study) were significantly less likely to show signs of behavior change after release than smaller blue marlin (Hoolihan et al., 2011a).The large variability (indicated by the large SD) in the

duration of behavior modification in the Hoolihan et al. (2011) estimates is indicative of the comparatively low resolution of transmitted summary data from PSAT tags used in their study compared to the sub-second resolution presented here. In addition, Hoolihan et al. (2011a) stipulate in their findings that species-specific behaviors and environmental conditions could not be taken into account. Comparisons of vertical movements from short term acoustic telemetry and acceleration studies (this study; Jolley Jr and Irby Jr, 1979; Holland et al., 1990; Block et al., 1992a; Gleiss et al., 2019), and longer duration implanted archival and PSATs (Schaefer et al., 2011; Chiang et al., 2015; Lam et al., 2015; Carlisle et al., 2017; Vaudo et al., 2018) suggest that, when investigated, recovery following release for tunas and billfishes is on the scale of hours rather than days, and that changes in vertical habitat use can largely be explained by differences in oceanographic conditions and prey distributions.

Likewise, physiological parameters suggest billfish are capable of rapid recovery. Tunas and billfish white muscle exhibit some of the highest, if not the highest, lactate levels and accompanying lactate dehydrogenase (LDH) activity of any vertebrate (Dickson, 1995; Bernal et al., 2010), thus facilitating rapid metabolism of accumulated lactate to pre-exercise levels, much faster than other fishes (Arthur et al., 1992). This is largely a result of these fishes large gill surface area (Wegner et al., 2010) and cardio-respiratory system being able to deliver oxygen and metabolic substrates at high rates compared to other species (Bernal et al., 2010). We therefore believe the findings presented here are an accurate representation of the species-specific recovery period for blue marlin and sailfish in the eastern tropical Pacific.

Conclusions

Here, we provide the first high-resolution insights into the recovery behavior of istiophorid billfish after release from a recreational fishery via accelerometry. We demonstrate the utility of and the ability to use (and recover) acceleration data loggers in these large pelagic fishes without a rigid dorsal fin conducive to tag attachment, as well as highly migratory species capable of long-distance movements. We show that post-release behavior and recovery periods are individual and species specific, even under identical environmental conditions and handling practices, indicating that fine-scale swimming and diving kinematics can provide insight to the underlying physiological impacts of recreational fisheries capture. While it was not specifically measured here, we propose that acceleration data loggers would be a useful method to determine the impact of various oceanographic conditions, handling practices and gear types on the

recovery of these highly sought-after recreational species. For example, because sailfish are smaller and more easily handled, they are often lifted out of the water for anglers to take a picture, exposing them to substantial time out of water, increasing stress and potentially post release mortality (Schlenker et al., 2016). In addition, fly fishing and lightweight gear has become a common angling practice for these species, considerably increasing fight time and therefore potential stress and recovery time. Gaining an understanding of impacts such as these would aid in sustainable catch and release fishing practices and fisheries management for these large, highly mobile predators in the face of global climate change.

Literature Cited

Andrzejaczek S, Gleiss AC, Lear KO, Pattiaratchi CB, Chapple T, Meekan M. 2019. Biologging tags reveal links between fine-scale horizontal and vertical movement behaviours in tiger sharks (Galeocerdo cuvier). Frontiers in Marine Science 6:229.

Arthur PG, West TG, Brill RW, Schulte PM, Hochachka PW. 1992. Recovery metabolism of skipjack tuna (Katsuwonus pelamis) white muscle: rapid and parallel changes in lactate and phosphocreatine after exercise. Canadian Journal of Zoology 70:1230-1239.

Bergman JN, Bennett JR, Binley AD, Cooke SJ, Fyson V, Hlina BL, Reid CH, Vala MA, Madliger CL. 2019. Scaling from individual physiological measures to population-level demographic change: case studies and future directions for conservation management. Biological Conservation 238:108242.

Bernal D, Sepulveda C, Musyl M, Brill RW. 2010. The eco-physiology of swimming movement patterns of tunas, billfishes and large pelagic sharks. In: Domenici P, Kapoor BG, editors. Fish Locomotion: an eco-ethological perspective. Enfield, NH, USA: Science Publishers. pp 437-483.

Block B, Booth D, Carey F. 1992a. Depth and temperature of the blue marlin, Makaira nigricans, observed by acoustic telemetry. Marine Biology 114:175-183.

Block BA. 1986. Structure of the brain and eye heater tissue in marlins, sailfish, and spearfishes. Journal of Morphology 190:169-189.

Block BA, Booth D, Carey FG. 1992b. Direct measurement of swimming speeds and depth of blue marlin. Journal of Experimental Biology 166:267-284.

Brill RW, Holts D, Chang R, Sullivan S, Dewar H, Carey F. 1993. Vertical and horizontal movements of striped marlin (Tetrapturus audax) near the Hawaiian Islands, determined

by ultrasonic telemetry, with simultaneous measurement of oceanic currents. Marine Biology 117:567-574.

Brill RW, Lowe TE, Cousins KL. 1998. How water temperature really limits the vertical movements of tunas and billfishes–it's the heart stupid. In: International Congress on Biology of Fish. American Fisheries Society, Towson University. p 4.

Brown JH, Gillooly JF, Allen AP, Savage VM, West GB. 2004. Toward a metabolic theory of ecology. Ecology 85:1771-1789.

Carlisle AB, Kochevar RE, Arostegui MC, Ganong JE, Castleton M, Schratwieser J, Block BA. 2017. Influence of temperature and oxygen on the distribution of blue marlin (Makaira nigricans) in the Central Pacific. Fisheries Oceanography 26:34-48.

Chiang W-C, Musyl MK, Sun C-L, DiNardo G, Hung H-M, Lin H-C, Chen S-C, Yeh S-Z, Chen W-Y, Kuo C-L. 2015. Seasonal movements and diving behaviour of black marlin (Istiompax indica) in the northwestern Pacific Ocean. Fisheries Research 166:92-102.

Coffey DM, Holland KN. 2015. First autonomous recording of in situ dissolved oxygen from free-ranging fish. Animal Biotelemetry 3:47.

Cooke S, Schramm H. 2007. Catch-and-release science and its application to conservation and management of recreational fisheries. Fisheries Management and Ecology 14:73-79.

Cremers J, Klugkist I. 2018. One direction? A tutorial for circular data analysis using R with examples in cognitive psychology. Frontiers in psychology 9:2040.

Davie PS. 1990. Pacific marlins: anatomy and physiology. Massey University, Palmerston North, New Zealand.

Dickson KA. 1995. Unique adaptations of the metabolic biochemistry of tunas and billfishes for life in the pelagic environment. Environmental Biology of Fishes 42:65-97.

Dobson G, Wood S, Daxboeck C, Perry S. 1986. Intracellular buffering and oxygen transport in the Pacific blue marlin (Makaira nigricans): adaptations to high-speed swimming. Physiological zoology 59:150-156.

Donaldson MR, Arlinghaus R, Hanson KC, Cooke SJ. 2008. Enhancing catch-and-release science with biotelemetry. Fish and Fisheries 9:79-105.

Evans R, McLain D, Bauer R. 1981. Atlantic Skipjack Tuna: Influences of Mean Environmental Conditions on Their Vulnerability to Surface Fishing Gear. Marine Fisheries Review 43:1-11.

Fiedler PC, Lavín MF. 2017. Oceanographic conditions of the eastern tropical Pacific. In: Coral Reefs of the Eastern Tropical Pacific. Springer. pp 59-83.

Gabaldon J, Turner EL, Johnson-Roberson M, Barton K, Johnson M, Anderson EJ, Shorter KA. 2019. Integration, calibration, and experimental verification of a speed sensor for swimming animals. IEEE Sensors Journal 19:3616-3625.

Gleiss AC, Norman B, Wilson RP. 2011. Moved by that sinking feeling: variable diving geometry underlies movement strategies in whale sharks. Functional Ecology 25:595-607.

Gleiss AC, Schallert RJ, Dale JJ, Wilson SG, Block BA. 2019. Direct measurement of swimming and diving kinematics of giant Atlantic bluefin tuna (Thunnus thynnus). Royal Society open science 6:190203.

Gleiss AC, Wright S, Liebsch N, Wilson RP, Norman B. 2013. Contrasting diel patterns in vertical movement and locomotor activity of whale sharks at Ningaloo Reef. Marine Biology 160:2981-2992.

Graves JE, Horodysky AZ. 2008. Does hook choice matter? Effects of three circle hook models on postrelease survival of white marlin. North American Journal of Fisheries Management 28:471-480.

Holland KN, Brill R, Chang RK. 1990. Horizontal and vertical movements of Pacific blue marlin captured and released using sportfishing gear. Fishery Bulletin 88:397.

Hoolihan JP, Luo J, Abascal FJ, Campana SE, De Metrio G, Dewar H, Domeier ML, Howey LA, Lutcavage ME, Musyl MK. 2011. Evaluating post-release behaviour modification in large pelagic fish deployed with pop-up satellite archival tags. ICES Journal of Marine Science 68:880-889.

Horodysky AZ, Cooke SJ, Brill RW. 2015. Physiology in the service of fisheries science: why thinking mechanistically matters. Reviews in Fish Biology and Fisheries 25:425-447.

Idrisi N, Capo TR, Luthy S, Serafy JE. 2003. Behavior, Oxygen Consumption and Survival of Stressed Juvenile Sailfish (Istiophorus platypterus) in Captivity. Marine and Freshwater Behavior and Physiology 36:51-57.

Jolley Jr JW, Irby Jr EW. 1979. Survival of tagged and released Atlantic sailfish (Istiophorus platypterus: Istiophoridae) determined with acoustical telemetry. Bulletin of Marine Science 29:155-169.

Karstensen J, Stramma L, Visbeck M. 2008. Oxygen minimum zones in the eastern tropical Atlantic and Pacific oceans. Progress in Oceanography 77:331-350.

Killen SS, Adriaenssens B, Marras S, Claireaux G, Cooke S. 2016. Context dependency of trait repeatability and its relevance for management and conservation of fish populations. Conservation Physiology 4.

Laffoley D, Baxter JM. 2019. Ocean deoxygenation: Everyone's problem - Causes, impacts, consequences and solutions. Full report. Gland, Switzerland: IUCN. 580 p.

Lam CH, Kiefer DA, Domeier ML. 2015. Habitat characterization for striped marlin in the Pacific Ocean. Fisheries Research 166:80-91.

Lennox RJ, Alós J, Arlinghaus R, Horodysky A, Klefoth T, Monk CT, Cooke SJ. 2017. What makes fish vulnerable to capture by hooks? A conceptual framework and a review of key determinants. Fish and Fisheries 18:986-1010.

Leung S, Mislan KAS, Muhling B, Brill R. 2019. The significance of ocean deoxygenation for open ocean tunas and billfishes. In: Laffoley D, Baxter JM, editors. Ocean deoxygenation: Everyone's problem - Causes, impacts, consequences and solutions. Gland, Switzerland: IUCN. pp 277 - 308.

Lewin W-C, Arlinghaus R, Mehner T. 2006. Documented and potential biological impacts of recreational fishing: insights for management and conservation. Reviews in Fisheries Science 14:305-367.

McKenzie DJ, Axelsson M, Chabot D, Claireaux G, Cooke SJ, Corner RA, De Boeck G, Domenici P, Guerreiro PM, Hamer B. 2016. Conservation physiology of marine fishes: state of the art and prospects for policy. Conservation physiology 4.

Musyl MK, Moyes CD, Brill RW, Mourato BL, West A, McNaughton LM, Chiang W-C, Sun C-L. 2015. Postrelease mortality in istiophorid billfish. Canadian Journal of Fisheries and Aquatic Sciences 72:538-556.

Myers AE, Hays GC. 2006. Do leatherback turtles Dermochelys coriacea forage during the breeding season? A combination of data-logging devices provide new insights. Marine Ecology Progress Series 322:259-267.

Pepperell J, Davis T. 1999. Post-release behaviour of black marlin, Makaira indica, caught off the Great Barrier Reef with sportfishing gear. Marine Biology 135:369-380.

Pewsey A, Neuhäuser M, Ruxton GD. 2013. Circular statistics in R. Oxford University Press.

Pinheiro J, Bates D, DebRoy S, Sarkar D, Team RC. 2007. Linear and nonlinear mixed effects models. 3:1-89.

Pörtner HO, Knust R. 2007. Climate change affects marine fishes through the oxygen limitation of thermal tolerance. science 315:95-97.

Prince ED, Goodyear CP. 2006. Hypoxia-based habitat compression of tropical pelagic fishes. Fisheries Oceanography 15:451-464.

Prince ED, Luo J, Phillip Goodyear C, Hoolihan JP, Snodgrass D, Orbesen ES, Serafy JE, Ortiz M, Schirripa MJ. 2010. Ocean scale hypoxia-based habitat compression of Atlantic istiophorid billfishes. Fisheries Oceanography 19:448-462.

Prince ED, Ortiz M, VENIzELOS A. 2002. A comparison of circle hook and" J" hook performance in recreational catch-and-release fisheries for billfish. In: American Fisheries Society Symposium: American Fisheries Society. pp 66-79.

R Core Team. 2019. R: A language and environment for statistical computing. In. Vienna, Austria: R Foundation for Statistical Computing.

Sakamoto KQ, Sato K, Ishizuka M, Watanuki Y, Takahashi A, Daunt F, Wanless S. 2009. Can ethograms be automatically generated using body acceleration data from free-ranging birds? PLoS one 4.

Schaefer KM, Fuller DW, Block BA. 2011. Movements, behavior, and habitat utilization of yellowfin tuna (Thunnus albacares) in the Pacific Ocean off Baja California, Mexico, determined from archival tag data analyses, including unscented Kalman filtering. Fisheries Research 112:22-37.

Schlenker LS, Latour RJ, Brill RW, Graves JE. 2016. Physiological stress and post-release mortality of white marlin (Kajikia albida) caught in the United States recreational fishery. Conservation Physiology 4.

Shepard EL, Wilson RP, Halsey LG, Quintana F, Laich AG, Gleiss AC, Liebsch N, Myers AE, Norman B. 2008. Derivation of body motion via appropriate smoothing of acceleration data. Aquatic Biology 4:235-241.

Steffensen JF, Lomholt JP. 1983. Energetic cost of active branchial ventilation in the sharksucker, Echeneis naucrates. Journal of Experimental Biology 103:185-192.

Stramma L, Prince ED, Schmidtko S, Luo J, Hoolihan JP, Visbeck M, Wallace DW, Brandt P, Körtzinger A. 2012. Expansion of oxygen minimum zones may reduce available habitat for tropical pelagic fishes. Nature Climate Change 2:33.

Vaudo J, Byrne M, Wetherbee BM, Harvey G, Mendillo Jr A, Shivji M. 2018. Horizontal and vertical movements of white marlin, Kajikia albida, tagged off the Yucatán Peninsula. ICES Journal of Marine Science 75:844-857.

Vaudo JJ, Wetherbee BM, Wood AD, Weng K, Howey-Jordan LA, Harvey GM, Shivji MS. 2016. Vertical movements of shortfin mako sharks Isurus oxyrinchus in the western North Atlantic Ocean are strongly influenced by temperature. Marine Ecology Progress Series 547:163-175.

Watanabe YY, Takahashi A. 2013. Linking animal-borne video to accelerometers reveals prey capture variability. Proceedings of the National Academy of Sciences 110:2199-2204.

Wegner NC, Sepulveda CA, Bull KB, Graham JB. 2010. Gill morphometrics in relation to gas transfer and ram ventilation in high-energy demand teleosts: Scombrids and billfishes. Journal of Morphology 271:36-49.

Whitmore BM, White CF, Gleiss AC, Whitney NM. 2016. A float-release package for recovering data-loggers from wild sharks. Journal of experimental marine biology and ecology 475:49-53.

Whitney NM, Pratt Jr HL, Pratt TC, Carrier JC. 2010. Identifying shark mating behaviour using three-dimensional acceleration loggers. Endangered Species Research 10:71-82.

Whitney NM, White CF, Gleiss AC, Schwieterman GD, Anderson P, Hueter RE, Skomal GB. 2016. A novel method for determining post-release mortality, behavior, and recovery period using acceleration data loggers. Fisheries Research 183:210-221.

Williams HJ, Holton MD, Shepard EL, Largey N, Norman B, Ryan PG, Duriez O, Scantlebury M, Quintana F, Magowan EA. 2017. Identification of animal movement patterns using tri-axial magnetometry. Movement ecology 5:6.

Wilson RP, Shepard E, Liebsch N. 2008. Prying into the intimate details of animal lives: use of a daily diary on animals. Endangered species research 4:123-137.

Wilson RP, White CR, Quintana F, Halsey LG, Liebsch N, Martin GR, Butler PJ. 2006. Moving towards acceleration for estimates of activity-specific metabolic rate in free-living animals: the case of the cormorant. Journal of Animal Ecology 75:1081-1090.

Wood S. 2015. Package 'mgcv'. R package version 1:29.

Yoda K, Sato K, Niizuma Y, Kurita M, Bost C, Le Maho Y, Naito Y. 1999. Precise monitoring of porpoising behaviour of Adélie penguins determined using acceleration data loggers. Journal of Experimental Biology 202:3121-3126.

CHAPTER III

PATROLLING THE BORDER: BILLFISH EXPLOIT THE HYPOXIC BOUNDARY CREATED BY THE WORLD'S LARGEST OXYGEN MINIMUM ZONE

Abstract

Pelagic predators must contend with low prey densities that are irregularly distributed and dynamic in space and time. Based on satellite imagery and telemetry data, many pelagic predators will concentrate horizontal movements on ephemeral surface fronts—gradients between water masses—because of enhanced local productivity and increased forage fish densities. Vertical fronts (e.g., thermoclines, oxyclines) can be spatially and temporally persistent, and aggregate lower trophic level and diel vertically migrating organisms due to sharp changes in water density or available oxygen. Thus, vertical fronts represent a stable and potentially energy rich habitat feature for diving pelagic predators but remain little explored in their capacity to enhance foraging opportunities. Here, we use a novel suite of high-resolution biologging data, including *in situ* derived oxygen saturation and video to document how two top predators in the pelagic ecosystem exploit the vertical fronts created by the oxygen minimum zone of the eastern tropical Pacific. Prey search behavior was dependent on dive shape, and significantly increased near the thermocline and hypoxic boundary for blue marlin (*Makaira nigricans*) and sailfish (*Istiophorus platypterus*), respectively. Further, we identify a foraging tactic not yet reported for pelagic predators and hypothesize that this behavior is used to briefly dive below the thermocline and hypoxic boundary (and by extension, below the prey) to ambush prey from below. We describe how habitat fronts created by low oxygen environments can influence pelagic ecosystems, which will become increasingly important to understand in the context of global change and expanding oxygen minimum zones. We anticipate that our findings are shared among many pelagic predators where strong vertical fronts occur, and additional high-resolution tagging is warranted to confirm this.

Introduction

Ecological theory predicts that when prey are sparse and patchily distributed, predators should move, forage, and engage in activity patterns that maximize energetic gain while minimizing energetic loss (Pyke et al., 1977; Stephens and Krebs, 1986). Because foraging success is positively related to resource density (Mysterud and Ims, 1998), predators should forage (e.g., elevate activity and search behavior) in habitats with high resource density (McMahon and Matter 2006). In the pelagic environment, oceanic fronts are one such location. Oceanic fronts—strong gradients in abiotic factor(s) (e.g., temperature) caused by the convergence of water masses with different properties—create hotspots of biogeochemical cycling and aggregate low trophic level organisms (Woodson and Litvin, 2015).

Because oceanic fronts influence prey distribution, studies of highly mobile marine predators often focus on movements and distribution in relation to fronts (Sequeira et al., 2018; Arostegui et al., 2022). While this information provides valuable insight of when and where predators encounter prey and use frontal habitat, they often lack the resolution necessary to describe how the fronts are exploited (but see Arostegui et al., 2022). Further, because satellite imagery of oceanic conditions is limited to surface waters, such studies of pelagic predator movements in relation to fronts have largely been restricted to horizontal movements and surface fronts. Yet, marine predators live in a three-dimensional habitat and must respond to variable prey density both horizontally and vertically to maximize energy acquisition.

Vertical fronts such as thermoclines, oxyclines and pycnoclines can be spatially and temporally persistent in oceanic basins, concentrate basal food resources, and act as barriers to many prey items seeking refuge during daylight hours (Derenbach et al., 1979; Stewart et al., 2019; Fortune et al., 2020). For example, little penguin (*Eudyptula minor*) prey encounter rates were positively correlated with well-stratified waters, as prey were less dispersed in the available habitat and concentrated at the thermocline (Ropert-Coudert et al., 2009). As such, vertical fronts have the potential to be rich in energy, but our knowledge of how top pelagic predators respond to and use these fronts on large scales remains limited.

The Eastern Tropical Pacific (ETP) features a narrow, productive surface layer of uniform temperature and oxygen saturation, followed by a sharp and shallow thermocline (Fiedler and Lavín, 2017). Coexistent with the thermocline is the upper boundary of the oxygen minimum layer, beyond which lies the world's largest naturally occurring oxygen minimum zone

(OMZ; Gallo and Levin, 2016). Because cold temperatures and hypoxic conditions limit the vertical and horizontal distribution of many fishes, predators and prey alike of the ETP are confined to surface waters above the OMZ, known as hypoxia-based habitat compression (Brill et al., 1998; Prince et al., 2010; Stramma et al., 2012). During daylight hours, as prey species attempt to escape predation pressure by moving into lower-lit waters, prey density increases around this hypoxic boundary (Bertrand et al., 2006; Bertrand et al., 2010; Bianchi et al., 2013). As such, the ETP provides an opportune environment to study the fine-scale vertical habitat use and hunting behavior of pelagic predators in relation to vertical fronts.

Information of predator habitat use and hunting behavior in relation to hypoxic boundaries is of economic and ecological interest as global climate change intensifies. Increasing global sea surface temperatures will serve to reduce global ocean oxygen content and strengthen upper ocean stratification, which will increase productivity in surface waters, fueling increased oxygen demand while simultaneously reducing oxygen supply to greater depths (Keeling et al., 2010). Under these scenarios, oxygen minimum zones will become shallower and increase in size, affecting new regions and ecosystems (Laffoley and Baxter, 2019). Thus, predator foraging behavior in the ETP could provide insight into future vertical habitat use of pelagic predators worldwide.

Here, we combine high-resolution biologging and animal-borne video of blue marlin (*Makaira nigricans*) and sailfish (*Istiophorus platypterus*) to examine the relationship between their vertical and horizontal movements in a vertically compressed habitat. Additionally, we determine how these highly migratory predators may exploit the vertical fronts created by an oxygen minimum zone to increase foraging opportunities.

Methods

Blue marlin and sailfish were caught using rod-and-reel on trolling lures or natural live bait off the Pacific coast of southeast Panama from September to November 2019. Each fish was brought alongside the vessel and a custom-designed biologging tag package was affixed to the dorsal musculature with two umbrella-style anchors using a custom-made tag applicator. Once both anchors were securely imbedded in the muscle, the tag was firmly cinched against the fish's body using two galvanic timed releases and a cable tie. Fish weight was estimated by an experienced captain.

The biologging tag package consisted of an inertial measurement unit (IMU; OpenTag 3.0; Loggerhead Instruments, Sarasota, FL, USA), video camera (DVL 2000M130; Little Leonardo, Tokyo, Japan) and a Smart Position and Temperature tag (SPOT-363A; Wildlife Computers, Redland, WA, USA) for package recovery. The IMU comprised a triaxial accelerometer, magnetometer, and gyroscope recording at 100 Hz, depth, temperature, and a small turbine-based fluid speed sensor recording at 1 Hz. A subset of IMUs were equipped with a small (12 mm diameter × 20 mm long) oxygen sensor (Micro Probe; OxyGuard, Farum, Denmark) that recorded *in situ* dissolved oxygen (% saturation) of the water at 1 Hz. For a detailed description on data products, methodology, and biologging tag package see Logan et al. (2022). Data used in the current study are from the tag deployments described in Logan et al. (2022) after excising the time prior to recovery for each fish. All fish were tagged under permit from the Ministerio de Ambiente, República de Panamá (SE/A-64-19), and procedures approved by Nova Southeastern University's Institutional Animal Care and Use Committee (2019.04.MS1).

Diel Habitat Use

Using animal-borne temperature and oxygen sensors, mean overall depth profiles were generated for each variable at 0.5 m depth intervals by pooling all individuals' depth, temperature, and oxygen data. The thermocline was calculated as the shallowest depth at which the water temperature differs from sea surface temperature by 0.8 °C (Fiedler, 2010). As there is no universal definition of what percent oxygen saturation constitutes an oxycline, we consider the oxycline to be the shallowest depth at which percent oxygen saturation begins to decline more drastically with depth than in the water above, which in our study was determined to be 90% of that at the surface (100% saturation). Similarly, because there is no single oxygen concentration that defines a universal level of hypoxic stress for all marine organisms (Seibel, 2011), we adopt the dissolved oxygen level of $\leq$ 3.5 mL L^{-1} threshold identified to induce stress in tropical pelagic fishes (Bushnell and Brill, 1991; Prince and Goodyear, 2006) as the hypoxic boundary for blue marlin and sailfish (which occurs at ~60-65% O_2 saturation at 19-25°C). All observations were categorically assigned to either day or night periods.

Dive shape

Variable dive shapes across diving marine taxa have been linked to a variety of behaviors (Carter et al., 2016; Braun et al., 2022). Because blue marlin and sailfish dives did not all follow

the same pattern, dive profiles were categorized based on their similarity of shape via cluster analysis. Here, we define a dive as a vertical excursion to a minimum of 10 m and lasting at least 20 s. Because gill breathing animals don't need to come to the surface, a depth threshold was necessary to isolate movements clearly directed away from the surface. Depths from each qualifying dive were either downsampled or interpolated (depending on duration of the dive) so that each dive consisted of 50 depths equally spaced across the dive duration. Depths were then scaled so the start and end of each dive were equal to zero and the maximum dive depth equal to one, thus standardizing dive depths and lengths (Schreer et al. 1998). Using the 'factoextra' package in R (Kassambara and Mundt, 2017), we conducted hybrid hierarchical k-means clustering on the standardized dive profiles. The optimal number of dive shapes (i.e., clusters) was determined using an ensemble approach in which the elbow method, the silhouette method and the gap statistic method (Tibshirani et al., 2001) were compared and evaluated for biological realism.

To determine how fish behavior varied among dive shapes, several environmental and behavioral statistics were summarized for each dive shape, including acceleration derived metrics of overall dynamic body accelerations (ODBA) and tailbeat frequency (TBF). Dive characteristics of each dive shape were compared within species using a multivariate analysis of variance (MANOVA). Where significant differences were identified, pairwise comparisons were examined using a non-parametric Games-Howell post-hoc test.

Path tortuosity and video

To investigate relationships between path tortuosity (a proxy for prey searching), vertical habitat characteristics and dive shape, general additive mixed models (GAMMs) were built in R using the mgcv package (Wood, 2015). Heading data (0–360°) were resampled to a 1-s frequency and used to calculate the turning angles of each individual by calculating the absolute difference in angle between consecutive observations. Then, turning angles were summed across 1-min periods, creating a continuous measure of path tortuosity. Because habitat characteristics of depth, temperature, and oxygen were correlated (Pearson correlation coefficients: 0.65–0.7), a principal component analysis (PCA) was conducted to reduce dimensionality and retain the greatest amount of information about the correlated variables in space. Principal components with greater than 10% of variance explained were included as candidate predictor variables in GAMMs. Tortuosity was the response variable, and habitat principal components and dive shape

were explanatory variables. The model was run using a Gaussian response distribution and identity link, and we used the corAR1 function to account for temporal auto-correlation in the data, with individual included as a random intercept (Zuur et al., 2009). Model fit was assessed by examining residual diagnostic plots, and Akaike's information criterion (AIC) was used to assess model performance against an intercept only model, with improved model fit indicated by a ΔAIC value > 2. Tortuosity was log-transformed prior to model fitting. Finally, the onboard video camera was used to ground-truth periods of high tortuosity, and interaction with con- and herterospecifics.

Results

Nine blue marlin and nine sailfish were caught and tagged between 2019-09-19 and 2019-11-04 (Table 3-1). Tags were attached for 36.2 ± 18.7 h (mean ± SD), recording 81 h and 75 h of video footage for blue marlin and sailfish, respectively. After censoring the time it took each individual to recover post-release (Table 3-1; see Logan et al. (2022)), 271 and 245 h of IMU data were retained for analysis for blue marlin and sailfish, respectively.

Table 3-1. Summary details of tagged blue marlin (BUM) and sailfish (SFA). Time retained indicates the amount of time used for analyses in this study, after removal of the unique recovery period for each fish from Logan et al. (2022).

Fish ID	Deployment Date	Estimated Mass (kg)	Total Tag Attachment Duration (h)	Time Retained (h)	Depth (m)		Water Temperature (°C)		% Oxygen Saturation	
					Median (IQR)	Range	Median (IQR)	Range	Median (IQR)	Range
BUM1	2019-09-22 12:00	160	14.8	7.1	2.8 (2.8 - 2.9)	2 - 35.7	27.5 (27.4 - 27.5)	26.5 - 27.7	86.6 (83.8 - 94.1)	69 - 98.8
BUM2	2019-09-24 12:40	205	34.0	25.3	3.9 (2.9 - 10.2)	0.1 - 52.7	27.7 (27.6 - 27.9)	19.1 - 28.7	94.5 (92.5 - 96.3)	10 - 100
BUM3	2019-10-03 12:29	115	35.9	25.6	22 (17.8 - 30.2)	4.6 - 43.3	27.1 (26.7 - 27.3)	20.7 - 27.6	91.5 (88.7 92.5)	18.8 - 95.1
BUM4	2019-10-03 13:41	90	36.4	29.4	1.2 (0.8 - 5.7)	0.7 - 40.6	27.9 (27.6 - 28.5)	25.6 - 29.9	97.4 (94.5 - 97.9)	60.1 - 99
BUM5	2019-10-05 14:33	90	35.9	18.6	0.6 (0.5 - 12)	0.2 - 41.3	27.1 (27.1 - 27.2)	24.9 - 28.3	97.1 (94.4 - 97.4)	57.4 - 98.5
BUM6	2019-10-09 14:15	115	32.1	21.7	2.9 (2.8 - 5)	1.6 - 51.9	27.6 (27.5 - 27.8)	21.9 - 28.7	90 (89.9 - 92.8)	30.8 - 98.6
BUM7	2019-10-21 11:27	115	32.7	24.6	1.3 (0.9 - 2)	0.1 - 51.6	27.5 (27.4 - 27.5)	22.5 - 27.8	97 (93.9 - 97.9)	30.8 - 99

BUM8	2019-10-25 14:35	180	67.0	58.0	4.8 (4.5 - 5.1)	0.3 - 55.4	27.6 (27.4 - 27.6)	22.7 - 27.9	95.2 (94.9 - 96.6)	22.9 - 100
BUM9	2019-10-30 12:03	70	70.5	59.1	0.5 (0.4 - 0.8)	0.1 - 52.3	27.7 (27.6 - 27.8)	23.7 - 28.1	97.5 (96.8 - 97.9)	21.6 - 100
SFA1	2019-09-19 10:38	50	16.8	11	4.2 (4.2 - 4.4)	0.1 - 55.2	27.5 (27.5 27.6)	19.9 - 27.8	93.5 (93.5 - 94.4)	20.8 - 99
SFA2	2019-09-23 12:00	30	13.4	8.8	1.4 (1.3 - 1.5)	0.1 - 7.5	27.8 (27.8 - 27.8)	27.7 - 27.9	98.7 (97.4 - 99.7)	92 - 100
SFA3	2019-10-09 11:41	25	33.5	28.5	1.9 (1.4 - 3.1)	0.2 - 67.9	27.6 (27.3 - 28.2)	21 - 28.9	88.4 (85.8 - 90.5)	7.5 - 99.7
SFA4	2019-10-14 11:20	45	36.8	32.7	3.6 (3.3 - 7.9)	0.2 - 46.9	27.5 (27.3 - 27.7)	22.8 - 28.2	92.7 (90.7 - 94.9)	24 - 100
SFA5	2019-10-15 13:17	45	60.3	55.0	3.8 (3.7 - 4)	0.02 - 63.8	27.8 (27.8 - 27.9)	19.9 - 28.4	91.3 (90.9 - 93.6)	9.4 - 99
SFA6	2019-10-18 09:53	45	67.2	62.4	1.9 (1.7 - 7.2)	0.01 - 62.4	27.5 (27.3 - 27.8)	20.9 - 28.7	98.7 (94.8 - 100)	6.4 - 100
SFA7	2019-10-27 11:13	35	38.7	33.4	2.2 (2.1 - 3)	0 - 46.5	27.8 (27.7 - 27.8)	25.5 - 28.2	95.1 (93.9 - 95.2)	46.8 - 99
SFA8	2019-10-31 10:13	45	18.9	13.3	2.9 (2.5 - 3.1)	1.6 - 37.5	28.1 (28.1 - 28.2)	27.1 - 28.3	93.2 (92.6 - 93.3)	62.2 - 97.9
SFA9*	2019-11-04 14:07	35	6.1	NA	2.4 (1.4 – 11.1)	0.6 – 33.9	28.4 (28.1 – 28.9)	27.3 - 29.1	94 (93.5 – 94.8)	82.3 - 100

*Eliminated from analyses due to short tag attachment duration; IQR = Interquartile Range

Diel Habitat Use

After combining water column profiles of depth, temperature and oxygen across all fish, the calculated thermocline (ΔSST 0.8°C) occurred at a depth of 31.3 ± 3.8 m, the oxycline (90% oxygen saturation) at 27.7 ± 2.7 m, and the hypoxic boundary (60-65% oxygen saturation) at 39.8 ± 2 m (figure 3-1A, 3-1D).

In general, blue marlin and sailfish spent most of their time in the upper mixed layer of the water column, though there were differences in depth use between day and night for each species. During the day, blue marlin mean depth was 5.3 ± 8.4 m with a maximum depth of 55 m (blue marlin 8). Blue marlin spent 88% of the day at depths of 0-10 m, and 96% of their time shallower than 30 m, in water temperatures of 27-28° C (90% of time), and at oxygen saturation levels of 90-100% (90% of time; Figure 3-1B, 3-1C). During daylight hours, blue marlin descended below the thermocline and oxycline 3% and 5% of their time, respectively, with 2.8 % of time spent around the thermocline (27-31 m; Figure 3-2B). Less than 1% of their time was spent below the hypoxic boundary. At night, blue marlin average depth was 4.7 ± 6.6 m with

90% of time spent between 0-10 m, 95% of time at water temperature between 27 and 28° C and 90% of time at oxygen saturation levels of 90-100% (Figure 3-1). Diving at night was less common, as blue marlin descended below the thermocline 2% of the time, below the oxycline 3% of the time, and below the hypoxic boundary < 0.5% of the time. When blue marlin descended below the mixed layer, they typically experienced Delta T of < 2°C, and Delta O_2 of < 10% O_2 saturation (Figure 3-2 C, D). Maximum Delta T and maximum Delta O_2 experienced were 8.5°C and 85% O_2 saturation, respectively.

Sailfish were more vertically active than blue marlin, yet also the spent most time within the mixed layer. During daylight hours, sailfish mean depth was 7.7 ± 12.4 m, with a maximum depth of 67.9 m (sailfish 3). Sailfish spent the majority (84%) of their daylight hours from 0-10 m depth, at water temperatures of 27-28°C (85%) and at oxygen saturation levels of 90-100% (76%; Figure 3-1E, 3-1F). During daylight hours, sailfish descended below the thermocline 10% of the time, below the oxycline 11% of the time, and below the hypoxic boundary 6% of the time, but showed an increase in proportion of time spent near the hypoxic boundary (~38 m; Figure 3-2B). Sailfish average depth at night was 6.1 ± 8.5 m, with 87% of time spent within 0-10 m, 94% of time in 27-28°C water and 81% of time at oxygen saturation levels of 90-100%. At night, sailfish descended below the thermocline 3% of the time, below the oxycline 5% of the time, and below the hypoxic boundary < 1% of the time. Maximum Delta T and Delta O_2 experienced by sailfish were 7.8°C and 87% O_2, respectively (Figure 3-2 C, D).

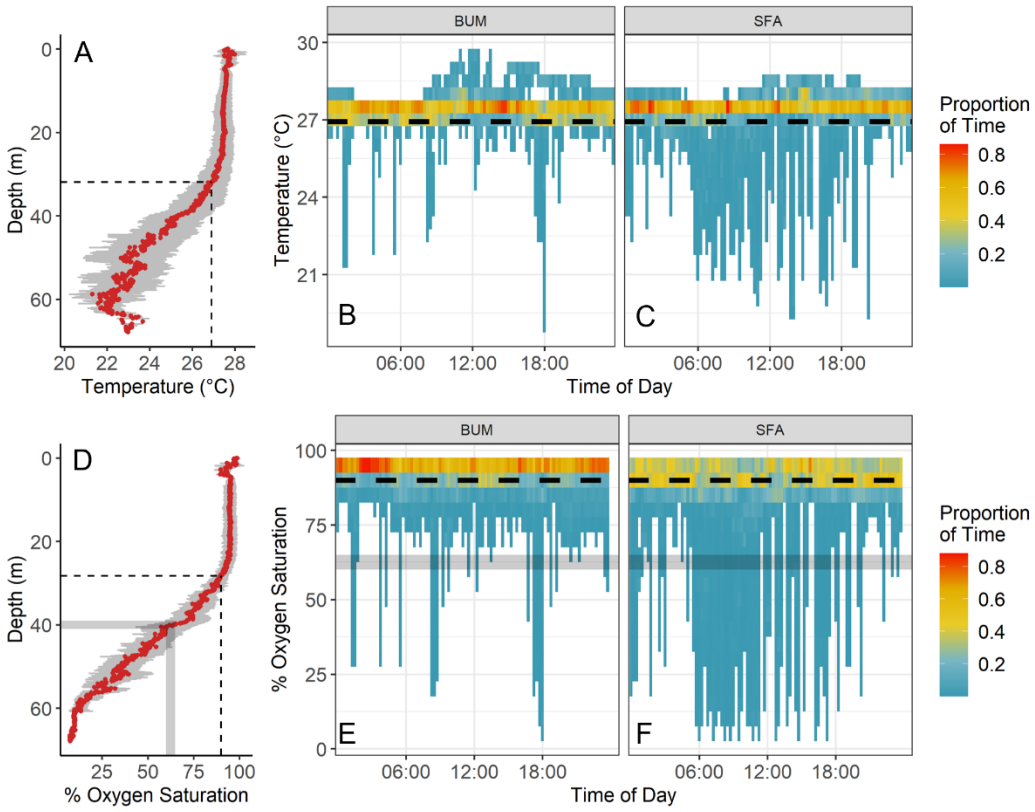

Figure 3-1. Vertical habitat characteristics and diel patterns in temperature and dissolved oxygen use. (A) Mean water column profiles of depth and temperature and (D) depth and % oxygen saturation measured from tagged fish (red) with grey shading indicating ±1 SD across all tags. (B, C) indicate mean time spent at temperature (0.5° bins) and (E, F) % oxygen saturation (5% bins) for blue marlin (blue marlin) and sailfish (sailfish). Dashed lines indicate the thermocline temperature in A-C and the oxycline % oxygen concentration in D-F. Shaded regions in D-F indicate the estimated % oxygen concentration of the 3.5 mL L^{-1} hypoxic boundary threshold. BUM = blue marlin, SFA = sailfish.

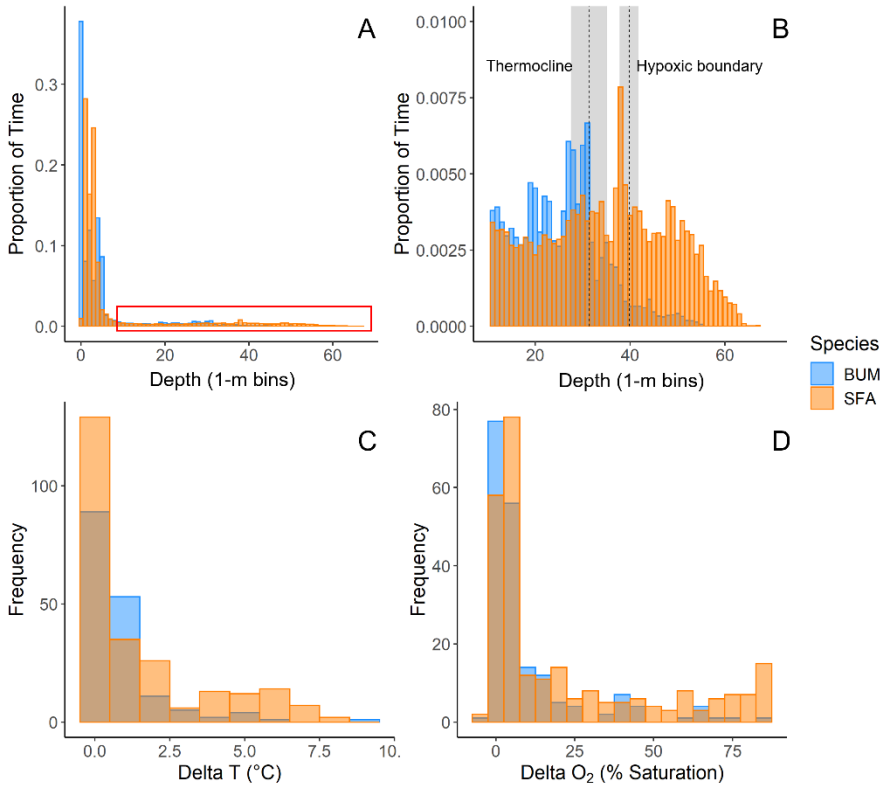

Figure 3-2. Vertical daytime distribution and minimum temperatures and % oxygen saturation experienced during dives by blue marlin (BUM) and sailfish (SFA). Percent time spent at 1-m depth intervals during daytime hours in (A), with (B) zoomed in on the tail of (A; red outline) to highlight increases near vertical habitat fronts. In B, vertical dotted lines and grey shading indicate the mean ± 1 SD depth of the thermocline and hypoxic boundary as determined *in situ* by biologging tags (see methods). (C) Minimum temperatures experienced relative to the mixed layer (Delta T; °C) and (D) % oxygen saturation relative to the mixed layer (Delta $\%O_2$ saturation) during dives.

Dive shape

A total of 176 blue marlin dives and 231 sailfish dives were classified. Upon visual inspection of the different dive shapes and previous knowledge of the diving behavior of pelagic fishes, the optimal number of dive shapes (clusters) for blue marlin and sailfish were selected as three and five, respectively (see Supplemental Figure S1). Both species displayed U, V, and W dive shapes, but sailfish also exhibited long-ascent (LA) and long-descent (LD) dive shapes (Figure 3-3). U dives featured a descent and ascent of similar duration separated by an extended bottom phase, while V dives lack the extended bottom phase. LD dives had a descent phase that lasted most of the dive, a limited bottom phase, and short ascent. LA dives had a short descent phase, a limited bottom phase, and an ascent that lasted most of the dive. W dives were

characterized by a rapid descent, followed by one or more small-scale vertical movements within the bottom phase of the dive, and a rapid ascent (Figure 3-3; Table 3-2).

Environmental and behavioral characteristics among dive shapes differed within blue marlin ($F_{(22,312)} = 10.34$, $p < 0.001$) and sailfish ($F_{(44,856)} = 7.78$, $p < 0.001$). U dives were the most common dive shape for blue marlin (51%) and sailfish (34%), followed by V dives in blue marlin (30%) and LA dives in sailfish (32%). For blue marlin, dives with an extended bottom phase (U and W) were deeper, during which fish experienced lower mean temperatures and oxygen concentrations than V dives (Table 3-2). Dive duration and bottom time were the longest during W dives, but neither ODBA, maximum ODBA nor TBF differed among dive shapes for blue marlin (Table 3-2). Sailfish displayed a greater variety of dive shapes than blue marlin, but in both species U and W dives were longer, deeper, colder and to lower oxygen saturation than other dive shapes (Table 3-2). Sailfish W dives had the deepest average and maximum depths of any dive shape for either species, and were also the longest duration dives performed by sailfish (Table 3-2).

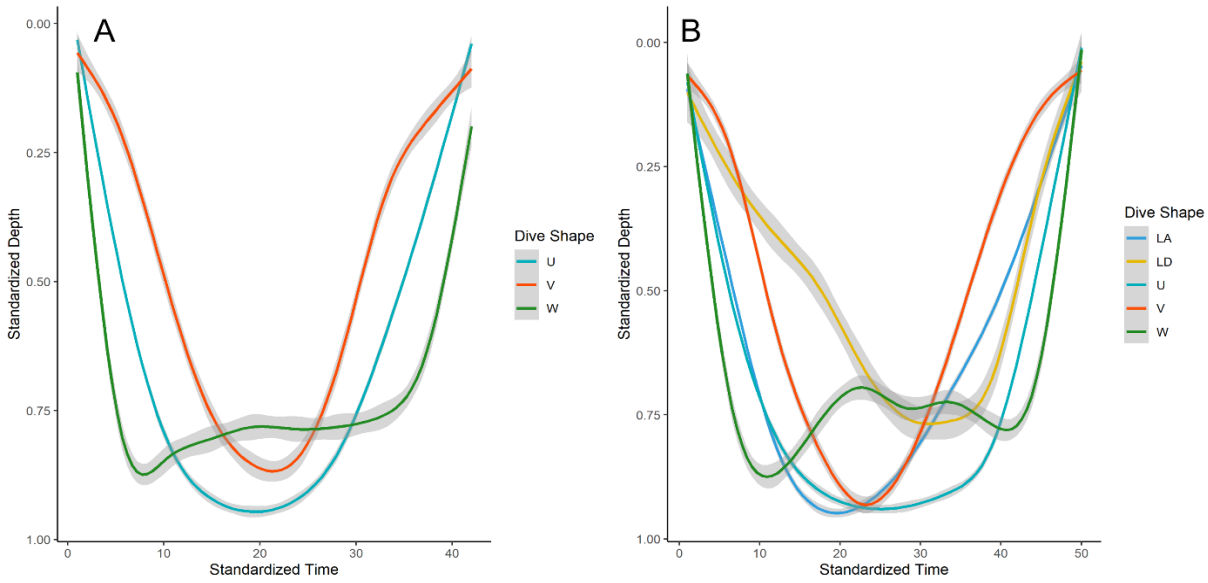

Figure 3-3. Smoothed dive shapes (solid lines) determined by hierarchical clustering of standardized dive profiles for blue marlin (A) and sailfish (B).

Table 3-2. Summary statistics (mean ± SD) for the dive shapes identified via hybrid hierarchical k-means clustering for blue marlin and sailfish. Statistical results are from a multivariate analysis of variance (MANOVA) of dive-shape characteristics. Values followed by the same letter are not significantly different at the 0.05 significance level, using a Games-Howell post-hoc test for pairwise comparisons.

Blue Marlin														
Dive		MANOVA												
Shape	n	F (df)	*P*	Mean Depth	Max Depth	Temperature	% Oxygen Saturation	Descent Rate	Ascent Rate	Duration (min)	Bottom Time (min)	ODBA	Max ODBA	TBF
U	89	(22,312) 10.34	< 0.001	17.8 ± 6.1 *a*	26 ± 10.1 *a*	27.3 ± 0.6 *a*	93 ± 7 *a*	0.13 ± 0.05 *a*	0.11 ± 0.03 *a*	10.9 ± 4.7 *a*	5.2 ± 2.5 *a*	0.061 ± 0.007 *a*	0.22 ± 0.24 *a*	0.51 ± 0.07 *a*
V	52			12.1 ± 4.8 *b*	21.8 ± 10.8 *b*	27.6 ± 0.3 *b*	95 ± 3 *b*	0.22 ± 0.21 *b*	0.17 ± 0.13 *b*	5.5 ± 4 *b*	1.6 ± 1.3 *b*	0.078 ± 0.04 *a*	0.38 ± 0.67 *a*	0.57 ± 0.2 *a*
W	35			18.9 ± 7.9 *a*	26 ± 11.5 *b*	27.2 ± 0.6 *a,b*	92 ± 8 *a*	0.15 ± 0.06 *a, b*	0.1 ± 0.04 *a*	22.7 ± 15.5 *c*	9.5 ± 7.5 *c*	0.064 ± 0.03 *a*	0.31 ± 0.32 *a*	0.53 ± 0.14 *a*
Sailfish														
LA	73	(44,856) 7.78	< 0.001	17.2 ± 8 *a*	25.5 ± 14.1 *a*	27.3 ± 0.9 *a*	89 ± 10 *a*	0.17 ± 0.09 *a*	0.13 ± 0.07 *a*	7.2 ± 4.6 *a*	2.9 ± 1.8 *a*	0.046 ± 0.01 *a*	0.22 ± 0.27 *a*	0.64 ± 0.06 *a*
LD	18			17.9 ± 6.9 *a*	34.1 ± 14.5 *a,b*	27.3 ± 0.6 *a*	89 ± 9 *a*	0.2 ± 0.09 *a*	0.45 ± 0.6 *a*	7.9 ± 4.8 *a,b*	1.7 ± 1.8 *a,b*	0.059 ± 0.03 *a*	0.29 ± 0.25 *a*	0.64 ± 0.12 *a*
U	78			25.5 ± 9.1 *b*	35.3 ± 13.5 *b*	26.7 ± 1.3 *b*	82 ± 15 *a,b*	0.16 ± 0.09 *a*	0.2 ± 0.4 *a,b*	12.3 ± 5.2 *c*	6.9 ± 3.2 *c*	0.05 ± 0.03 *a*	0.41 ± 1.4 *a*	0.62 ± 0.09 *a*
V	35			15.2 ± 6.9 *a*	26.4 ± 13.2 *a*	27.3 ± 0.7 *a*	90 ± 10 *a*	0.24 ± 0.13 *a, b*	0.23 ± 0.15 *b*	4.5 ± 3.9 *a,b*	1.3 ± 0.9 *a,b*	0.057 ± 0.02 *a,b*	0.27 ± 0.3 *a*	0.69 ± 0.1 *a,b*
W	27			30.9 ± 10 *b*	45.3 ± 15.9 *b,c*	26.1 ± 1.4 *b*	74 ± 16 *b*	0.19 ± 0.05 *a*	0.2 ± 0.08 *b*	18.7 ± 10.1 *d*	6.9 ± 4.8 *c*	0.056 ± 0.01 *a,b*	0.27 ± 0.13 *a*	0.66 ± 0.07 *a*

Path tortuosity and video

Physical water column characteristics (temperature, % oxygen saturation, depth) and dive shape were examined to determine their influence on fish path tortuosity. Because blue marlin and sailfish are visual predators, only daytime dives were used. Path tortuosity was different among dive shapes for both species (blue marlin Kruskal-Wallis $\chi^2 = 25.3$, df = 2, $p < 0.001$; sailfish $\chi^2 = 25.8$, df = 4, $p < 0.001$). Pairwise comparisons revealed blue marlin dive tortuosity was greatest for W dives, followed by U dives and V dives (Supplemental Table S1) and sailfish dive tortuosity was greatest for W and U dives, followed by LA dives (Supplemental Table S2).

The first principal component (PC1) of depth, ambient water temperature and ambient % oxygen saturation explained 79% of variance, and the second principal component (PC2) explained 11.5% of variance so both were included in candidate GAMMs. Large and similar loadings on PC1 for depth (0.57), temperature (-0.57) and oxygen (-0.59) indicate that each variable was an important contributor to PC1, and that increasing values of PC1 indicate deep, cold, and oxygen poor water. Loadings were similarly large on PC2 for depth (-0.71) and temperature (-0.7), but not oxygen (-0.001), such that increases in PC2 are indicative of shallower but cold water.

Blue marlin, path tortuosity was best described by the model that included the interaction of water temperature and dive shape, which explained 51.8% of deviance of path tortuosity (Supplemental Table S3). Blue marlin exhibited increased tortuosity at low temperatures during U and W dives; tortuosity increased during the coldest portion (below ~22 °C) in U dives (Figure 3-4a) and was elevated in W dives starting at the thermocline (~27 °C) and extending into colder water (Figure 3-4b). Tortuosity was not impacted by temperature during V dives.

The best fitting model for sailfish path tortuosity included PC1, PC2 and dive shape, explaining 58.9% of deviance (Supplemental Table S4). Path tortuosity was low at the lowest PC1 values, corresponding to movements near the surface (Figure 3-5A, C). However, sailfish path tortuosity increased at and adjacent to the hypoxic boundary. For example, sailfish tortuosity increased at PC1 values ranging from ~3.5 to 11 (Figure 3-5A), corresponding to a median depth of 39 m (IQR 36 – 45 m), temperature of 25.4 °C (IQR 24.2 - 26.2 °C) and % oxygen saturation of 65% (IQR 50 – 76%). Similarly, sailfish tortuosity increased along PC2 values of 2 – 3 (Figure 3-5B), corresponding to a similar median depth of 41 m (IQR 2-51 m), temperature of 22.4 °C (IQR 21.6 – 25.3 °C) and oxygen saturation of 48% (IQR 29 – 90%).

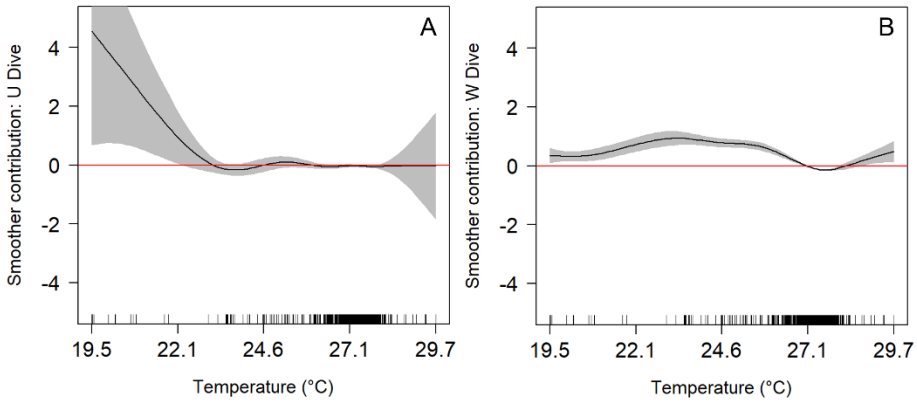

Figure 3-4. Response curves from the best-fit general additive mixed model (black solid line) for blue marlin tortuosity by dive shape. Shaded areas represent 95% confidence limits and positive values on y-axis (above red line) indicate increased tortuosity by blue marlin. Ticks on x-axis denote values for which there are data. V-dives are omitted because there was no relationship.

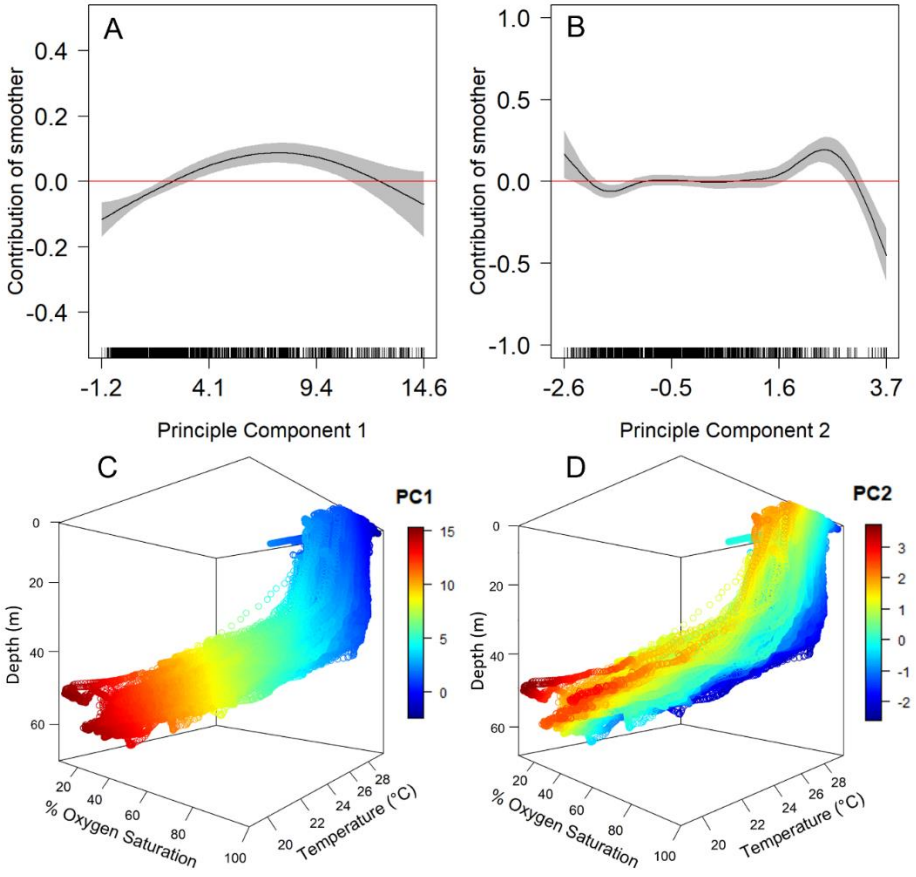

Figure 3-5. (A-B) Response curves from the best-fit general additive mixed model (black solid line) for sailfish path tortuosity. Shaded areas represent 95% confidence; positive values on y-axis (above red line) indicate increased tortuosity by sailfish. (C-D) Principal component scores (values given by color scale) as distributed in coordinates of co-located depth, water temperature, and dissolved oxygen saturation.

In total, we obtained 156 h of video footage (81 h blue marlin and 75 h sailfish), which captured interactions with con- and heterospecifics. For example, video enabled identification of high activity periods, or when other animals were present in the field of view of the animal carrying the tag package. During sailfish tag deployments, other sailfish were encountered on numerous occasions both at the surface and at depth, indicating behaviors expressed by the tagged individual were shared among untagged fish (Figure 3-6). No con- or heterospecific interaction was observed in any blue marlin footage. Furthermore, video footage showed very little visible light past ~50 m during daylight hours (Figure 3-6).

Repetitive diving below the hypoxic boundary during W-dives was common among sailfish. This behavior was characterized by rapid descents to below the hypoxic boundary where the fish would remain for a short period, return to just above the hypoxic boundary for a short period where percent oxygen saturations were high, and then dive back down below the hypoxic boundary for another brief period (Figure 3-6). This behavior was often performed one or more times before returning to the surface (Figure 3-6).

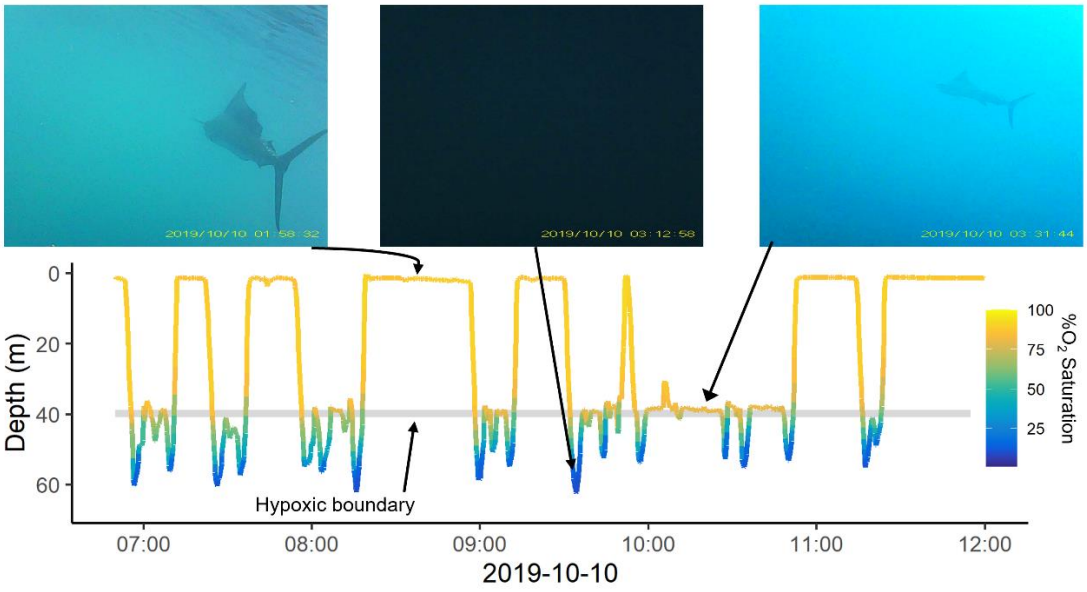

Figure 3-6. Excerpt of diving behavior from sailfish 3's full dataset. Video cameras were used to identify periods of conspecific interaction and ambient light, inset images across top panel. In the bottom panel depth is color coded to % oxygen saturation from the animal-borne oxygen sensor, with the gray horizontal line representing the hypoxic boundary (60 – 65% oxygen saturation).

Discussion

Despite blue marlin and sailfish being ubiquitous in tropical and subtropical pelagic waters, and their economic and ecological importance, most information relating to their habitat

use comes from course-scale satellite transmitting tags (Braun et al., 2015). As such, their fine-scale diving and foraging behavior, and interaction with environmental features has lagged behind other pelagic predators (e.g., sharks and tunas; but see Arostegui et al., 2022). This information is hindered by the challenges associated with direct observation of billfish behavior due to their cryptic nature and inability to be maintained in captivity. Here, we combined a suite of biologging technologies to document the fine-scale habitat use of blue marlin and sailfish in the vertically compressed ETP. Further, we report on a previously undocumented behavior that may be widespread among highly mobile marine predators, and an important component of their behavior and foraging success.

We found substantial evidence of vertical habitat compression due to the sharp and simultaneous declines in both temperature and dissolved oxygen concentration at shallow (~30-40 m) depths. Hypoxia and low temperatures are known to limit the horizontal and vertical distribution of istiophorid billfish, with a synergistic effect when they act in concert (Prince et al., 2010; Carlisle et al., 2017). For example, blue marlin in the central Pacific made shallower dives in regions where both oxygen and temperature were limiting at depth, but less so when only one was limiting (Carlisle et al., 2017). Due to cardiac temperature thresholds, istiophorid billfish maximum diving depths are predicted to be limited by a temperature difference relative to the surface mixed layer of 8°C (ΔT 8°C), rather than absolute water temperature (Brill et al., 1993). Our results are consistent with this finding for both species, with minimum maximum ΔT of 7.8°C for sailfish and 8.5°C for blue marlin.

Contrary to temperature, absolute oxygen concentration should limit dive depth regardless of surface oxygen levels. Species that share similar physiology, gill morphology, and respiratory mode to istiophorid billfish have been shown to experience physiological stress when dissolved oxygen (DO) decreases below 3.5 mL L^{-1} (Bushnell and Brill, 1991; Wegner et al., 2010), which occurred at ~40 m during the study period. However, of the fish that dove past these depths, they did not remain there for extended periods, even during long duration dives. Marlin and sailfish often remained at or near the 3.5 mL L^{-1} isopleth (38 – 40 m), and made periodic, brief forays below the isopleth (Figures 3-1, 3-2, 3-6). While sustained activity at these oxygen levels is not possible, blue, black (*Istiompax indica*) and striped marlin (*Kajikia audax*) have been observed to make brief 'spike' dives to depths with DO < 3.5 mL L^{-1} in the Eastern Tropical Atlantic and Indian Ocean, where oxygen minimum zones also exist near the surface

(Prince et al., 2010; Rohner et al., 2022). These findings suggest that the 3.5 mL L^{-1} boundary is not an absolute barrier to istiophorid vertical movements, but limits diving (Prince et al., 2010; this study). It should be noted that Rohner et al. (2022) and Prince et al. (2010) used climatological modeled oxygen data, suggesting caution when interpreting oxygen levels actually experienced. Here, we confirm via animal-borne oxygen sensor measurements that tagged billfish move into water with ambient oxygen concentrations < 3.5 mL L^{-1} for brief periods.

Motivations for diving in marine predators have been linked to several interacting factors, including energy conservation, behavioral thermoregulation, navigation, and foraging (Carey et al., 1990; Thompson et al., 1991; Klimley et al., 2002; Gleiss et al., 2011). For example, by moving both horizontally and vertically, animals may reduce energy consumption while simultaneously increasing prey encounter rate without substantially increasing distance traveled (Andrzejaczek et al., 2020). Variable dive shapes, which have been observed in a wide range of pelagic predator taxa (Beck et al., 2003; Seminoff et al., 2006; Kerstetter et al., 2011) may also serve various purposes. V and U dives are among the most common and are thought to correspond to transiting and/or prey searching (V dives), or prey patch exploitation (i.e., foraging; U dives). However, U dives were the most common dive shape exhibited here for blue marlin and sailfish (51% and 34%, respectively), yet only one foraging attempt was caught on video. Therefore, rather than prey patch exploitation, we hypothesize that pelagic predators performing U dives (where dive depth is much shallower than bottom depth) are more likely searching for prey higher in the water column (i.e., looking for silhouettes) or searching along features that congregate prey (e.g., thermocline, pycnocline). Due to the high temporal resolution data obtained here, we identified additional dive shapes not yet reported for billfish, including W, LD and LA. LA dives were the second most common dive shape exhibited by sailfish (Table 3-2), suggesting sailfish often perform slow and shallow ascents, likely searching for prey in surface waters from below. Like U dives, W dives are proposed to be foraging dives in seabirds and pinnipeds (Bailleul et al., 2007; Halsey et al., 2007), and we provide evidence below of a similar function for billfish in the ETP.

The preferred prey of blue marlin and sailfish in the ETP (e.g., carangids, clupeids, scombrids) are subjected to the same vertical habitat restrictions as istiophorid billfish (Evans et al., 1981; Prince and Goodyear, 2006). Because many of these prey species are diel vertical

migrators (Luo et al., 2000; Yasuda et al., 2018), and ram ventilation is limited by the upper margins of oxygen minimum zones (Bianchi et al., 2013), the abundance of these prey fish increases around this oxygen boundary during daylight hours (Bertrand et al., 2006; Bertrand et al., 2010). For example, in Pacific Nicaraguan waters, thread herring (*Opisthonema libertate*) biomass was found to be highest immediately above the 3–4 mL L^{-1} DO isopleth during daylight hours (Ehrhardt and Fitchett, 2006). For blue marlin and sailfish, path tortuosity was highest during U and W dives at depths near the thermocline and the 3–4 mL L^{-1} DO isopleth. Blue marlin path tortuosity was high at cold temperatures during U dives, and below the thermocline during W dives. Sailfish path tortuosity was also greatest during U and W dives and displayed a peak in tortuosity at a median depth of 39 m and median oxygen saturation of 65% (~3.4 mL L^{-1}), which are remarkably similar to the calculated hypoxic boundary (39.8 ± 2 m; 60-65% O_2 saturation). Straight line movement is the most energetically efficient form of travel, and optimal search strategies should continue in straight lines unless the potential benefits of turning offset the cost (Wilson et al., 2013b). Tortuous movements are known to occur during prey searching behavior and have been linked to increased foraging success in many marine animals (Austin et al., 2006; Adachi et al., 2017). As such, based on path tortuosity and physical characteristics of each dive type, we propose that V, LD, and LA dives (low tortuosity) were transiting and passive prey searching, while U and W dives (high tortuosity) were active prey searching and foraging dives near vertical habitat fronts with increased prey abundance.

The propensity for sailfish to repeatedly descend below the hypoxic boundary during the bottom phase of W dives suggests these descents are intentional (e.g., Figure 3-6). We propose this behavior represents a foraging tactic where sailfish briefly dive below the hypoxic boundary (and by extension, below the prey) and search for prey silhouettes backlit by downwelling surface light. Istiophorids possess several adaptations supporting this hypothesis. For example, the marlin eye is acutely adapted for sensitivity at low light levels such as those experienced during deep foraging dives in the ETP (Figure 3-6; Fritsches et al., 2003b). Similarly, high retinal cell density and the three visual pigments necessary for trichromatic color vision are only present together in the ventral part of the eye, indicative of color vision and high visual acuity in the visual field above and ahead of the animal (Fritsches et al., 2003a). Furthermore, istiophorids possess a thermogenic organ beneath the brain, adjacent to the eyes that generates and maintains elevated temperatures relative to ambient (Block, 1986). During vertical movements into cold

low-light waters, heating by this organ results in the maintenance of high speed of vision, and up to an order of magnitude greater temporal resolution of the eyes compared to their prey (Fritsches et al., 2005). Together, these features suggest that marlin and sailfish are specially adapted to hunt in cool, dark waters and ambushing prey from below. A conceptual framework for the evolution, maintenance, and importance of ambush predation in the pelagic environment supports this, suggesting that due to the lack of vertical structure to hide behind, many pelagic predators must attack from below (Bakun, 2022a; Bakun, 2022b). Bluefin tuna have been observed to make frequent bounce dives through the thermocline during the day in highly stratified waters, suggested to be foraging dives (Kitagawa et al., 2000) but may be an example of the behavior we describe here. Indeed, the only predation attempt caught on video during tag deployments was during a W dive of sailfish 6, where the pursuit was initiated at depth in cold, low oxygen, dimly-lit water (57 m; 22°C; 10-20% O_2 saturation), featured a rapid ascent (reaching 3.1 ms^{-1}), and ended at the surface (Logan et al., 2023).

Conclusions

Here we have provided insights into predator diving and foraging behavior along vertical fronts as well as how these predators respond to and use low oxygen environments. Given the limited spatial coverage of this study in relation to the large geographic range of these species, it is likely the behaviors exhibited here are not characteristic to these species as a whole, and foraging strategies may be plastic depending on the environmental conditions experienced. However, we believe that new high-resolution biologging methods, such as those used here, will reveal the use of vertical fronts by marine predators is more widespread than currently represented in the literature. Further, the collective influence of climate change, global deoxygenation and shoaling oxygen minimum zones will reduce available habitat throughout the world's oceans and affect many marine organisms through direct and indirect pathways. Because apex predators play important roles in structuring and regulating ecosystems, understanding how they will respond to and use low oxygen environments and the habitat fronts they create, as we have presented here, is needed so real-time management strategies are best equipped to respond to changing open-ocean ecosystems.

CHAPTER IV

HUNTING BEHAVIOR OF A SOLITARY SAILFISH *ISTIOPHORUS PLATYPTERUS* AND ESTIMATED ENERGY GAIN AFTER PREY CAPTURE

This chapter was originally published as Logan R.K., Luongo S.M., Vaudo J.J., Wetherbee B.M., Shivji M.S. (2023) Hunting behavior of a solitary sailfish *Istiophorus platypterus* and estimated energy gain after prey capture. *Scientific Reports* 13:1484. doi.org/10.1038/s41598-023-28748-0

Abstract

Foraging behavior and interaction with prey is an integral component of the ecological niche of predators but is inherently difficult to observe for highly mobile animals in the marine environment. Billfishes have been described as energy speculators, expending a large amount of energy foraging, expecting to offset high costs with periodic high energetic gain. Surface-based group feeding of sailfish, *Istiophorus platypterus,* is commonly observed, yet sailfish are believed to be largely solitary roaming predators with high metabolic requirements, suggesting that individual foraging also represents a major component of predator-prey interactions. Here, we use biologging data and video to examine daily activity levels and foraging behavior, estimate metabolic costs, and document a solitary predation event for a 40 kg sailfish. We estimate a median active metabolic rate of 218.9 ± 70.5 mgO_2 kg^{-1} h^{-1} which increased to 518.8 ± 586.3 mgO_2 kg^{-1} h^{-1} during prey pursuit. Assuming a successful predation, we estimate a daily net energy gain of 2.4 MJ (5.1 MJ acquired, 2.7 MJ expended), supporting the energy speculator model. While group hunting may be a common activity used by sailfish to acquire energy, our calculations indicate that opportunistic individual foraging events offer a net energy return that contributes to the fitness of these highly mobile predators.

Introduction

Predator–prey interaction is a cornerstone of ecology, intrinsically linked to individual fitness and population level dynamics of both predators and prey, and ultimately relates to the evolutionary success of populations (Stephens and Krebs, 1986; Krebs et al., 1995). Foraging behavior and energetic gains and losses associated with foraging, predation and consumption impinge directly on the physiology and behavior of all animals (Stephens and Krebs, 1986; Brown et al., 2004). For many large pelagic marine predators, the rarity of observations of predatory events and challenges of documenting hunting behavior have hindered understanding of behavioral strategies, trophic relationships and associated energetics in marine ecosystems (Watanabe and Goldbogen, 2021).

Istiophorid billfishes (marlins) are known for their unique morphology, power, and high-speed predatory potential. In sailfish (*Istiophorus platypterus*), an epipelagic predator inhabiting tropical to subtropical waters worldwide (Collette and Graves, 2019), group hunting behavior is well documented and involves multiple individuals herding a school of prey fish (i.e. bait ball) toward the water's surface. Individual sailfish enter the school and laterally slash their bill in an attempt stun/kill prey for consumption (Domenici et al., 2014; Herbert-Read et al., 2016; Kurvers et al., 2017). This tactic is facilitated by morphological adaptations including the bill, a streamlined body shape, enlarged dorsal fin that acts to stabilize the sailfish as it slashes the bill, and a caudal fin with a high aspect ratio enabling bursts of speed of up to 8.8 ms^{-1} during bait-ball interactions (Marras et al., 2015).

Outside of bait-ball hunting aggregations, however, sailfish are believed to be solitary roaming predators. Because of the difficulty of maintaining sailfish in captivity, energetic requirements have not been directly measured for adults (but see Idrisi et al., 2003), yet due to various life history and morphological traits, sailfish are presumed to have a high metabolic rate (Block, 1986; Wegner et al., 2010; Killen et al., 2016b). As such, in addition to bait-ball hunting events, solitary sailfish likely need to capitalize on encounters with prey to support this high metabolic rate. However, due to an elusive pelagic lifestyle, individual sailfish hunting behavior has not been documented and energetic relationships of such events have not been investigated. Recently, sailfish have been described as lateralized predators, preferring to attack from one side (right or left) of their prey, depending on the individual (Kurvers et al., 2017). This is theorized to have evolved via group hunting, where multiple sailfish take turns attacking a bait-ball,

preventing the prey from learning which side the attack may come from (Kurvers et al., 2017). However, in one-on-one predator-prey interactions, lateralization could be costly to the predator's hunting success because it would increase the predictability of where an attack will come from (Rogers, 2002; Ghirlanda et al., 2009). Lack of information on hunting behavior and energetics of such events, which have direct bearing on ecological interactions of top predators, results in a limited understanding of their role in oceanic ecosystems and overall fitness (Collette et al., 2011).

Knowledge of daily activity levels and energy dynamics of hunting behavior and foraging events in billfishes and other top marine predators will improve our understanding of behavioral alterations associated with changing environmental conditions, such as warming and deoxygenation (Whitlock et al., 2015). Because activity level has a major impact on an animal's energy budget, there is a need for estimates of active metabolism of large aquatic predators to inform future energetic and trophic models. Here, using an animal-borne datalogger with video, we report on the daily activity of an individual sailfish in the Eastern Tropical Pacific over a 24 h period. We describe an observation of a foraging event, the lateralization of the strikes during the event, and place these events in the broader context of the daily activities of this individual to estimate the daily net energetic benefit of the predation event.

Methods

The sailfish (estimated to be 40 kg by an experienced captain, and calculated to be 1.85 m per Wares and Sakagawa (1974)) was caught via rod and reel from a recreational sportfishing vessel using standard trolling gear with natural bait off the Pacific coast of southeast Panama (7.53 N, 78.53 W). The fish was brought alongside the vessel and a custom-designed biologging tag package was attached to the dorsal musculature with two umbrella dart anchors (Figure 1). Once both anchors were securely imbedded in the muscle, the tag was cinched against the body using two galvanic timed releases (International Fishing Devices Inc., Northland, New Zealand) and a cable tie. Only six minutes elapsed from when the fish was hooked to release. The tag consisted of an acceleration data logger (tri-axial accelerometer, magnetometer and gyroscope recording at 100 Hz), depth and temperature sensors, and a small turbine-based fluid speed sensor recording at 1 Hz (OpenTag 3.0, Loggerhead Instruments, Sarasota, FL; see supplemental data for swim speed calibration; Figure S1, S2). Finally, the tag package contained a miniaturized video camera (68 mm × 21 mm × 22 mm; Little Leonardo, Tokyo, Japan) and a

Smart Position and Temperature tag (SPOT-363A; Wildlife Computers, Redland WA) to aid in package recovery. The entire tag package was 18 x 7 cm at the leading edge, increasing to 18 x 10.5 cm at the trailing edge, weighing 335 g in air (~0.8% of sailfish body weight; 4-10% of the frontal cross-sectional area of the sailfish; see supplemental methods for estimated drag). Upon dissolution of the galvanic timed releases, the package released from the fish and was recovered at sea using a UHF handheld receiver (AOR AR8200, USA).

Data were analyzed using Igor Pro v. 8.0.4.2 (Wavemetrics, Inc., Lake Oswego, OR, USA) and RStudio v. 1.4.1106 (R Core Team, 2019). The static component of acceleration was calculated using a 3-s box smoothing window on the raw acceleration data as this was visually determined to sufficiently remove the dynamic component of acceleration (Shepard et al., 2008). Tag attachment angle was corrected by rotating the raw acceleration data such that the X and Y axis had a mean of zero. Body pitch was then calculated from the anterior-posterior axis of the static component of acceleration. The lateral axis of the gyroscope was used to determine directionality of the strikes during the predation event, and calculate the tailbeat frequency using a continuous wavelet transformation (Sakamoto et al., 2009; Andrzejaczek et al., 2019). Finally, a compass heading and reconstructed track were generated from the magnetometer data using the *magHead* function in the gRumble R package (White et al., 2017).

To estimate the sailfish's active metabolic rate and energy expenditure, we used the relationship between oxygen consumption and swim speed for adult dolphinfish (*Coryphaena hippurus*) (Stieglitz et al., 2016), with the assumption this relationship is consistent across fish length (Weihs, 1973; Beamish, 1978). See section 2 of the supplementary material for a detailed description of why dolphinfish was chosen as the proxy species and further description of metabolic rate calculations. Oxygen consumption (MO_2; $mgO_2\ kg^{-1}\ h^{-1}$) was estimated using the equation $\log(MO_2) = [cU + \log(d)]$, where c and d are the slope and intercept of the logarithmic regression, and U is the swim speed of the sailfish (BLs^{-1}; Figure S3). MO_2 was calculated continuously for every speed measurement throughout the 24 hours from the sailfish tag data, and we then took the inverse log of MO_2 and corrected for mass of the dolphinfish (M_D) in (Stieglitz et al., 2016) to obtain VO_2 ($mgO_2\ h^{-1}$). Oxygen consumption for the 40 kg sailfish was then calculated using the equation:

$$\mathrm{AMR_E} = VO_2 \left(\frac{\mathrm{M_S}}{\mathrm{M_D}} \right)^{\mathrm{b}}$$

where AMR_E is the estimated active metabolic rate ($mgO_2\ h^{-1}$), $\dot{V}O_2$ is the oxygen consumption at each swim speed, b is the mass scaling exponent, and M_S is the sailfish mass (kg). AMR_E was corrected for temperature using a Q_{10} of 1.83 (Clarke and Johnston, 1999; Killen et al., 2010) and was made mass-specific using the estimated mass of the sailfish (see section 2 of the supplementary information for more detail).

Because a proxy species was used for the calculation, we allowed for variation in parameter estimates of b, c, d, and M_D with an iterative approach (10,000 iterations) and randomly sampled values for these parameters from normal distributions with means and standard deviations equal to published values where available (Table S1, Figure S4). The median of all iterations was used as the AMR_E, with the interquartile range (IQR) used to represent a range of possible AMR_E values (Figure S5). Sailfish swim speed (ms^{-1}) was converted to BL s^{-1} after estimating the length using previously published length – mass relationships (Wares and Sakagawa, 1974). To calculate energy expenditure of the day and the predation event, we used an oxy caloric coefficient of 0.013 kJ mgO_2^{-1} (Elliott and Davison, 1975), and 8.03 kJ g^{-1} wet weight for *Auxis* spp. energy content (Abitia-Cardenas et al., 1997). Prey mass of 635 g was estimated for a 35 cm TL tuna using the length-weight relationship for *A. thazard* (Froese and Pauly, 2010).

Results and Discussion

We used a custom designed biologging tag package with onboard video to describe a 3D high-resolution pursuit between a solitary sailfish and an individual small tuna in open water, representing the first time such an interaction has been documented. The sailfish was tagged at 09:53 on 18 October 2019, and the tag package remained attached to the sailfish for 67 h. However, analyses here are limited to the 24 h period in which the predation event took place (19 October – 20 October; ~14 h after tagging and ~9 h after post-release recovery (Logan et al., 2022)) because this coincides with the time period the video camera was recording during daylight hours (on at 0600, off at 1800, sunrise and sunset, respectively) enabling us to ground-truth acceleration signals. Biologging data and accompanying video show the sailfish performing oscillatory dives between the surface and depths of 40 – 50 m during daylight hours. At night, fewer dives were performed and the sailfish generally remained within the top 10 – 20 m of the water column (Fig. 4-1A), leading to a greater range of temperatures experienced during the day (day 20.9 – 27.9°C; night 26.5 – 28.2°C). Due to the temperature dependence of the estimated

active metabolic rate (AMR_E), the cooler temperatures at depth led to a reduced AMR_E during daylight hours (212.9 ± 89.1 mgO_2 kg^{-1} h^{-1}) compared to night (224.7 ± 44.4 mgO_2 kg^{-1} h^{-1}). Additionally, AMR_E initially increases with depth due to increased swim speeds during diving (Fig. 4-1B), until the thermocline is reached in the 30 – 40 m depth bin, at which point AMR_E decreases with further increased depth (Fig. 4-1B, C). However, due to thermal inertia of large-bodied fishes (Holland et al., 1992; Nakamura et al., 2015; Watanabe et al., 2021), it is possible that the sailfish's body retained heat during the short (14.7 ± 1.7 min) excursions below the thermocline and did not drop to ambient temperature. As such, the metabolic rate calculated at depth may be underestimated with the temperature correction performed here. For example, during the dive in which the predation event occurred (Figure 4-1; Table 4-1), if body temperature was assumed equivalent to surface temperature throughout the dive, estimated metabolic rates would increase by 18% compared to if the metabolic rates were temperature corrected according to the tag's external temperature reading (Table S2). Yet, because the majority (> 90%) of time over the 24 hours was spent above the thermocline, the temperature correction has little impact on the daily calculated AMR_E and subsequent energy expenditure (<1% difference; Table S3).

The sailfish exhibited greatly reduced tailbeat activity and swimming speeds ($\leq$0.25 ms^{-1}; 0.14 BLs^{-1}) when near the surface (Figure 4-1), characteristic of basking behavior exhibited by swordfish and other istiophorid billfishes (Sepulveda et al., 2018; Rohner et al., 2022). Basking is believed to serve thermoregulatory purposes (Rohner et al., 2022), but would also serve to reduce energy expenditure for billfishes facilitated by their swim bladders (Block et al., 1992b). Indeed, basking behavior observed here led to a significant reduction in AMR_E (186.6 ± 3.1 mgO_2 kg^{-1} h^{-1}; T_{37520} = -158.3, $p < 0.001$), when compared to active swimming behavior with strong and sustained tailbeats during dives (261.1 ± 91.1 mgO_2 kg^{-1} h^{-1}; mean swimming speed 0.56 ± 0.2 ms^{-1}; 0.3 ± 0.1 BL^{-1}).

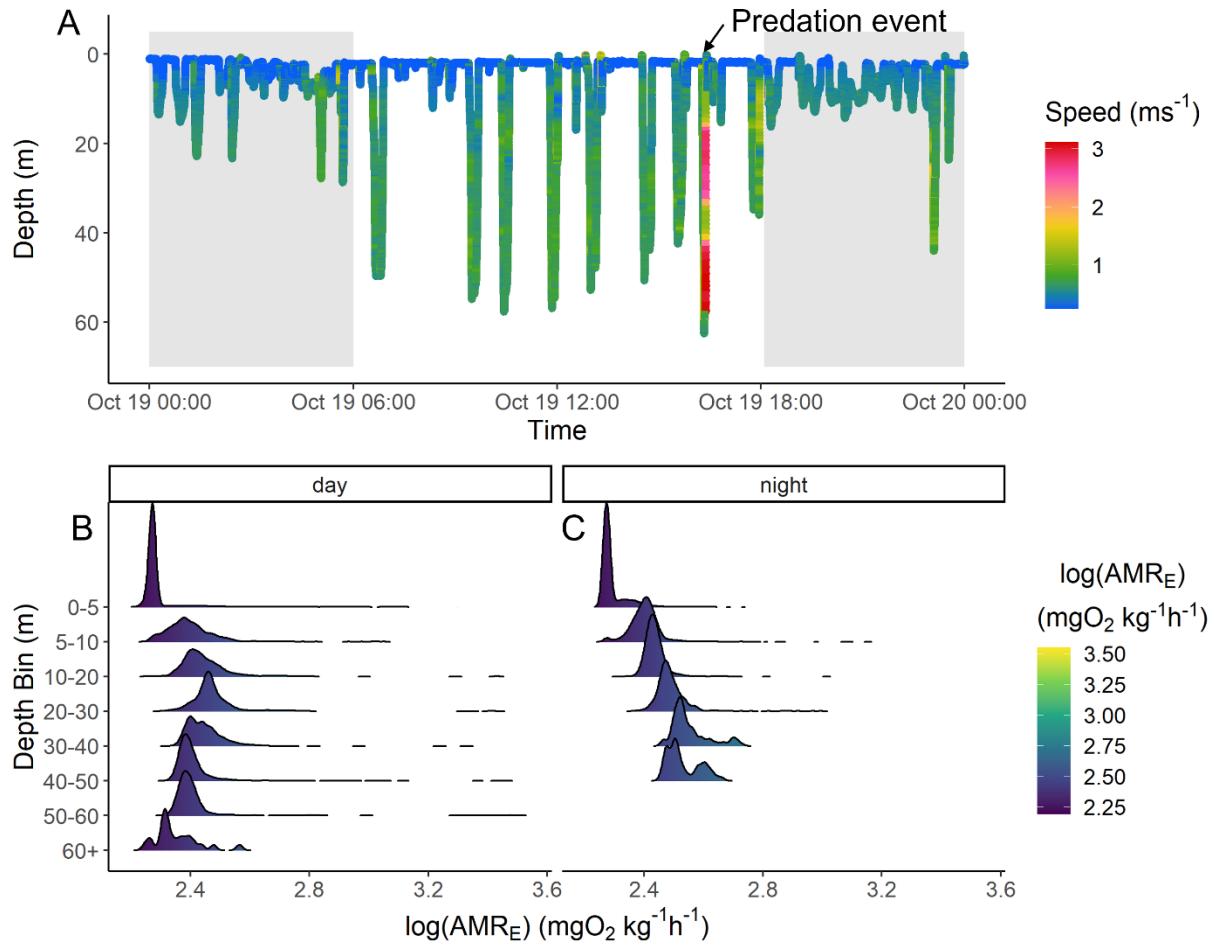

Figure 4-1. Summary 24 h depth, speed and estimated metabolic rate. Depth trace over the course of the 24 h monitoring period in A, and binned depth density histograms of the log transformed median estimated active metabolic rate (AMR_E; $mgO_2\ kg^{-1}h^{-1}$) for day and night periods in B and C, respectively. In A, color of the depth trace indicates speed (ms^{-1}), and shaded regions represent night hours. The dive in which the predation event took place is indicated with an arrow in A.

Table 4-1. Summary statistics for dives performed by the sailfish during daylight hours compared to the dive in which the predation event took place. Values are presented as mean ± SD where applicable.

	Daytime Dives (n=8)	Pursuit Dive
Duration (min)	14.7 ± 1.7	6.7
Max Depth (m)	50 ± 7.5	62.4
Descent Rate (ms^{-1})	0.18 ± 0.03	0.24 ± 0.21
Ascent Rate (ms^{-1})	0.17 ± 0.03	1.3 ± 0.43
Max AMR_E ($mgO_2\ kg^{-1}\ h^{-1}$)	498.2 ± 92.2	3,283.8
Energy used (MJ)	0.03 ± 0.003	0.04

The dive in which the predation event took place occurred roughly 31 h into the 67 h that the tag package remained attached to the sailfish (Figure 4-2A). At 16:15 2019-10-19, the sailfish dove from the surface to a depth of 62.4 m with a mean (± SD) vertical velocity (VV) of 0.24 ± 0.21 ms^{-1}, where it remained for a short period before ascending to ~40 m (Figure 4-2B). During the ascent, multiple possible prey items are seen in the video (Figure 4-2C), and there was a brief increase in speed and tailbeat frequency (TBF), before the fish's depth leveled off for ~2 minutes. The fish then dove again to 57.5 m, where visible light almost completely attenuated (Figure 4-2D), and a change in locomotory mode from slow and steady swimming to rapid and forceful tailbeats occurred, beginning a rapid ascent (VV = 1.3 ± 0.43 ms^{-1}), with speeds reaching 3.1 ms^{-1} (1.7 body lengths [BL] s^{-1}), and a body pitch of 54.6 ± 16.1° (maximum of 77.6°; Figure 4-2B). It should be noted that due to the rapid ascent, the temperature readout of the tag lagged behind true ambient temperature (e.g., temperature of the descent compared to temperature of the ascent; Figure 4-2B). Summary statistics for the dive in which the predation event took place are compared to all other daytime dives (Table 4-1).

The prey that was pursued during the predation event first became visible in the video when the sailfish reached the surface (Figure 4-2E). The sailfish made several attempts to capture the prey, often breaking the surface of the water (supplemental video). From the video, the prey appeared to be a frigate or bullet tuna (*Auxis thazard brachydorax* or *A. rochei eudorax*), both of which are common in the region and known sailfish prey (Collette and Aadland, 1996; Collette and Graves, 2019). During the rapid ascent and while at the surface, TBF and swimming speed remained high (1.6 ± 0.7 Hz and 1.7 ± 0.84 ms^{-1}, respectively, maximum of 2.92 ms^{-1}). At the surface, there were frequent changes in heading and the tuna appeared in the video several times (Figure 4-2B; Figure 4-3D; supplemental video). At one point, the tuna engaged in antipredator behavior presumably to 'hide', by swimming very close to the sailfish in front of the video camera along its right flank and out of its peripheral view (Figure 4-2F; supplemental video). After roughly 60 s from the tuna's first appearance on camera, the video and biologging data suggest that the sailfish caught the tuna or terminated the pursuit (Figure 4-2B). Because the mouth of the sailfish was not in view of the camera, it is uncertain if the foraging attempt was successful; however, the tuna was last seen directly in front of the sailfish, immediately followed by a headshake (often characteristic of swallowing / prey

manipulation for shallowing) and resumption of slow steady swimming by the sailfish, suggesting it was successful (Figure 4-2B; supplementary video).

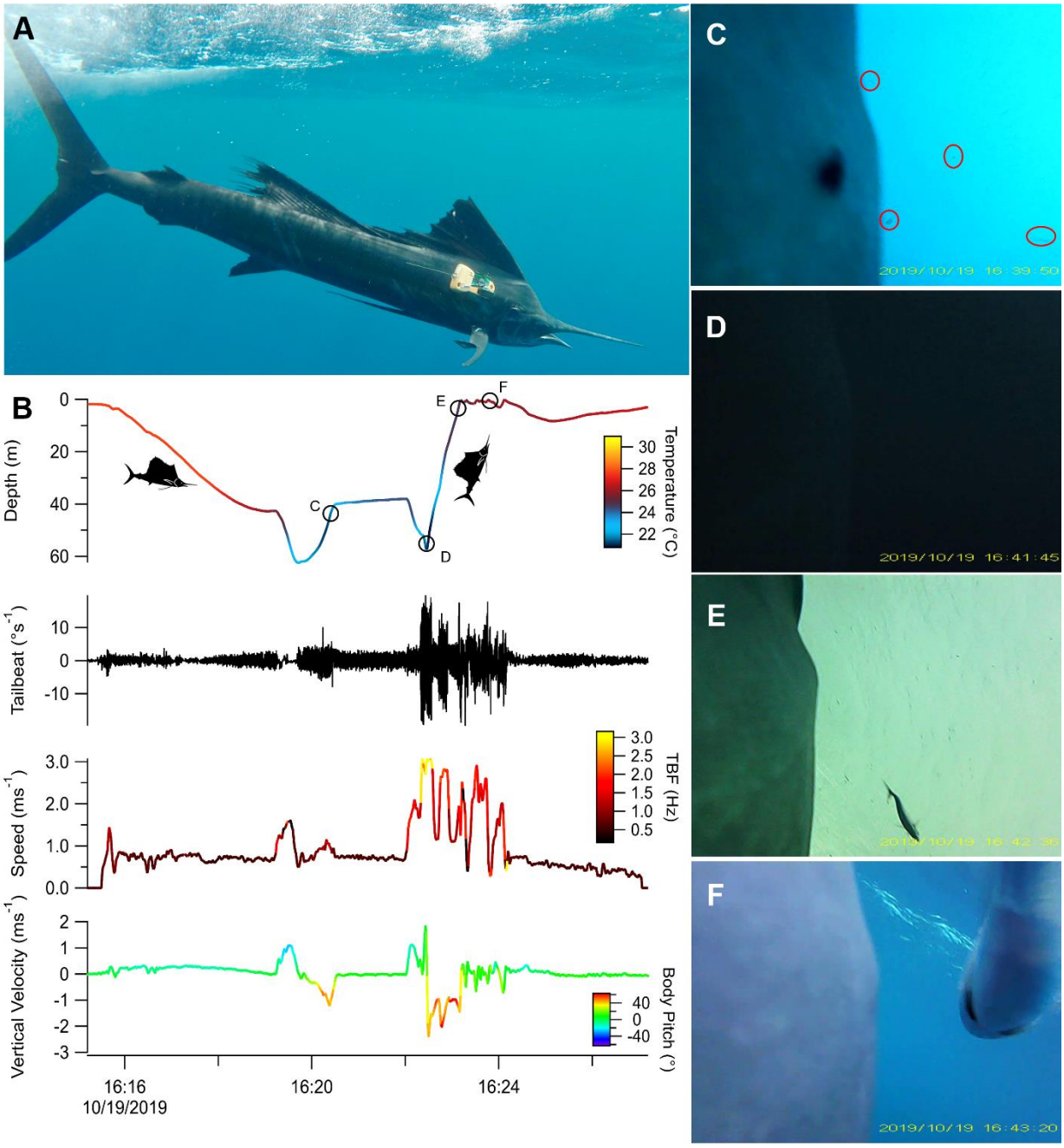

Figure 4-2. Sailfish activity before, during and after the predation event. (A) Biologging float package attached to sailfish. (B) Depth, temperature, tailbeats (°sec^{-1}), speed (ms^{-1}), tailbeat frequency (TBF; Hz), vertical velocity (ms^{-1}) and body pitch angle (°) of the dive in which the event occurred. The timing and depth associated with each image (C-F) are identified by circles on the depth profile in (B). (C) The sailfish ascends from 60 m and encounters multiple potential prey items, outlined in red. (D) The available light is notably low at this depth (~60 m) and decreases rapidly with depth to almost zero light. (E) First observation of the prey pursued in the predation event. (F) Prey possibly attempting to 'hide' from the sailfish by swimming very close to it during the pursuit.

During the 24 h monitoring period, the mean estimated active metabolic rate (AMR_E; $mgO_2\ kg^{-1}\ h^{-1}$) of the sailfish for the median, 25th and 75th percentile of all 10,000 iterations were 218.9 ± 70.5, 156.6 ± 48.4 and 307 ± 102.9 $mgO_2\ kg^{-1}\ h^{-1}$, respectively (Table 4-2, Figure S5). Using the median iteration, during the dive where the predation occurred, mean AMR_E was 518.8 ± 586.3 (IQR 361.2 – 748.5) $mgO_2\ kg^{-1}\ h^{-1}$ (Figure 4-3). From this median iteration, we estimate that 2.7 MJ (IQR 1.9 – 3.8 MJ) of energy was expended over the course of the day, where only 1% (0.04 MJ) was expended during the pursuit (Table 4-2). The estimated energy content of the tuna was 5.1 MJ (calculated from Abitia-Cardenas et al., 1997), and assuming a successful predation outcome, this encounter resulted in a net energy gain of 2.4 MJ (IQR 1.3 – 3.2 MJ). However, if this predation was unsuccessful, the cost of this pursuit was only 1% of the energy expenditure for the day. For a sailfish of this size, this daily energy expenditure equates to the required consumption of ~0.5 tuna d^{-1} to sustain daily metabolic costs estimated for the median AMR_E (218.9 $mgO_2\ kg^{-1}\ h^{-1}$; see section 3 of supplemental methods for details of calculation).

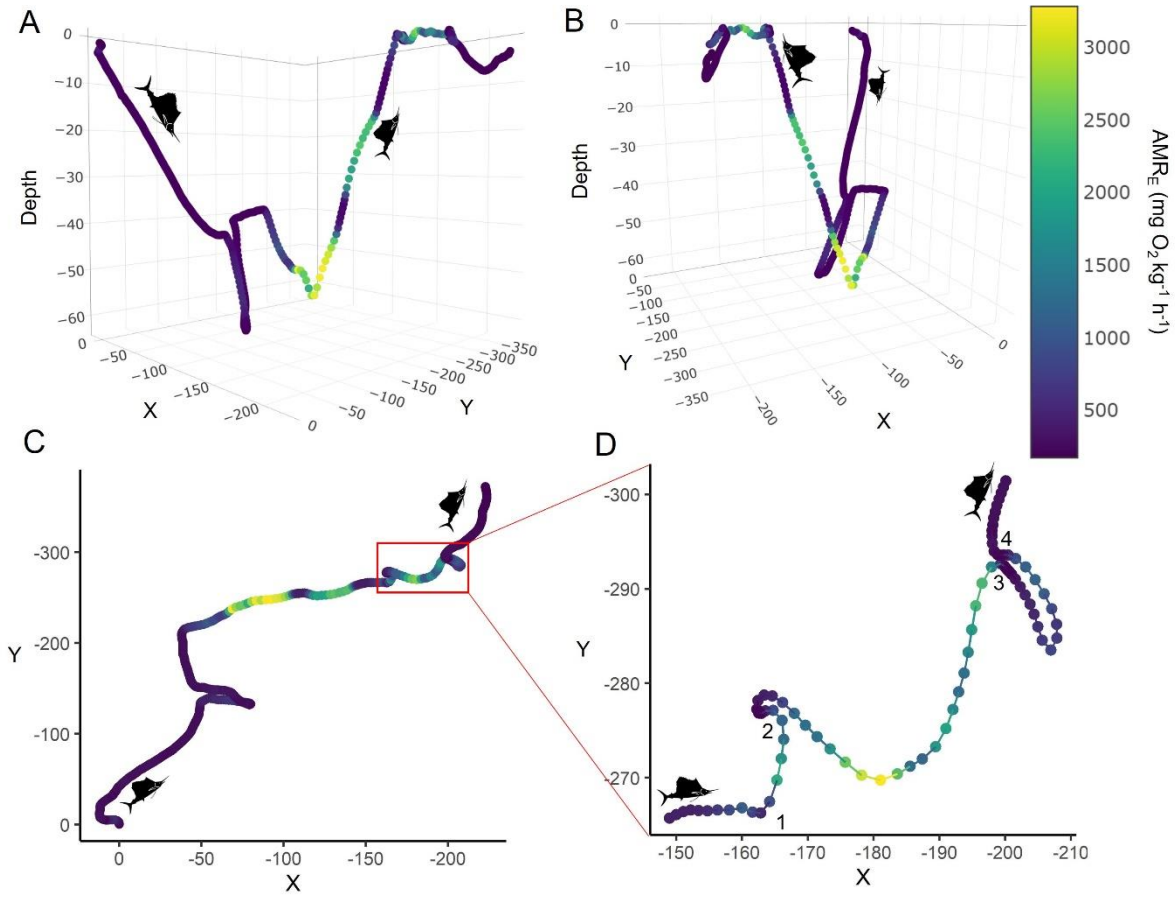

Figure 4-3. Reconstructed 3D track of the dive in which the predation event took place, colored by the mean estimated active metabolic rate (AMR_E; mgO_2 kg^{-1} h^{-1}). A and B show different perspectives of the depth profile and associated changes in heading, while C and D are overhead (2D) views, with D being zoomed in on the pursuit portion of the encounter at the surface. The numbers displayed in D represent the approximate location of the sequential capture attempts as seen in the supplemental footage. Sailfish silhouettes indicate direction of travel.

Table 4-2. Estimated active metabolic rate (AMR_E; mgO_2 kg^{-1} h^{-1}) and energy expenditure (MJ) during the dive where the predation occurred, and overall for the 24 h period for the 25th, median and 75th percentile of the 10,000 iterations of randomly sampled parameter estimates used to calculate AMR_E. Values are presented as mean ± SD where applicable.

	Pursuit Dive		Overall	
	AMR_E	MJ	AMR_E	MJ
25th Percentile	361.2 ± 390.4	0.03	156.6 ± 48.4	1.9
Median	518.8 ± 586.3	0.04	218.9 ± 70.5	2.7
75th Percentile	748.5 ± 874.3	0.06	307 ± 102.9	3.8

We observed a willingness for this individual sailfish to attack from both sides of the prey. The alternating pattern of positive, negative, positive, negative (Figure 4-4A – D) in the

degrees of rotation s^{-1} immediately prior to and during each strike suggests that the sailfish attacked from different sides of the prey in each successive strike. This behavior is in contrast to Kurvers et al. (Kurvers et al., 2017), who found that during bait-ball hunting aggregations with multiple sailfish, individual sailfish were strongly lateralized and would tend to strike from the same side each time they entered the bait-ball. Attacking from different sides in succession is a novel finding for sailfish and suggests behavioral plasticity within different hunting scenarios (i.e., group vs solitary hunting). In one-on-one hunting situations when neither the predator nor prey are in a group setting, it would benefit the predator to avoid lateralization because the prey can quickly learn any tendencies the predator may have (McGhee et al., 2013; Kurvers et al., 2017).

One noteworthy finding was the relatively low maximum speed attained by the sailfish (3.1 ms^{-1}) during the encounter with the prey. Sailfish are believed to be one of the fastest swimming fish (Lane, 1941; Block et al., 1992b) with recent estimates suggesting maximum speeds of 8.2 – 8.3 ± 1.4 ms^{-1} (Marras et al., 2015; Svendsen et al., 2016), and predator–prey interactions might be expected to be events where maximal speeds are exhibited by both predator and prey (Marras et al., 2015). However, because it is the prey that sets the speed, timing of accelerations, decelerations and turns, the predator is either reacting to or predicting what the prey will do to enable trajectory interception and capture which culminates in lower than maximal predator speeds during pursuits (Wilson et al., 2018). Additionally, theoretical models predict that if prey are slower than their predators, as is the case here (Domenici, 2001), prey should avoid the predator by turning rather than trying to increase separation by travelling as fast as possible (Wilson et al., 2018). For example, Wilson et al. (Wilson et al., 2018) demonstrated that if a prey animal is moving as fast as possible, it cannot accelerate forwards and must either turn or continue straight, making its movements more predictable and interceptable, compared to a slow moving prey that has more escape options (speed up, slow down, turn) and is therefore less predictable. As such, sailfish and their prey are likely avoiding maximum speeds during one-on-one encounters in open water (Chittka et al., 2009). Additionally, previous studies have noted that cursorial and avian predators will slow down in the moments prior to an attack to increase maneuverability when in close proximity to prey (Combes et al., 2013; Wilson et al., 2013a; Wilson et al., 2018), which was also observed here (Figure 4-4E – H). Furthermore, morphological adaptations of sailfish (i.e., the bill) can be moved through the water more rapidly

than the whole body (Marras et al., 2015), potentially allowing sailfish to rely on these morphological 'weapons', rather than speed during one-on-one pursuits to increase capture success rates. We also observed a tendency of the sailfish to approach the prey from below in each capture attempt (Figure 4-4I – L).

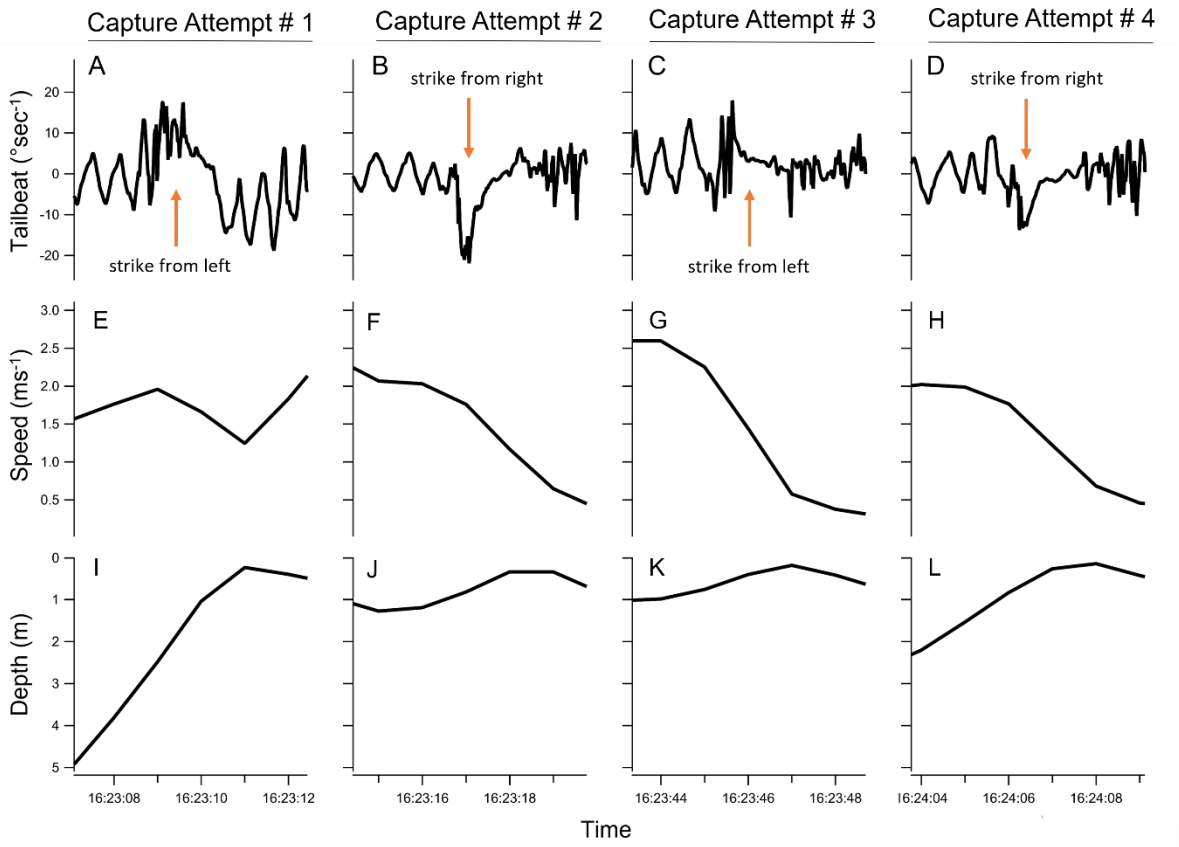

Figure 4-4. Zoomed in portions (1 sec intervals) of the tailbeat (°rotation sec^{-1}), speed (ms^{-1}) and depth (m) of the four different capture attempts (A-D, respectively) during the one-on-one pursuit (see supplemental video).

Direct observation of natural predation events by marine predators are rare (Papastamatiou et al., 2018; Andrzejaczek et al., 2019), particularly for pelagic fish predators where visual observation is difficult, prey is sparse, and feeding rates are low compared to that of marine mammals and seabirds (Papastamatiou et al., 2018). For the predation event presented here, based on the footage of potential prey items near the thermocline (Figure 4-2C; supplementary video), the observed increase in speed and TBF immediately prior to the rapid

ascent (Figures 4-2B; 4-3A), and the shorter than average dive time (Table 4-1), we propose that the prey item was encountered at depth, and chased to the surface (Domenici et al., 2014). Given the shallow thermocline and co-occurring oxycline present in the Eastern Tropical Pacific (Prince and Goodyear, 2006), and the potential for these features to concentrate prey (Derenbach et al., 1979; Stewart et al., 2019; Fortune et al., 2020), we hypothesize that oscillatory dives in the mixed layer are prey-searching dives to increase foraging opportunities (Nakamura et al., 2011). Due to their unique metabolic biochemistry suited to life in the open ocean, tunas and billfishes have long been described as energy speculators, gambling high and continual energy output, expecting to offset the costs with periodic high energetic gain events (Stevens and Neill, 1978; Brill, 1987; Dickson, 1995). The estimated energy gain of 2.4 MJ resulting from the prey encounter in the 24 h period described here is consistent with energy speculation behavior, but also suggests this sailfish would need to regularly forage on high energy prey to support its metabolic requirements. Because the video camera was only recording for the daylight hours of the 24 h period analyzed here, we cannot say if any other feeding events occurred during the remainder of the track; however, there were two other similar bursts of activity identified in the acceleration data during the following day prior to the tag releasing from the fish. As such, energy obtained from individual foraging events like that described here may be an important energy supply for the routine energy requirements of these high metabolic performers between opportunistic, large energy gain, group hunting bait-ball foraging events where multiple prey can be consumed in a short amount of time.

Conclusions

This biologger deployment yielded animal-borne video, triaxial acceleration, gyroscope and magnetometer data, and depth, temperature, and speed data of a rare predation event, along with a full 24 h period of behavioral and activity data providing a one-of-a-kind dataset for this top predator. We estimated a range of values in which this sailfish's active metabolic rate likely occurred (IQR 156 ± 48 to 307 ± 102, median 219 ± 70; $mgO_2\ kg^{-1}\ h^{-1}$ at 0.21 ± 0.1 BLs^{-1}; Table 2), and cursory interspecific comparisons suggest our estimates of metabolic rate fall within the range of expected values (Blank et al., 2007; Sepulveda et al., 2007; Payne et al., 2015; Anderson et al., 2022). However, it should be noted that because dolphinfish were used as the proxy species and they do not possess cranial endothermy as sailfish do, the estimates presented here are likely an underestimation. Furthermore, the measurements presented here are based on a

single sailfish, and individual variability in diving behavior would impact estimated metabolic costs. Undoubtedly, as new methods are developed to directly quantify oxygen consumption of large fishes (e.g., Payne et al., 2015), estimates of metabolic rate will become more accurate and will enable estimates for additional physiological measurements, such as aerobic scope and cost of transport. However, we provide the first detailed description of activity levels and hunting behavior of an individual free-ranging sailfish and estimate of the energetics of a rare predation event. These estimates suggest that while the energetic gains from this predation event were substantial compared to what was expended during the pursuit, the amount of energy burned in search of prey over the course of the day and night was considerable. Until methods to directly quantify metabolic costs of large pelagic predators are developed, the approach we have taken could be used as a starting point to inform future energetic and trophic models and improve our understanding of the role of these pelagic predators in our oceans.

Literature Cited

Abitia-Cardenas LA, Galvan-Magaña F, Rodriguez-Romero J. 1997. Food habits and energy values of prey of striped marlin, Tetrapturus audax, off the coast of Mexico. Fishery Bulletin:360-368.

Anderson J, Spurgeon E, Stirling B, May JI, Rex P, Hyla B, McCullough S, Thompson M, Lowe C. 2022. High resolution acoustic telemetry reveals swim speeds and inferred field metabolic rates in juvenile white sharks (Carcharodon carcharias). PLoS ONE 17.

Andrzejaczek S, Gleiss AC, Lear KO, Pattiaratchi CB, Chapple T, Meekan M. 2019. Biologging tags reveal links between fine-scale horizontal and vertical movement behaviours in tiger sharks (Galeocerdo cuvier). Frontiers in Marine Science 6:229.

Beamish F. 1978. Swimming capacity. In ‘Fish Physiology. Vol. VII’.(Eds WS Hoar and DJ Randall.) pp. 101–187. In: Academic Press: New York.

Blank JM, Farwell CJ, Morrissette JM, Schallert RJ, Block BA. 2007. Influence of swimming speed on metabolic rates of juvenile Pacific bluefin tuna and yellowfin tuna. Physiological and Biochemical Zoology 80:167-177.

Block BA. 1986. Structure of the brain and eye heater tissue in marlins, sailfish, and spearfishes. Journal of Morphology 190:169-189.

Block BA, Booth D, Carey FG. 1992. Direct measurement of swimming speeds and depth of blue marlin. Journal of Experimental Biology 166:267-284.

Brill RW. 1987. On the standard metabolic rates of tropical tunas, including the effect of body size and acute temperature change. Fisheries Bulletin 85:25-35.

Brown JH, Gillooly JF, Allen AP, Savage VM, West GB. 2004. Toward a metabolic theory of ecology. Ecology 85:1771-1789.

Chittka L, Skorupski P, Raine NE. 2009. Speed–accuracy tradeoffs in animal decision making. Trends in ecology & evolution 24:400-407.

Clarke A, Johnston NM. 1999. Scaling of metabolic rate with body mass and temperature in teleost fish. Journal of animal ecology 68:893-905.

Collette B, Carpenter K, Polidoro B, Juan-Jordá M, Boustany A, Die DJ, Elfes C, Fox W, Graves J, Harrison L. 2011. High value and long life—double jeopardy for tunas and billfishes. Science 333:291-292.

Collette B, Graves J. 2019. Tunas and billfishes of the world. Johns Hopkins University Press.

Collette BB, Aadland C. 1996. Revision of the frigate tunas (Scombridae, Auxis), with descriptions of two new subspecies from the eastern Pacific. Fishery Bulletin.

Combes S, Salcedo M, Pandit M, Iwasaki J. 2013. Capture success and efficiency of dragonflies pursuing different types of prey. Integrative and comparative biology 53:787-798.

Derenbach J, Astheimer H, Hansen H, Leach H. 1979. Vertical microscale distribution of phytoplankton in relation to the thermocline. Marine Ecology Progress Series 1:187-193.

Dickson KA. 1995. Unique adaptations of the metabolic biochemistry of tunas and billfishes for life in the pelagic environment. Environmental Biology of Fishes 42:65-97.

Domenici P. 2001. The scaling of locomotor performance in predator–prey encounters: from fish to killer whales. Comparative Biochemistry and Physiology Part A: Molecular & Integrative Physiology 131:169-182.

Domenici P, Wilson A, Kurvers R, Marras S, Herbert-Read JE, Steffensen J, Krause S, Viblanc P, Couillaud P, Krause J. 2014. How sailfish use their bills to capture schooling prey. Proceedings of the Royal Society B: Biological Sciences 281:20140444.

Elliott J, Davison W. 1975. Energy equivalents of oxygen consumption in animal energetics. Oecologia 19:195-201.

Fortune SM, Ferguson SH, Trites AW, Hudson JM, Baumgartner MF. 2020. Bowhead whales use two foraging strategies in response to fine-scale differences in zooplankton vertical distribution. Scientific reports 10:1-18.

Froese R, Pauly D. 2010. FishBase. In: Fisheries Centre, University of British Columbia.

Ghirlanda S, Frasnelli E, Vallortigara G. 2009. Intraspecific competition and coordination in the evolution of lateralization. Philosophical Transactions of the Royal Society B: Biological Sciences 364:861-866.

Herbert-Read JE, Romanczuk P, Krause S, Strömbom D, Couillaud P, Domenici P, Kurvers RH, Marras S, Steffensen JF, Wilson AD. 2016. Proto-cooperation: group hunting sailfish improve hunting success by alternating attacks on grouping prey. Proceedings of the Royal Society B: Biological Sciences 283:20161671.

Holland KN, Brill RW, Chang RK, Sibert JR, Fournier DA. 1992. Physiological and behavioural thermoregulation in bigeye tuna (Thunnus obesus). Nature 358:410-412.

Idrisi N, Capo TR, Luthy S, Serafy JE. 2003. Behavior, Oxygen Consumption and Survival of Stressed Juvenile Sailfish (Istiophorus platypterus) in Captivity. Marine and Freshwater Behavior and Physiology 36:51-57.

Killen SS, Atkinson D, Glazier DS. 2010. The intraspecific scaling of metabolic rate with body mass in fishes depends on lifestyle and temperature. Ecology letters 13:184-193.

Killen SS, Glazier DS, Rezende EL, Clark TD, Atkinson D, Willener AS, Halsey LG. 2016. Ecological influences and morphological correlates of resting and maximal metabolic rates across teleost fish species. The American Naturalist 187:592-606.

Krebs CJ, Boutin S, Boonstra R, Sinclair A, Smith J, Dale MR, Martin K, Turkington R. 1995. Impact of food and predation on the snowshoe hare cycle. Science 269:1112-1115.

Kurvers RH, Krause S, Viblanc PE, Herbert-Read JE, Zaslansky P, Domenici P, Marras S, Steffensen JF, Svendsen MB, Wilson AD. 2017. The evolution of lateralization in group hunting sailfish. Current Biology 27:521-526.

Lane F. 1941. How fast do fish swim. Country Life (London) 90:534-535.

Logan RK, Vaudo JJ, Lowe CG, Wetherbee BM, Shivji MS. 2022. High-resolution post-release behaviour and recovery periods of two highly prized recreational sportfish: the blue marlin and sailfish. ICES Journal of Marine Science 79:2055-2068.

Marras S, Noda T, Steffensen JF, Svendsen MB, Krause J, Wilson AD, Kurvers RH, Herbert-Read J, Boswell KM, Domenici P. 2015. Not so fast: swimming behavior of sailfish during predator–prey interactions using high-speed video and accelerometry. Integrative and comparative biology 55:719-727.

McGhee KE, Pintor LM, Bell AM. 2013. Reciprocal behavioral plasticity and behavioral types during predator-prey interactions. The American Naturalist 182:704-717.

Nakamura I, Goto Y, Sato K. 2015. Ocean sunfish rewarm at the surface after deep excursions to forage for siphonophores. Journal of Animal Ecology 84:590-603.

Nakamura I, Watanabe YY, Papastamatiou YP, Sato K, Meyer CG. 2011. Yo-yo vertical movements suggest a foraging strategy for tiger sharks Galeocerdo cuvier. Marine Ecology Progress Series 424:237-246.

Papastamatiou YP, Meyer CG, Watanabe YY, Heithaus MR. 2018. Animal-borne video cameras and their use to study shark ecology and conservation. Shark Research: Emerging Technologies and Applications for the Field and Laboratory:83-91.

Payne NL, Snelling EP, Fitzpatrick R, Seymour J, Courtney R, Barnett A, Watanabe YY, Sims DW, Squire Jr L, Semmens JM. 2015. A new method for resolving uncertainty of energy requirements in large water breathers: the 'mega-flume' seagoing swim-tunnel respirometer. Methods in Ecology and Evolution 6:668-677.

Prince ED, Goodyear CP. 2006. Hypoxia-based habitat compression of tropical pelagic fishes. Fisheries Oceanography 15:451-464.

R Core Team. 2019. R: A language and environment for statistical computing. In. Vienna, Austria: R Foundation for Statistical Computing.

Rogers LJ. 2002. Advantages and disadvantages of lateralization. Comparative vertebrate lateralization:126-153.

Rohner CA, Bealey R, Fulanda BM, Prebble CE, Williams SM, Pierce SJ. 2022. Vertical habitat use by black and striped marlin in the Western Indian Ocean. Marine Ecology Progress Series 690:165-183.

Sakamoto KQ, Sato K, Ishizuka M, Watanuki Y, Takahashi A, Daunt F, Wanless S. 2009. Can ethograms be automatically generated using body acceleration data from free-ranging birds? PLoS one 4.

Sepulveda C, Graham J, Bernal D. 2007. Aerobic metabolic rates of swimming juvenile mako sharks, Isurus oxyrinchus. Marine Biology 152:1087-1094.

Sepulveda CA, Aalbers SA, Heberer C, Kohin S, Dewar H. 2018. Movements and behaviors of swordfish Xiphias gladius in the United States pacific leatherback conservation area. Fisheries Oceanography 27:381-394.

Shepard EL, Wilson RP, Halsey LG, Quintana F, Laich AG, Gleiss AC, Liebsch N, Myers AE, Norman B. 2008. Derivation of body motion via appropriate smoothing of acceleration data. Aquatic Biology 4:235-241.

Stephens DW, Krebs JR. 1986. Foraging theory. Princeton University Press.

Stevens ED, Neill WH. 1978. Body temperature relations of tunas, especially skipjack. In: Hoar WS, Randall DJ, editors. Fish Physiology. New York: Academic Press. pp 315-359.

Stewart JD, Smith TT, Marshall G, Abernathy K, Fonseca-Ponce IA, Froman N, Stevens GM. 2019. Novel applications of animal-borne Crittercams reveal thermocline feeding in two species of manta ray. Marine Ecology Progress Series 632:145-158.

Stieglitz JD, Mager EM, Hoenig RH, Benetti DD, Grosell M. 2016. Impacts of Deepwater Horizon crude oil exposure on adult mahi-mahi (Coryphaena hippurus) swim performance. Environmental Toxicology and Chemistry 35:2613-2622.

Svendsen MB, Domenici P, Marras S, Krause J, Boswell KM, Rodriguez-Pinto I, Wilson AD, Kurvers RH, Viblanc PE, Finger JS. 2016. Maximum swimming speeds of sailfish and three other large marine predatory fish species based on muscle contraction time and stride length: a myth revisited. Biology open 5:1415-1419.

Wares PG, Sakagawa GT. 1974. Some Morphometrics of Billfishes From the Eastern Pacific Ocean. In: Shomura RS, Williams F, editors. Proceedings of the International Billfish Symposium. Kailua-Kona, Hawaii: NOAA Technical Report. pp 107-120.

Watanabe YY, Goldbogen JA. 2021. Too big to study? The biologging approach to understanding the behavioural energetics of ocean giants. Journal of Experimental Biology 224:jeb202747.

Watanabe YY, Nakamura I, Chiang W-C. 2021. Behavioural thermoregulation linked to foraging in blue sharks. Marine biology 168:1-10.

Wegner NC, Sepulveda CA, Bull KB, Graham JB. 2010. Gill morphometrics in relation to gas transfer and ram ventilation in high-energy demand teleosts: Scombrids and billfishes. Journal of Morphology 271:36-49.

Weihs D. 1973. Optimal fish cruising speed. Nature 245:48-50.

White CF, Moxley J, Jorgensen S. 2017. gRumble. In. https://github.com/MBayOtolith/gRumble.

Whitlock RE, Hazen EL, Walli A, Farwell C, Bograd SJ, Foley DG, Castleton M, Block BA. 2015. Direct quantification of energy intake in an apex marine predator suggests physiology is a key driver of migrations. Science Advances 1:e1400270.

Wilson AM, Hubel TY, Wilshin SD, Lowe JC, Lorenc M, Dewhirst OP, Bartlam-Brooks HL, Diack R, Bennitt E, Golabek KA. 2018. Biomechanics of predator–prey arms race in lion, zebra, cheetah and impala. Nature 554:183-188.

Wilson AM, Lowe J, Roskilly K, Hudson PE, Golabek K, McNutt J. 2013. Locomotion dynamics of hunting in wild cheetahs. Nature 498:185-189.

CHAPTER V

SEASONALLY MEDIATED NICHE PARTITIONING IN A VERTICALLY COMPRESSED PELAGIC PREDATOR GUILD

Abstract

The presence and diversity of top predators is critical for healthy ecosystem function and stability. As such, identifying the mechanisms by which sympatric top predators partition available resources in a habitat-limited environment can contribute to future community ecosystem conservation, given predicted widespread reductions in bio-available habitat. We quantified niche partitioning among three highly mobile, large pelagic predators, blue marlin (*Makaira nigricans*), black marlin (*Istiompax indica*), and sailfish (*Istiophorus platypterus*), in the vertically compressed (i.e., temperature and oxygen limited) habitat of the eastern tropical Pacific, using a decade of recreational fisheries data, multi-year satellite tracking with high-resolution vertical diving data, and stable isotope analysis. Fishery and three-dimensional spatial data suggested high overall spatial and temporal overlap among species, but seasonal and diel variability in vertical habitat use promoted spatial partitioning within the water column during periods of high prey abundance. Furthermore, isotopic data indicated low trophic overlap over long time scales, supporting differences in foraging behavior identified in diving data among these predators. Niche partitioning coupled with behavioral plasticity among this predator guild provides a mechanism for the maintenance of high predator species diversity in a spatially restricted habitat, and has important implications for how sympatric predators in other ocean regions may respond and adapt to further natural and human-driven environmental change.

Introduction

Within ecosystems, sympatric predators with similar ecological requirements may coexist by exhibiting some form of niche separation to reduce interspecific competition (Pianka, 1974; Schoener, 1974). Niche separation occurs in a variety of forms, and is often observed along spatial or temporal shifts in habitat use (Vanak et al., 2013; Karanth et al., 2017). Competitive interactions may be further reduced among sympatric predators via separation of their trophic axes (i.e., having different diets) (Croxall et al., 1997; McCauley et al., 2012; Browning et al., 2014). Because top predators can exert strong influences on ecological communities but are often the most anthropogenically impacted groups, identifying mechanisms by which resources are partitioned by sympatric predators contributes to species-specific conservation and management of marine ecosystems (Botsford et al., 1997; Pauly et al., 1998; Petchey et al., 1999).

Billfishes (family Istiophoridae) are highly migratory top predators in the pelagic environment yet seasonally co-occur in high abundances in coastal regions with narrow continental shelves (Nakamura, 1985; Torres Rojas et al., 2013; Varghese et al., 2014). One of these regions is the Pacific coast of Central America, known for high catch rates of multiple billfishes (e.g. Sailfish, *Istiophorus platypterus*, Blue Marlin *Makaira nigricans*, Striped Marlin, *Kajikia audax*, Black Marlin, *Istiompax indica*) (Miyabe and Bayliff, 1987; Pohlot and Ehrhardt, 2018; Marín-Enríquez et al., 2019). In Panama, recreational billfish catches are high during the dry season (December – April) when the Intertropical Convergence Zone (ITCZ) is pushed south by northerly trade winds, resulting in upwelling of cool, nutrient rich waters (Fiedler and Lavín, 2017). Surface chlorophyll concentration peaks during this time, creating a surge in surface productivity in the region (D'Croz and O'Dea, 2007). During the wet season (May – November), the trade winds relax, upwelling decreases, surface waters return to a warm, nutrient poor, low productivity state (D'Croz and O'Dea, 2007), and coastal billfish sightings decline (Haulsee et al., 2022). In addition to seasonal atmospheric variability, the eastern tropical Pacific (ETP) contains several interacting oceanographic features leading to a strong and shallow thermocline year-round, and a large naturally occurring oxygen minimum zone beneath the thermocline (Fiedler and Lavín, 2017). Seasonal upwelling causes this thermocline to shoal as shallow as 25-30 m (Xie et al., 2005). Because cold temperatures and hypoxic conditions below the thermocline cause a reduction of the bio-available habitat for high-oxygen demand species such as billfish

(Brill and Lutcavage, 2001), these predators are restricted to the mixed layer, a condition known as hypoxia-based habitat compression (Prince et al., 2010; Stramma et al., 2012).

While many studies have examined either movement patterns or trophic positions of various billfishes (Chiang et al., 2015; Lam et al., 2015; Lam et al., 2016; Carlisle et al., 2017; Rosas-Luis et al., 2017; Williams et al., 2017b), none have integrated spatial tracking and isotopic analysis to examine niche dynamics in this co-occurring predator guild. Blue marlin [hereafter BUM], black marlin [BAM] and sailfish [SFA] prefer similar water temperatures, and are similarly vertically restricted by low temperature and oxygen at depth, particularly in the ETP (Prince and Goodyear, 2006; Prince et al., 2010; Braun et al., 2015). In addition, the stomach contents of BUM and SFA landed in the ETP indicate a dominance (97% and 96.2%, respectively) of surface oriented teleost prey (e.g., *Auxis* spp.; Rosas-Luis et al., 2017; pers. obs.). Comparable blood heamatocrit and haemoglobin concentrations, and similar gill morphologies indicate that physiologically, limitations among billfishes could be similar (Wells and Davie, 1985; Dobson et al., 1986; Johnson, 1986; Davie, 1990). As such, interspecific interactions among these similar billfishes are likely high while occupying the vertically compressed ETP.

In seasonally dynamic habitats like the ETP, billfishes must cope with fluctuations in environmental conditions and resource availability that may increase interactions with other billfishes and other pelagic predators (Correa and Winemiller, 2014). Understanding how billfishes respond to environmental variability and periods of high and low prey abundance has important implications for how they may impact the pelagic ecosystem, but also for predicting how populations and communities will respond to larger scale climatic change (Carroll et al., 2021). For instance, global oxygen minimum zones are predicted to grow both vertically and horizontally, and hypoxia-based habitat compression will begin to affect new regions and new ecosystems (Laffoley and Baxter, 2019; Leung et al., 2019). As such, understanding the mechanisms of coexistence among the billfish guild in the ETP provides an opportunity to study how sympatric predators in other regions may respond and adapt to vertical habitat compression, and how the billfish complex in the ETP may fare in light of further environmental change.

Taken together, the seasonal resource availability, similar habitat preferences and diet, and physiological limitations suggest that BUM, BAM and SFA have the potential for high ecological niche overlap in the vertically compressed ETP. Here, we employ a combination of

methodological and data approaches using long-term recreational fishery data, multi-year horizontal telemetry tracking, high-resolution vertical movements data, and stable isotope analysis to better understand the spatial, temporal, and trophic mechanisms that facilitate coexistence of these closely related sympatric top predators.

Methods

Tagging and sample collection

BUM, BAM, and SFA were caught off the Pacific coast of southeast Panama (Table 4-1) based out of Tropic Star Lodge, Piñas Bay from November 2018 to February 2022 via rod-and-reel, trolling lures or natural bait. Each fish was brought alongside the vessel, assessed for physical trauma associated with capture, and its weight estimated by an experienced captain. A subset of these fish was tagged with a pop-up satellite archival transmitting tag (miniPAT, Wildlife Computers, Redmond WA, USA) anchored into the dorsal musculature using either an umbrella- or titanium-style dart. Tags were painted with an anti-fouling coating and tethered to the dart with 30 cm of 1.8-mm diameter fluorocarbon monofilament (136-kg tensile strength). Fish were kept in the water during tagging.

Prior to release a small fin clip (< 2 cm) was taken from the distal end of the pectoral fin for stable isotope analysis. All samples were rinsed with fresh seawater, placed in vials, immediately stored on ice for 5-7 hours while at sea, and then frozen until further processing.

Data and sample processing

Horizontal Tracks

Only tags attached for > 10 d were used in analyses. Horizontal tracks of billfish were reconstructed using the Global Position Estimator 3 (GPE3, Wildlife Computers), which uses the tag records of light, temperature, depth, and reference data on sea surface temperature and bathymetry with a user-defined movement speed to determine the most likely path. For each fish, we ran several iterations of the model varying the speed parameter (0.5 increments from 0.5 – 2.5 ms^{-1}) and selected the most probable track that converged but limited large spikes and gaps between successive locations. Estimated tracks were further filtered in R (R Core Team, 2019) using a speed-distance-angle algorithm (Freitas et al., 2008) to remove improbable locations (e.g. spikes in the movement trajectory). Tracks and depth time-series were trimmed to remove locations or data that indicated the tag was no longer attached to the fish (e.g. premature tag release) or the individual had died.

Depth and temperature

Tags were initially programmed to detach from the fish after 365 days in 2018, but duration was reduced to 240 days in the 2019 and 2021 tagging seasons after low initial tag reporting success. Tags recorded and archived depth (± 0.5 m) and temperature (± 0.5° C) at 3 or 5-s intervals every other day for 240 and 365 d programmed attachment durations, respectively. Once released from the fish, tags transmitted summaries of the archived data via satellite uplink through the Argos system. Archived data were summarized into 24-h temperature–depth profiles across eight different depths distributed between the minimum and maximum depths recorded for the 24-h period. Tags also transmitted depth data as a time-series of 150-s intervals, revealing fine-scale depth data across each track. However, typically only a subset of the archived data was successfully received via satellite resulting in gaps within the data.

Stable isotope analysis

Frozen fin samples were dried in a food dehydrator at 60° C for 24 – 48 h, powdered, and 0.5 – 1.5 mg of each sample packed into tin capsules. Isotopic analysis was performed at the University of California Davis stable isotope facility (Davis, CA, USA). δ13C and δ15N values are reported as per mille (‰) relative to international standards Vienna Pee Dee Belemnite (V-PDB) and atmospheric nitrogen, respectively.

Data Analysis

Presence and Habitat Use

To examine long-term seasonal presence of billfish near the tagging location, daily recreational billfish catch records from Tropic Star Lodge were obtained for 2010 – 2020. Because a catch inherently depends on the angler's ability to bring the fish to the boat, we used fish raises (or sightings) as our metric of fish presence. To standardize for differences in the number of boats fishing per day (fishing effort), we calculated daily sightings per unit effort (SPUE) as fish raised divided by the number of boats that fished (Haulsee et al., 2022), and then averaged SPUE per month. Tropic Star Lodge closes annually during the months of October and most of November, so these months were omitted from analyses. To examine how fish movements compared to seasonal SPUE trends, we calculated the distances from each fish's daily locations from the reconstructed tracks to the tagging location (~ 7.5 N, 78.4 W) and to the nearest coast. Distance to the coast was compared among species with a general linear mixed

model (GLMM), with individual as a random factor and a first order autocorrelation structure of days at liberty within individual to account for temporal autocorrelation.

Vertical movement patterns were compared at a range of temporal resolutions among species using transmitted 150-s interval time-series depth data. For each day of the study period with time-series data, hourly mean depth was calculated for each fish. To determine how mean depth varied throughout the 24-h period, seasonally and annually among species, we used generalized additive mixed models in the R package mgcv (Wood, 2015) with mean depth as the response variable and various combinations of species, hour of day, season (wet and dry), the interaction between species and season, and tagging year as explanatory variables with individual set as a random factor. Because fish tagged in a season spanned multiple calendar years (e.g., November 2018 – February 2019), tagging year was set as the tagging season (first year of tagging, second year of tagging, etc.) rather than absolute year (e.g., 2018, 2019). Hour of day was run using cyclic cubic splines and grouped by species and season. The final model was run using a Gamma response distribution and log link, and model fit and residuals were inspected using the gam.check() function.

We used linear mixed effects models (LMEs) to determine how individual dive characteristics varied among species. Dive characteristics were obtained from the transmitted depth time-series data using the "diveMove" package in R (Luque, 2007). This package identifies dives below a specified depth (we used 10 m) in a time-series, and for each dive identifies dive phases (i.e., descent, bottom, and ascent) using a cubic spline model. Specific behaviors of interest (response variables, modeled separately) were number of dives per day, mean depth of the bottom phase, maximum dive depth, bottom phase duration, total dive duration, and the 'distance' covered during the bottom phase of dives (calculated as the sum of absolute depth differences while at the bottom of each dive; i.e., the amount of "wiggling" at the bottom of a dive). Because these metrics will depend on the amount of time-series data obtained per day for each species, we first performed a LME on the amount of daily time-series messages obtained by species, with individual as a random variable and a first order autocorrelation structure of days at liberty within individual. There was no difference in the amount of daily time-series data obtained between species ($F_{2,63} = 0.94$, $p = 0.39$; Table S1), so no further standardization was performed. Each response variable was summarized (e.g., total, mean, maximum, depending on the variable) for each fish for each day. LMEs were fit in R using the

nlme package (Pinheiro et al., 2017) with restricted maximum likelihood. Models included species with individual as a random variable, and a first order autocorrelation structure of days at liberty within individual to account for temporal autocorrelation within each fish. Reported ΔAIC values of best fit models were compared to an intercept only model of the same structure. Where significance was indicated between species, multiple comparisons of means were performed via Tukey contrasts. Preliminary analysis showed little difference in diving behavior between species during the wet season (e.g., mean, max dive depth), so only dives during the dry season were analyzed when most fish were in close proximity to the tagging region and continental shelf.

To examine horizontal and vertical space use concurrently among the three species, three-dimensional utilization distributions (3D UDs) were calculated. In three-dimensional habitats, shared space tends to be overestimated when portrayed only in 2 dimensions (latitude and longitude only; Simfendorfer et al., 2012), therefore 3D UDs (latitude, longitude and depth) were estimated using the R package 'ks' (Duong, 2007). Core (50%) and extent (95%) 3D UDs were calculated both seasonally and overall, for each species and compared to determine the amount of spatiotemporal overlap in 3D habitat use. To get the full extent of potential vertical habitat occupied, daily maximum depth was used for the vertical axis. To determine a multiplier for the smoothing factor matrices, we used methods analogous to Simpfendorfer et al. (2012) and Bubley et al. (2020), and the plug-in bandwidth selector was used with a multiplier of 5 being applied to all smoothing factor matrices. The total volume of overlap between the core and extent 3D UDs was then calculated, and then divided by the volume of the respective species' probability contours to obtain a proportion of overlapping UDs for each species.

Stable Isotope Analysis

Despite being captured over multiple years, all individuals within a species were grouped to assure robust sample sizes for subsequent statistical analyses, and the long isotopic integration time of fin tissue likely incorporates trophic behavior across multiple seasons (Matich et al., 2010). To examine trophic niche variation within and between species, we first examined differences in the distribution of $\delta^{13}C$ and $\delta^{15}N$ values among billfishes using Kruskal–Wallis tests due to unequal sample sizes and variances. Post-hoc multiple comparisons between species' means were evaluated using a Dunn test with p-values adjust using the Holm method. Second, we calculated three established niche metrics: $\delta^{13}C$ range (CR), $\delta^{15}N$ range (NR) based on point

estimates for each species (Layman et al., 2007), and standard ellipse area (SEA; Jackson et al., 2011). CR is used to infer variability in habitat-use, whereas NR is used to assess diversity in trophic levels exhibited by individuals across the sampling community (Layman et al., 2007). SEA estimates were calculated using the SIBER R package (Jackson et al., 2011) using a maximum likelihood approach and represents a bivariate estimation of trophic niche width. Due to variable sample sizes for the different billfishes, we calculated small sample size corrected (SEA_C), and Bayesian estimates of SEA (SEA_B [median values]). Bayesian estimates were run over 10,000 iterations trimmed by the first 1,000 (Jackson et al., 2011).

Trophic niche overlap between species was determined using the 'nicheROVER' R package (Swanson et al., 2015). 'nicheROVER' uses Bayesian methods to calculate the probability of the size of the isotopic niche area of species A inside that of species B, and vice versa, and is not sensitive to variations in sample size (Swanson et al. 2015). Overlap estimates were run for 10,000 iterations and incorporated 95% of the niche region size to represent overlap in total trophic niche space.

Results

In total, 47 BUM, 55 BAM and 75 SFA were caught and either sampled, tagged, or both. Of these, 30 BUM, 46 BAM and 30 SFA were tagged with miniPATs. Seventeen tags (16%) did not report, and after discarding tags with short duration deployments (<10 d) or that exhibited patterns of post-release mortality, data were retained for 24 BUM, 23 BAM and 19 SFA (Table 4-1). Cumulatively, there were 7,602 d of tracking data (5,970 dry season, 1,632 wet season) with mean (± SD) days at liberty of 120 ± 69, 115 ± 65, and 114 ± 53 d for BUM, BAM and SFA, respectively. Over the course of the deployments, the average straight-line distance (the distance from tagging to pop-up location) travelled was 609 ± 587, 327 ± 228, and 581 ± 402 km for BUM, BAM and SFA, respectively. Length of the reconstructed tracks averaged 2,681 ± 1,754 for BUM, 2,097 ± 1,077 for BAM, and 2,384 ± 1,318 km for SFA. No difference was detected among the days at liberty (one-way ANOVA; $F_{(2)}=0.05$, $p = 0.95$), straight-line distance travelled ($F_{(2)}=2.87$, $p = 0.06$), or the cumulative distance travelled ($F_{(2)}=0.99$, $p = 0.37$) among species. However, species differed in their daily distance to the coast (GLMM, $F_{(2,63)} = 8$, $p < 0.001$). BAM remained closest to the coast throughout their tracking periods (121 ± 114 km; BUM – BAM, Est. = 18.9, SE = 4.8, Z = 3.9, $p < 0.001$; SFA – BAM, Est. = 12.4, SE = 5.2, Z = 2.4, $p = 0.03$), but BUM and SFA were not different (BUM 228 ± 256 km, SFA 173 ± 132 km; p

= 0.19). Yet, in general all three species remained in the ETP where the available vertical habitat is severely compressed due to a shallow thermocline and reduced oxygen saturation at depth (Figure 4-1). BAM showed fidelity to the ETP throughout the year, with the mean distance over time from tag location remaining below 500 km (Figure S1). For BUM and SFA, mean distance over time from tagging location showed an increase followed by a decrease, indicating an offshore movement followed by a return migration to the tagging region after ~ 125 DAL (Figures S1a). Given that the majority of BUM and SFA were tagged in late November and early December (Table 4-1), these fish were returning to the tagging region in May and June, coinciding with the rise in BUM and SFA SPUE at Tropic Star Lodge (Figure S1b). All three species have high SPUE in January and February, followed by a decrease March, and subsequent increase beginning in June and July. BUM and BAM show a steady increase from July to December, whereas SFA peak in July, but remain high through the end of the year (Figure S1b).

Table 4-1. Tagging summary by species for black marlin, blue marlin, and sailfish.

Species	Estimated Weight (kg)	Deployment			Pop-up			Days at Liberty
		Date (m/d/y)	Lat	Long	Date (m/d/y)	Lat	Long	
Black	170	11/27/2018	7.52	-78.48	2/11/2019	6.35	-82.21	76
Black	135	12/6/2018	7.53	-78.47	6/1/2019	7.61	-81.22	177
Black	125	1/27/2019	7.52	-78.28	3/11/2019	5.1	-78.66	43
Black	205	1/28/2019	7.5	-78.29	7/18/2019	5.34	-82.14	171
Black	90	2/3/2019	7.57	-78.33	10/7/2019	8.41	-78.45	246
Black	115	2/4/2019	7.6	-78.3	4/28/2019	6.92	-82.21	83
Black	90	11/27/2019	7.6	-78.32	4/13/2020	7.08	-79.9	138
Black	270	1/26/2020	7.49	-78.34	4/25/2020	6.39	-81.58	90
Black	80	2/2/2020	7.56	-78.39	9/29/2020	5.1	-79.4	240
Black	180	2/4/2020	7.53	-78.45	5/6/2020	6.17	-78.73	92
Black	100	2/4/2020	7.53	-78.37	5/12/2020	6.78	-78.57	98
Black	215	2/9/2020	7.56	-78.36	4/27/2020	6.51	-81.32	78
Black	115	2/10/2020	7.52	-78.38	4/26/2020	8.22	-78.39	76
Black	230	2/10/2020	7.47	-78.27	9/8/2020	0.04	-80.48	211
Black	160	2/11/2020	7.46	-78.29	4/1/2020	6.94	-80.99	50
Black	180	2/12/2020	7.5	-78.38	4/30/2020	8.3	-78.47	76
Black	115	12/3/2021	7.59	-78.32	4/11/2022	7	-79.64	129
Black	180	12/5/2021	7.58	-78.33	12/29/2021	5.93	-80.9	24
Black	320	12/11/2021	7.59	-78.33	5/12/2022	5.8	-77.89	152
Black	205	1/27/2022	7.59	-78.59	3/17/2022	4.73	-84.66	47
Black	125	1/28/2022	7.58	-78.58	4/10/2022	8.41	-78.63	72

Black	180	1/31/2022	7.58	-78.58	4/19/2022	0.22	-80.09	78
Black	180	1/31/2022	7.58	-78.58	8/22/2022	7.05	-81.82	203
Blue	90	11/24/2018	7.53	-78.47	1/25/2019	6.25	-78.97	62
Blue	135	11/24/2018	7.52	-78.46	3/7/2019	4.95	-86.04	103
Blue	100	11/25/2018	7.51	-78.46	2/21/2019	1.58	-94.3	88
Blue	115	11/27/2018	7.52	-78.47	3/15/2019	5.85	-82.29	108
Blue	135	11/29/2018	7.49	-78.37	1/26/2019	-2.39	-86.84	58
Blue	75	11/30/2018	7.52	-78.47	12/27/2018	6.57	-79.79	27
Blue	90	11/30/2018	7.52	-78.47	2/7/2019	6.91	-78.04	69
Blue	90	12/1/2018	7.49	-78.38	2/5/2019	7.05	-82.47	66
Blue	115	11/24/2019	7.35	-78.44	5/30/2020	8.56	-84.21	188
Blue	150	11/24/2019	7.38	-78.45	2/3/2020	8.63	-85.49	71
Blue	115	11/28/2019	7.57	-78.43	5/9/2020	3.07	-87.68	163
Blue	135	1/27/2020	7.53	-78.49	9/24/2020	7.12	-78.85	241
Blue	80	1/28/2020	7.58	-78.57	4/1/2020	8.07	-99.3	64
Blue	80	1/28/2020	7.57	-78.48	9/25/2020	7.19	-78.57	241
Blue	115	1/29/2020	7.55	-78.57	6/9/2020	6.93	-81.31	132
Blue	125	1/29/2020	7.59	-78.59	5/7/2020	5.14	-78.82	100
Blue	230	1/29/2020	7.58	-78.57	6/28/2020	3.79	-77.88	151
Blue	180	11/14/2021	7.73	-78.63	1/14/2022	5.59	-80.76	61
Blue	115	11/22/2021	7.55	-78.52	6/20/2022	3.08	-78.69	210
Blue	135	11/22/2021	7.37	-78.38	7/20/2022	5.87	-78.17	240
Blue	205	11/22/2021	7.38	-78.41	12/18/2021	8.65	-78.88	26
Blue	135	11/24/2021	7.48	-78.38	4/12/2022	8.14	-88.29	139
Blue	115	11/25/2021	7.47	-78.46	6/11/2022	5.15	-77.98	198
Blue	115	12/1/2021	7.5	-78.47	2/12/2022	2.8	-81.17	72
Sail	45	11/25/2018	7.52	-78.47	1/6/2019	4.03	-79.63	42
Sail	35	11/29/2018	7.51	-78.46	1/31/2019	2.69	-89.7	63
Sail	35	11/29/2018	7.41	-78.38	3/2/2019	5.53	-83.27	94
Sail	30	11/30/2018	7.51	-78.33	4/21/2019	4.28	-78.1	142
Sail	30	12/1/2018	7.49	-78.38	3/9/2019	5.82	-82.35	98
Sail	35	12/3/2018	7.52	-78.41	5/18/2019	6.31	-77.52	166
Sail	40	11/22/2019	7.41	-78.67	3/25/2020	3.12	-87.77	124
Sail	35	11/27/2019	7.55	-78.39	3/19/2020	4.6	-89.3	113
Sail	30	11/29/2019	7.55	-78.41	7/27/2020	6.61	-79.25	241
Sail	40	11/29/2019	7.6	-78.35	1/24/2020	8.46	-78.96	56
Sail	35	11/30/2019	7.55	-78.57	1/23/2020	7.84	-85.85	53
Sail	35	1/22/2020	7.57	-78.54	3/7/2020	3.63	-78.58	44
Sail	40	1/22/2020	7.59	-78.57	6/29/2020	-0.95	-80.64	159
Sail	40	1/23/2020	7.55	-78.53	4/6/2020	5.68	-80.87	74
Sail	25	11/17/2021	7.29	-78.58	4/11/2022	9.92	-88.74	145
Sail	35	11/20/2021	7.65	-78.55	3/1/2022	4.43	-81.93	101
Sail	40	11/21/2021	7.45	-78.45	4/18/2022	5.94	-80.89	148
Sail	30	11/22/2021	7.49	-78.51	3/29/2022	8.1	-81.99	127
Sail	35	11/22/2021	7.47	-78.49	5/24/2022	6.61	-79.57	183

Vertical and Horizontal Habitat Use

For all species, the majority of time during daylight hours (80 ± 18%, 62 ± 19%, 58 ± 16% for BAM, BUM and SFA, respectively) were spent in water ≤ 10 m. Overall, BAM average daytime depth was 12 ± 15 m, followed by BUM 17 ± 19 m and SFA 22 ± 23 m. Percent of daytime spent deeper than 10 m was significantly different among species and season (Type III two-way ANOVA for unbalanced designs; species, df = 2, F = 13.5, $p < 0.001$; season, df = 1, F = 4.6, p = 0.03). SFA and BUM spent significantly more time below 10 m than BAM (Estimate = 0.2, SE = 0.04, T = 4.7, $p < 0.001$ and Estimate = 0.3, SE = 0.04, T = 4.2, $p < 0.001$, respectively). In the dry season, BAM spent less time below 10 m (13 ± 7%) compared to the wet season (34 ± 29%; T = -2.2, df = 9.4, p = 0.05), where BUM and SFA spent similar proportions of time below 10 m in both the dry and wet seasons (BUM 34 ± 17% and 43 ± 20%, p = 0.2; SFA 44 ± 12% and 38 ± 20%, p = 0.4, respectively).

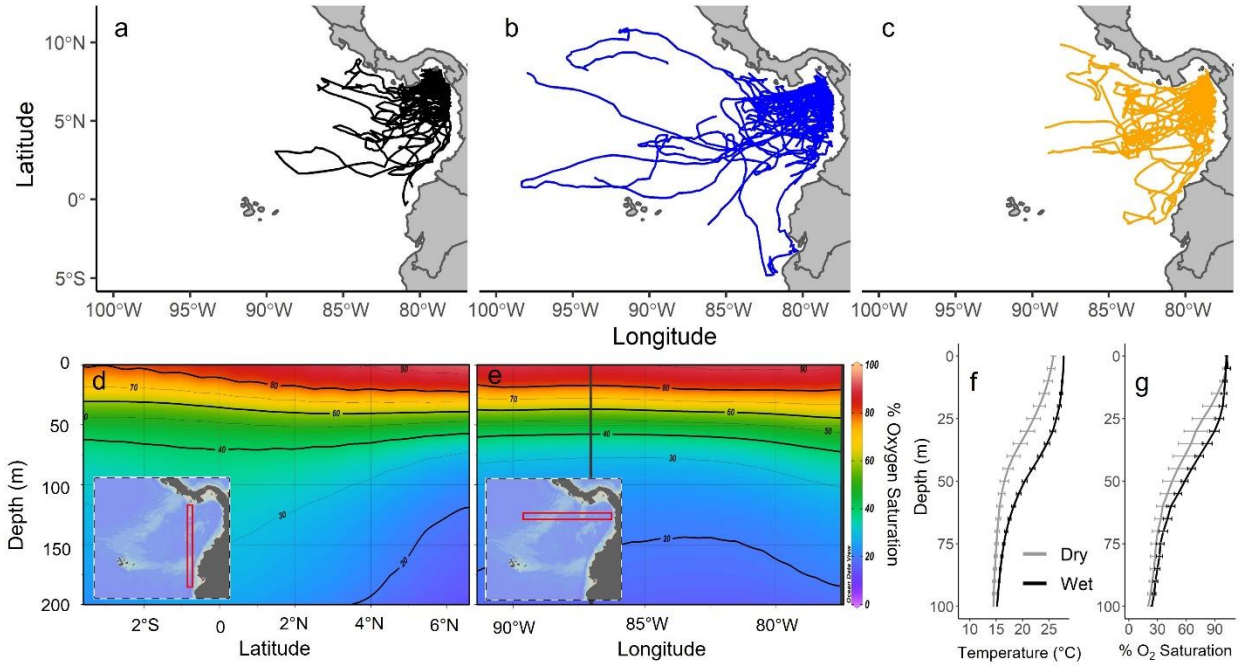

Figure 4-1. Reconstructed tracks of (a) black marlin (b) blue marlin and (c) sailfish along with the mean annual meridional (d) and zonal (e) sections of percent oxygen saturation at the red outlined latitudinal and longitudinal bands indicated in the inset plots, and the seasonal (wet vs dry) mean (± SE) temperature (f) and percent oxygen saturation (g) at 5 m depth intervals at the tagging site. Data for d – g were obtained from NOAA's National Centers for Environmental Information World Ocean Atlas 2018. Note the vertical black line in (e) is an oceanic island.

Average depth of each species was best explained by hour of day and season. The inclusion of tagging year did not improve model fit, so this was removed for the most parsimonious model (Table S2). The overall best fit model included an interaction between species and season within the hour of day smoother (% deviance explained = 65.5%; Table S2). All species displayed patterns consistent with diel vertical migration during both seasons, where fish were shallow at night and dived deeper during the day (Figure 4-2). During the wet season, all species showed substantial overlap in their predicted mean depth throughout the 24-h cycle (Figure 4-2a), with only slight differences in hourly mean depth response curves (Figure 4-2c-e). However, during the dry season, predicted mean daytime depths were nonoverlapping. On average, SFA were the deepest of the three, followed by BUM, and BAM the shallowest (Figure 4-2b). During the dry season, the relative timing and strength of this diel pattern was different for each species (Figure S2). Where SFA reached their peak (are deepest) in early morning hours (~06:00 – 08:00), BUM and BAM did not peak until the late afternoon (~15:00 – 17:00; Figure 2b, Figure S2). BUM and SFA were significantly deeper than BAM during all daylight hours (Figure 4-2f, g). SFA were deeper than BUM in the morning from sunrise until ~10:00, and then at ~16:00 BUM average depth becomes deeper while SFA gets shallower (Figure 4-2b, h; Figure S2). As such, there becomes a large difference in mean depth of BUM and SFA from 16:00 – 20:00 (Fig. 4-2h) where BUM were deeper until sunset, and then mean depth is not different between BUM and SFA during the night (Figure 4-2h).

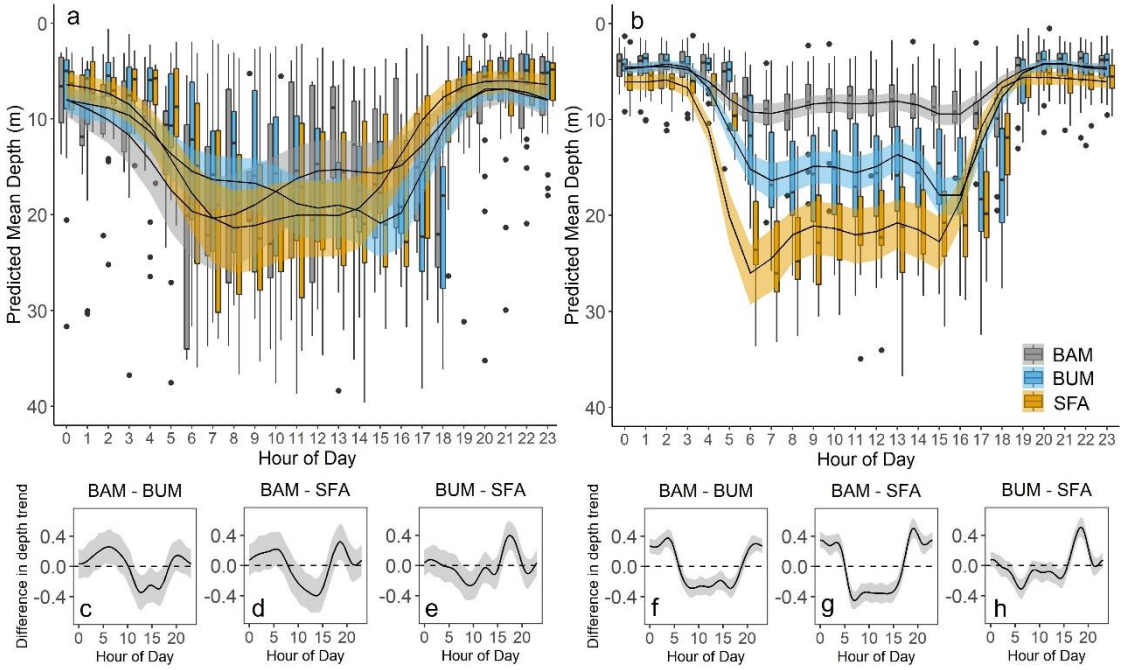

Figure 4-2. Seasonal diel vertical behavior of billfish in the eastern tropical Pacific. Grouped boxplot of black marlin (BAM), blue marlin (BUM) and sailfish (SFA) hourly depth overlaid with the predicted hourly mean depth (solid black line) and 95% confidence intervals (colored shading) from the GAMM output during the wet season (a) and dry season (b), along with the difference between the GAMM partial effects response curves during the wet season (c – e) and the dry season (f – h). Mean depth was determined to be significantly different between species where the confidence intervals do not overlap 0 (horizontal dashed line) in c – h.

In total, 18,889 BUM, 17,356 BAM, and 34,229 SFA dives from the dry season were analyzed. Linear mixed effects model predictions showed that BAM dived to shallower mean and maximum depths than both BUM and SFA (Figure 4-3a, b; Table S3). While BAM spent roughly the same amount of time in the bottom phase of a dive as SFA, they covered significantly less distance than both BUM and SFA (Figure 4-3c, d). BAM performed a similar number of dives everyday to BUM, however, each dive was on average shorter in duration than BUM dives, but similar to SFA dives (Figure 4-3e, f). SFA mean bottom depth and mean maximum depth were similar to that of BUM, but SFA performed more dives per day than either BUM or BAM, with dives being shorter in both bottom phase and overall duration. However, even though SFA dive duration and bottom time were shorter than those of both BUM and BAM, SFA bottom 'distance' was not different than that of BUM, and greater than that of BAM suggesting SFA were very vertically active during their brief time at the bottom of a dive (Figure

4-3). While SFA performed the greatest number of dives throughout the day, more dives were performed and bottom distance covered was greatest in the early morning hours, and generally decreased until sunset (Figure 4-3i). In contrast, number of dives and bottom distance covered during BUM dives was low in the morning and peaked in the late afternoon (Figure 4-3g, h).

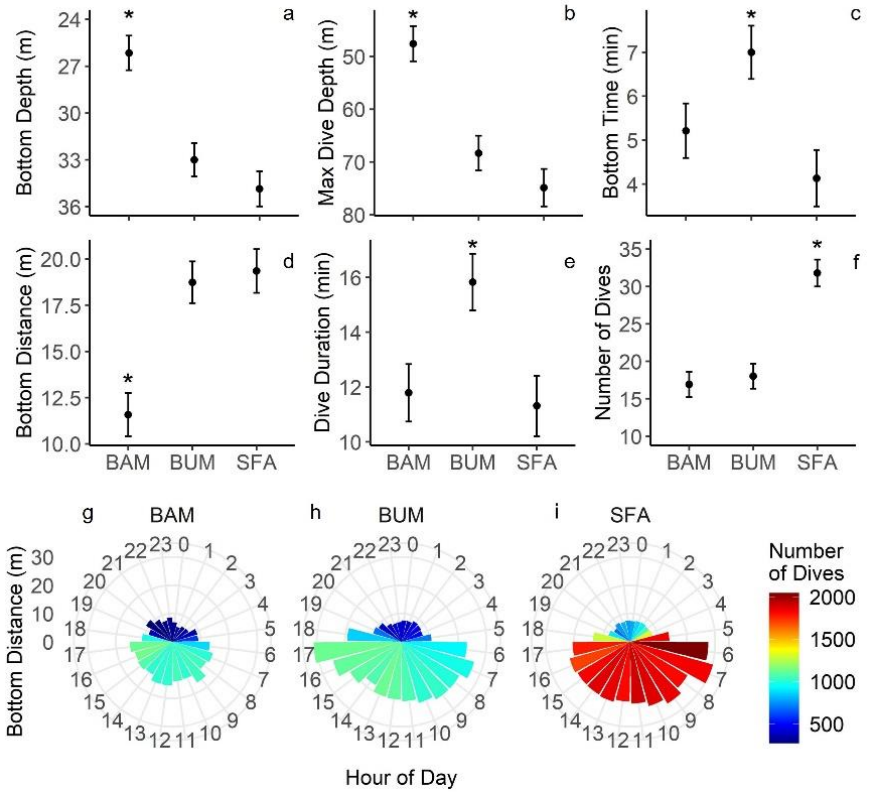

Figure 4-3. Best-fit linear mixed effect model predictions (± 95% CI) of black marlin (BAM), blue marlin (BUM) and sailfish (SFA) daily dive behaviors for all dives extracted during the dry season from 150-s timeseries depth data (a – f), paired with diel diving activity of bottom distance covered during a dive, colored by the number of dives performed in each hour of the day (g – i). Only dives > 10 m were considered. In a – f, statistical significance from other species is indicated by "*".

In general, BUM used the largest volumes of water as they moved furthest away from the tagging location (Table 4-2; Figures 4-1, 4-4; Figure S1). While BAM horizontal movements were greater than BUM movements in the wet season, BUM average maximum depth (102.1 ± 59.7 m) was nearly double BAM maximum depth (59.3 ± 26.8 m), leading to a larger volume of water used. Similarly, although BUM core and extent UDs extend further offshore than those of

SFA, the volume of water used is similar for the core habitat and is comparable between the extent UDs due to SFA diving to deeper maximum depths than BUM (Figure 4-4).

Core (50%) and extent (95%) volume use for all species showed a large amount of habitat overlap both seasonally and overall (Figure 4-4; Figure S3). In the wet season, core habitat overlap ranged from 28 – 71%, while extent habitat overlap ranged from 37 – 81% (Figure S3). Although the extent UD of each species was generally larger in the dry season (likely an artifact of more tracking days in the dry season), core UD sizes were similar between wet and dry seasons (Table 4-2). Maximum proportion of habitat overlap tended to be larger in the dry season for both the core and extent UDs, ranging from 14 – 87% overlap, and 16 – 100% overlap, respectively (Figure S4). Overall, BAM 3D core and extent habitat use were nearly completely overlapped by both BUM and SFA habitat use areas, but BAM overlapped relatively little of both BUM and SFA 3D habitat use (20-32%; Figure 4-4). However, SFA and BUM had high 3D core habitat overlap in the wet (44 – 69%) and dry (64 – 80%) seasons, and overall (70 – 77%; Figure 4-4; Figure S3).

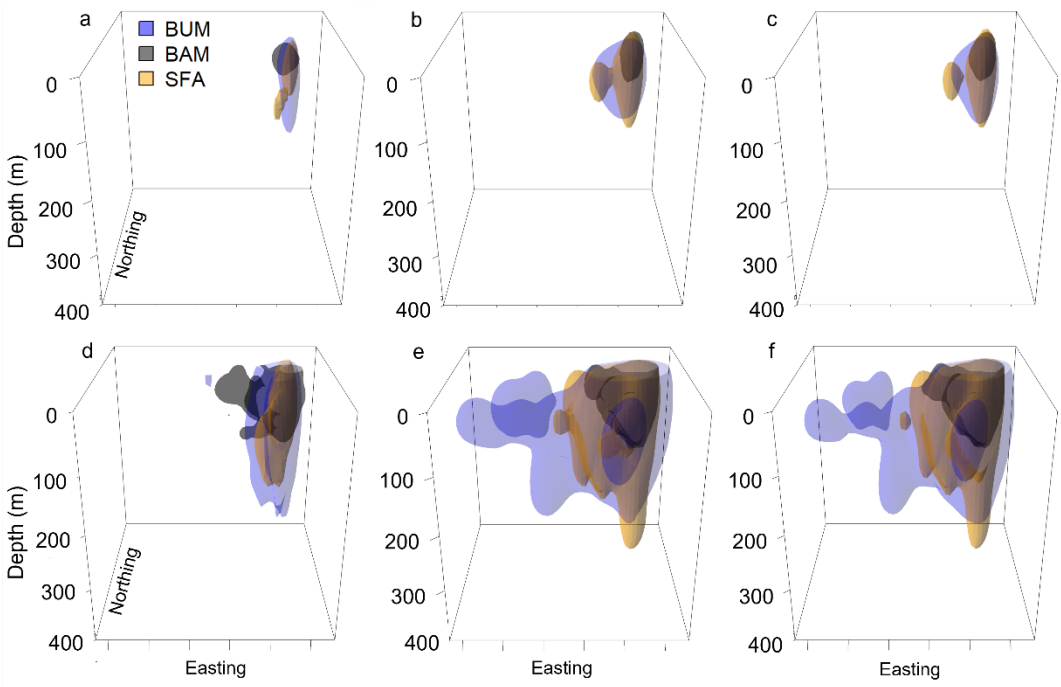

Figure 4-4. Overlap between 3-dimensional core (50%; a-c) and extent (95%; d-f) utilization distributions for blue marlin (BUM, blue), black marlin (BAM, black) and sailfish (SFA, orange) in the eastern tropical Pacific. 3D UDs are shown for the wet season (a, d), dry season (b, e) and overall (c, f). The depth dimension used was maximum daily depth. All figures are plotted on the same 3D spatial scale (x, y, z).

Table 4-2. Volumes of three-dimensional utilization distributions for blue marlin (BUM), black marlin (BAM) and sailfish (SFA) during the wet season (April – November), dry season (December – March) and overall. Volume is given in km^3.

	Wet		Dry		Overall	
	50	95	50	95	50	95
BUM	1.00×10^4	1.02×10^5	2.70×10^4	3.80×10^5	2.10×10^4	3.10×10^5
BAM	5.00×10^3	6.60×10^4	5.00×10^3	6.00×10^4	5.00×10^3	6.00×10^4
SFA	6.00×10^3	4.60×10^4	2.00×10^4	1.90×10^5	2.10×10^4	1.90×10^5

Stable Isotope Analysis

Billfish stable carbon isotope values ranged from –16.0‰ to –12.7‰ and stable nitrogen isotope values ranged from 10.8‰ to 14.9‰ (Figure 4-5a). Stable carbon and nitrogen isotope values differed among species (Kruskal–Wallis test carbon, $\chi 2 = 61.3$, df = 2, $p < 0.001$; nitrogen, $\chi 2 = 46.5$, df = 2, $p < 0.001$). Specifically, mean $\delta^{13}C$ values for SFA were lower than

BUM (Dunn test, $Z = 5.8$, $p < 0.001$) and BAM values ($Z = 6.7$, $p < 0.001$). $\delta^{15}N$ values differed between all three species; SFA were the lowest (SFA – BUM, $Z = 2.8$, $p = 0.005$; SFA – BAM, $Z = 6.7$, $p < 0.001$) and BAM were the highest (BAM – BUM, $Z = 3.6$, $p < 0.001$).

Carbon range estimates were greatest for SFA, and the same for BUM and BAM (Table 4-3). However, nitrogen range estimates were the lowest for SFA, and greatest for BAM (Table 4-3). SEA varied between species but followed similar patterns to NR estimates. SEA estimates for BAM and BUM were greater than those of SFA (Table 4-3). SEA_C and SEA_B estimates exhibited similar values (Table 4-3, Figure 4-5b). Low total trophic niche overlap was observed between the three species ($\leq$ 30.8% across all species comparisons), the lowest overlap occurred between SFA and BAM (< 1%) and the greatest overlap occurred between BUM and BAM (23.4 – 30.8%; Table 4-4, Figure S4).

Table 4-3. Summary statistics [mean (SD)] of black marlin (BAM), blue marlin (BUM), and sailfish (SFA) estimated weight and stable isotope values, with isotopic niche metrics including $\delta^{13}C$ and $\delta^{15}N$ ranges (‰); standard ellipse area (SEA), small sample size corrected SEA (SEA_C), and Bayesian estimates of SEA (SEA_B; median values shown).

Species	n	Est. Weight	$\delta^{13}C$ (‰)	$\delta^{15}N$ (‰)	$\delta^{13}C$ range (CR)	$\delta^{15}N$ range (NR)	SEA (‰^{2})	SEA_C (‰^{2})	SEA_B (‰^{2})
BAM	17	175 (65)	-13.5 (0.49)	13.3 (0.57)	1.5	2.5	0.85	0.91	0.88
BUM	21	135 (65)	-13.9 (0.38)	12.1 (0.52)	1.5	2.1	0.61	0.64	0.62
SFA	45	35 (5)	-15.1 (0.44)	11.8 (0.23)	1.9	0.8	0.29	0.3	0.3

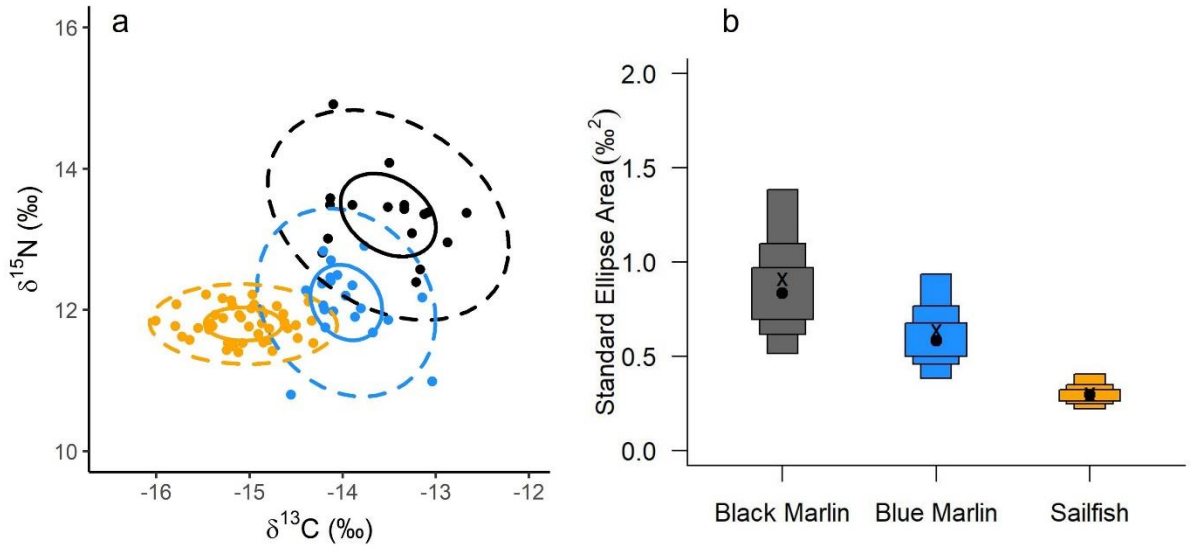

Figure 4-5. (a) Core trophic niche (40% of data, solid lines) and total trophic niche (95% of data dashed lines) estimates for black marlin (black), blue marlin (blue) and sailfish (orange). (b) SEA_B estimates with 50%, 75%, and 95% credible intervals (the X represents maximum likelihood estimated SEA_C).

Table 4-4. Total trophic niche overlap (%) between black marlin (BAM), blue marlin (BUM), and sailfish (SFA) in the eastern tropical Pacific. Two different overlap estimates are presented for each species comparison based on whether the total trophic niche of species A is being compared to species B, or vice versa.

		Species B		
		BAM	BUM	SFA
Species A	BAM	-	23.4	0.1
	BUM	30.8	-	15.9
	SFA	0.4	22.8	-

Discussion

Using long-term recreational fisheries data in combination with horizontal tracking, high resolution vertical movements, and stable isotope data collected over multiple years, we revealed a high amount of long-term and 3D habitat overlap, temporal partitioning of vertical habitat, and low trophic overlap among blue marlin, black marlin and sailfish in the ETP. While differences in life history, morphological, and physiological constraints may be important factors in facilitating habitat partitioning in some sympatric, pelagic species (Brill and Lutcavage, 2001; Bernal et al., 2017), the hypoxia-based habitat compression in the ETP results in these three

billfish species being restricted to the same environmental conditions and seasonal prey productivity. Therefore, the niche partitioning described here is not likely driven by physiological or morphological constraints, but more likely represents behavioral mechanisms used to alleviate resource competition among this predator guild in a vertically compressed habitat.

Recreational fishing records demonstrate a strong, long-term seasonal pattern of co-occurrence among these billfishes in the ETP, and we document a high proportion of 3D spatial overlap between them. Core use areas were relatively small and showed high overlap among species (20% – 91%) compared to the 4% and 38% of 3D core habitat overlap between BUM and SFA, and SFA and white marlin (*Kajikia albida*), respectively, in the western north Atlantic (Bubley et al., 2020). In addition, the tendency for tagged fish to remain near Panamanian waters after long periods of time is noteworthy for these highly mobile species. Among other billfish movement studies with similarly long tag deployments, displacement distance is often positively correlated with days at liberty. For example, BUM tagged in the north Pacific were 1,276 ± 2,191 km from the tagging location after 112 ± 75 (median ± inter-quartile range; n = 69) days at liberty (Dale et al., 2022). Similarly, BAM tagged near the Great Barrier Reef were 2,146 ± 1,226 km (mean ± SD; n = 42) from the tag location after 8 – 180 d (Domeier and Speare, 2012). These distances, despite similar or fewer days at liberty to our tagged fish, are roughly twice and seven-times the mean displacement distances we found for BUM and BAM (609 ± 587 and 327 ± 228 km, respectively). SFA are the most site attached of the ten billfishes reviewed by Braun et al. (2015), and their displacement distance reported here (581 ± 402 km) was similar to or slightly greater than those of other SFA studies in the Atlantic (Orbesen et al., 2008; Lam et al., 2016). The low overall displacement distances reported here for BUM, BAM and SFA suggests fidelity to Panamanian and adjacent waters and thus high potential for horizontal overlap, and when combined with restricted vertical habitat use, suggests niche partitioning may be behaviorally mediated in this environment.

Pelagic species vertical movements are often hypothesized to be driven by foraging behavior (Sepulveda et al., 2004; Bestley et al., 2008; Braun et al., 2022). In the ETP, shoaling of the thermocline and oxycline during the dry season further compresses the already restricted vertical habitat available to these predators, likely evoking increased interspecies competition for available prey. As such, the seasonal partitioning in vertical habitat documented here would

serve to reduce competitive overlap, creating niche partitioning within this pelagic predator guild. Indeed, during the dry season when coastal productivity is at its peak, fishery SPUE is high for all species, and core 3D spatial overlap is high, we documented a substantial separation of mean depth use that was consistent across years. During the dry season, BAM made use of very shallow average depths, SFA used the deepest average depths, and BUM used intermediate depths. This vertical behavior is in stark contrast to many previous studies of vertical habitat use among these species. For example, SFA were generally thought to be the most surface-oriented billfish, spending a greater proportion of time in water < 10 m than BUM (Prince and Goodyear, 2006; Braun et al., 2015; Bubley et al., 2020; Madigan et al., 2021). Also, similar sized BAM (~100-250 kg) had a mean hourly daytime depth of ~70 – 80 m in the western Pacific (Williams et al., 2017b), compared to a mean hourly daytime depth of 12 ± 15 m observed for BAM in our study. During the wet season, BUM, BAM and SFA used similar depths throughout the day, similar to that observed for BUM, SFA and white marlin in the western north Atlantic (Bubley et al., 2020) where seasonal changes are not as stark and vertical habitat compression does not exist. This suggests that when coastal productivity is lower, vertical habitat compression reduced, and core 3D habitat overlap decreases, sympatric billfish predators homogenize their diving behavior and are able use similar depths to one another throughout the day.

Predator guilds in other ecosystems are known to display seasonal and temporal variation in hunting behavior and habitat use to relax interspecific interference and competition (Metz et al., 2012; Hinke et al., 2015; Matich et al., 2017). For example, within a large carnivore guild with overlapping area use in western Zambia, Dröge et al. (2017) documented that wild dogs (*Lycaon pictus*) and cheetahs (*Acinonyx jubatus*) concentrate hunting efforts on time windows that avoid nighttime hunting by lions (*Panthera leo*) and spotted hyenas (*Crocuta crocuta*). Similarly, three species of predatory fishes in a temperate reservoir were observed to seasonally partition horizontal and vertical habitat in response to seasonal reservoir stratification (Westrelin et al., 2022). For example, during periods when the water column was well-mixed (autumn and winter), fish partitioned vertical habitat, but during summer the reservoir became vertically stratified, and all species compressed to surface waters resorted to horizontal partitioning (Westrelin et al., 2022).

We identified both seasonal and diel differences in vertical habitat use and found key differences in the diving behavior driving the habitat partitioning among the billfishes monitored

here. For example, although SFA hourly daytime depth was deeper than BUM during the dry season, both species dove to the same mean and maximum depths. However, SFA's deeper average depths were driven by SFA preforming nearly twice as many, but much shorter duration, dives per day than BUM. Variation in dive duration and frequency can likely be explained by morphological differences between BUM and SFA, as SFA are smaller and more laterally compressed, limiting their capacity to retain body heat when exploring colder depths for extended periods (Hoolihan et al., 2011b). However, BUM and BAM tagged in this study were of similar body size (Tables 1 and 3), thus differences in depth use cannot be explained by morphological differences between them. Furthermore, SFA performed most of their dives in the early morning hours, during which they covered more bottom distance (a proxy for prey searching or chasing; see Logan et al., 2023), whereas BUM performed more dives and covered more bottom distance in the late afternoon. Lear et al. (2021) recently described diel temporal niche partitioning within a coastal sympatric guild of six shark species, where peaks in activity patterns were spread throughout the 24-h cycle. While BAM were using a shallower portion of the water column, BUM and SFA were exploiting the same depths, but were potentially alleviating interaction with one another via diel partitioning of diving activity. These findings provide new insights into the mechanisms underpinning resource partitioning among highly mobile, large diving pelagic predators, and are complemented by direct data of feeding habits.

Not only did we identify seasonal partitioning of vertical habitat, but over long-time scales we documented strong interspecific differences in foraging as well. Because non-lethal blood sampling (fast-turnover tissue) is not feasible for these large fishes, we do not have the temporal resolution necessary to determine seasonal changes in diet, and our fin tissue samples likely represent prey assimilated over multiple seasons (Matich et al., 2010). Interestingly, although SFA are reported to be the most coastal of the billfishes (Braun et al., 2015), our tracking data demonstrate that BAM were the most coastally inclined while SFA used more offshore habitats, further indicated by SFA being the most depleted in $\delta^{13}C$ of the three species. However, SFA also had the smallest nitrogen range and SEA, indicating a small amount of trophic diversity and a more specialized foraging tactic by preying on functionally similar prey groups (Layman et al., 2007). Rosas-Luis et al. (2017) report similar findings for muscle tissue of SFA caught in nearby waters of Ecuador, with low $\delta^{15}N$ variability and high $\delta^{13}C$ variability. The higher $\delta^{13}C$ values of BUM and BAM suggests that they forage differently, potentially

consuming prey from more coastal, high productivity regions associated with the strong seasonal upwelling events of the ETP, which favor the enrichment of primary production (Stock et al., 2017). Furthermore, the increased $\delta^{15}N$ values, larger nitrogen ranges and greater SEAs of BUM and BAM indicate feeding on higher trophic levels and more generalist foraging behavior than SFA, as BUM and BAM are larger and have a larger mouth gape, and are able to consume a wider variety of prey items (Keppeler et al., 2020). Because we lack spatially explicit baseline isotope data, patterns of inshore and offshore feeding cannot be fully discerned. However, these results demonstrate that seasonal differences in vertical habitat use can lead to long term changes in the trophic niche of pelagic predators, and highlight the power of complimentary methodologies to gain insights into movements and behavior in mediating competition among sympatric predators.

These data also have important implications for interaction potential with surface-based commercial fisheries in the region, which is the dominant type of fishing that occurs in the ETP (IATTC, 2018). Commercial and artisanal surface and shallow-set longlines targeting highly profitable species (e.g., yellowfin tuna (*Thunnus albacares*), dolphinfish (*Coryphaena hippurus*)) are prevalent in this region, and are the most likely fisheries to interact with billfish (Kitchell et al., 2004). Our results suggest that the billfishes of the ETP may be disproportionately affected depending on the season. For example, BAM mean depth and proximity to the coast during the dry season may significantly increase the likelihood of interaction with these fisheries compared to BUM and SFA, although all species use shallow waters in the ETP compared to other parts of their range. However, BAM are currently listed as data deficient on the IUCN Red List (Collette et al., 2022), and have historically been misidentified in fishery catch statistics (Williams et al., 2018). As such, reliable data on bycatch, landings, and effort for this species are urgently needed to determine if additional management efforts are required for this species.

Top predators and predator diversity in ecosystems have been identified as critical components for ecosystem function and stability, and monitoring of these species can therefore help guide ecosystem science and conservation efforts (Sinclair et al., 2003; Estes et al., 2016; Hazen et al., 2019). In this era of unprecedented environmental change and habitat destruction, shifts in the geographic distribution of many species are already evident, and are only predicted increase (Parmesan, 2006), with oxygen limitation and altered oxygen distribution suggested to be a major factor contributing to further changes in large pelagic predator horizontal and vertical

distributions (Leung et al., 2019; Rubalcaba et al., 2020). The data we have presented here demonstrates that the billfish complex in the ETP uses a suite of mechanisms to promote coexistence in a vertically restricted habitat, and leads to the hypothesis that sympatric predators in other pelagic ecosystems currently unaffected by oxygen minimum zones may be able to behaviorally adapt and respond to predicted widespread vertical habitat compression.

Chapter VI

CONCLUSION

Due to their large body size, difficulty and expense of capture, and dispersed elusive nature, paired with their inability to be kept in captivity, information of billfish biology, physiology, and ecology has lagged behind other marine predators. Concurrently, their high mobility, epipelagic lifestyle, long lifespan, and marketable meat contribute to their high vulnerability to various fishing gears and environmental change. Understanding how billfish interact with and recover from fishery interaction, how the environment influences their movements, hunting, and depth use, and how they interact with other billfish species aids our ability to improve population assessments and management. In this dissertation, I have provided a substantial step forward in our understanding of billfish biology and ecology for three species that have been historically challenging to study at high resolutions. The data contained within this dissertation is poised to aid future advances in billfish ecology as methods and technologies continue to improve.

Using the novel tag package I designed and implemented in Chapter II, fishery managers now have a detailed understanding of how billfish behaviorally respond to and recover from globally practiced recreational catch-and-release fishing. Because of the hypoxia-based habitat compression present in the eastern tropical Pacific, blue marlin and sailfish tagged in this study were unable to dive to deeper waters with cooler temperatures, as documented in other locations throughout their range (Block et al., 1992a). However, tagged fish did dive to the upper boundary of the oxygen minimum zone, and exhibited increased swim speeds for several hours as a mechanism of increased oxygen transfer at the gills. As such, we documented relatively rapid behavioral recovery for sailfish and blue marlin (4.9 ± 2.8 h and 9.0 ± 3.2 h, respectively) from catch and release fishing.

After removing all data prior to recovery for each fish as determined in Chapter II, Chapter III investigated blue marlin and sailfish high-resolution habitat use, fine-scale interaction with vertical habitat features, and hunting behavior. Because the vast majority of previous movement studies of billfish have implemented comparatively low-resolution data gathered from satellite transmitting tags, they often lack the resolution necessary to describe how environmental features (e.g., fronts) are exploited by billfish. In this chapter, I describe a novel hunting method for billfish in the ETP, in which they utilize the low temperatures and low oxygen boundaries that concentrate prey, dive below the boundary, and ambush prey from below. These findings

represent some of the first documented instances of large pelagic predators exploiting a large, naturally occurring vertical habitat front, and provide new insights into pelagic predator hunting techniques around the world that should be investigated further in other locations.

In light of the hunting hypothesis put forward in Chapter III (that predators in highly stratified environments will dive below the vertical fronts to ambush prey from below), Chapter IV provides support for this hypothesis with a documented foraging attempt by a sailfish. Because acceleration signals could be ground-truthed with animal borne video, in this chapter I describe at a very high resolution the activity patterns and hunting behavior of a solitary sailfish, representing the first time such interaction has been documented. I then took the analysis one step further by estimating the active metabolic rate of the sailfish, the amount of energy likely expended by the sailfish throughout the course of 24 hours, during the predation event, and the amount of energy that it would have gained assuming a successful capture of the prey tuna. These findings represent the first such estimations of free-ranging sailfish metabolic rates, and sheds much needed light on the poorly understood ecophysiology of these top predators.

As a result of the vertically compressed habitat of the ETP and the high abundance of blue marlin, black marlin and sailfish in this region, the final chapter (Chapter V) aimed to resolve how all these large predators could successfully coexist. By leveraging a decade of recreational fisheries data, multi-year satellite tracking with high-resolution vertical diving data, and stable isotope analysis, I found that seasonal and diel variability in vertical habitat use promoted spatial partitioning within the water column during periods of high prey abundance. Furthermore, isotopic data supported low trophic overlap over long time scales, supporting differences in foraging behavior identified by dive data. Niche partitioning coupled with behavioral plasticity among this predator guild provides evidence for the maintenance of high predator species diversity in a vertically restricted habitat, and has important implications for how sympatric predators in other regions may respond and adapt to further natural and human-driven environmental change.

Of course, many interesting questions arose during this work, with not enough time to pursue them all. For example, in Chapter II, in order to remain consistent across fish, all individuals were caught and tagged using the same methodology to remain consistent, and minimize stress put on the animal. However, I see a number of opportunities for this work to be

extended to more species that are popular in recreational fisheries, and implementing various capture techniques to see how they may impact recovery time. For example, fly-fishing with light-weight tackle for big game fish, such as marlin, is becoming increasingly popular, which can significantly increase fight durations, and may potentially increase recovery times, or inhibit recovery altogether. In the high-resolution habitat use and hunting behavior analysis presented in Chapter III and IV, I was able to quantify hunting behavior in the ETP; however this work would benefit from further exploration of hunting behaviors in other regions without a defined oxygen minimum zone to determine how behavior changes across habitat variability. Furthermore, because sailfish cannot be kept in captivity, I was required to use a proxy species (dolphinfish *Coryphaena hippurus*) to estimate the amount of oxygen consumed, and therefore the metabolic rate of the sailfish. As such, the resulting values are only estimations and should not be taken as exact values. However, until such methods are developed to gather oxygen consumption data from large pelagic fishes, the use of proxy species is the best alternative for estimating energetic dynamics of pelagic predators.

Finally, Chapter V provides substantial evidence of seasonally driven vertical habitat partitioning among this predator guild; however, this work would be improved by additional tracking data spanning the entire year. Due to the nature of satellite tags detaching prematurely from billfish, most of the tracking data used in Chapter V is during the dry season because that is when tagging took place, and many tags did not remain attached for the wet season. Tagging at different times of the year would allow for more in depth analysis of habitat partitioning and how these predators coexist in high abundances. Similarly, because these are large, powerful fish that can only be restrained momentarily, we were only able to collect pectoral fin tissue from a sample of individuals. However, if a restraint technique could be implemented that allowed for increased time to access the fish, several tissue types could be sampled to investigate temporally relevant changes in diet, and potentially new tagging methods could be developed to increase tag retention time, or new tag types altogether (e.g., SPOT, implant archival tag, etc.,).

Overall, this dissertation provides significant advances to our collective knowledge of billfish biology and ecology, particularly in relation to one another and their environment. While it was not a motivation at the initiation of the project, performing this work in the eastern tropical Pacific fortuitously allowed me to expand the breadth of this research, and frame it in the context

of global change, and global deoxygenation of our oceans. In this era of unprecedented environmental change, global oxygen minimum zones are predicted to grow both vertically and horizontally, and hypoxia-based habitat compression will begin to affect new regions and new ecosystems. As such, understanding how top predators of an ecosystem respond to catch and release, how they may utilize low oxygen habitat or highly stratified habitats, and their mechanisms of coexistence provides an opportunity to study how sympatric predators in other regions may respond and adapt to vertical habitat compression, and how the billfish complex in the ETP may fare in light of further environmental change using the data generated from this dissertation.

Appendix A: Chapter II Supplemental Information

Supplemental Tables

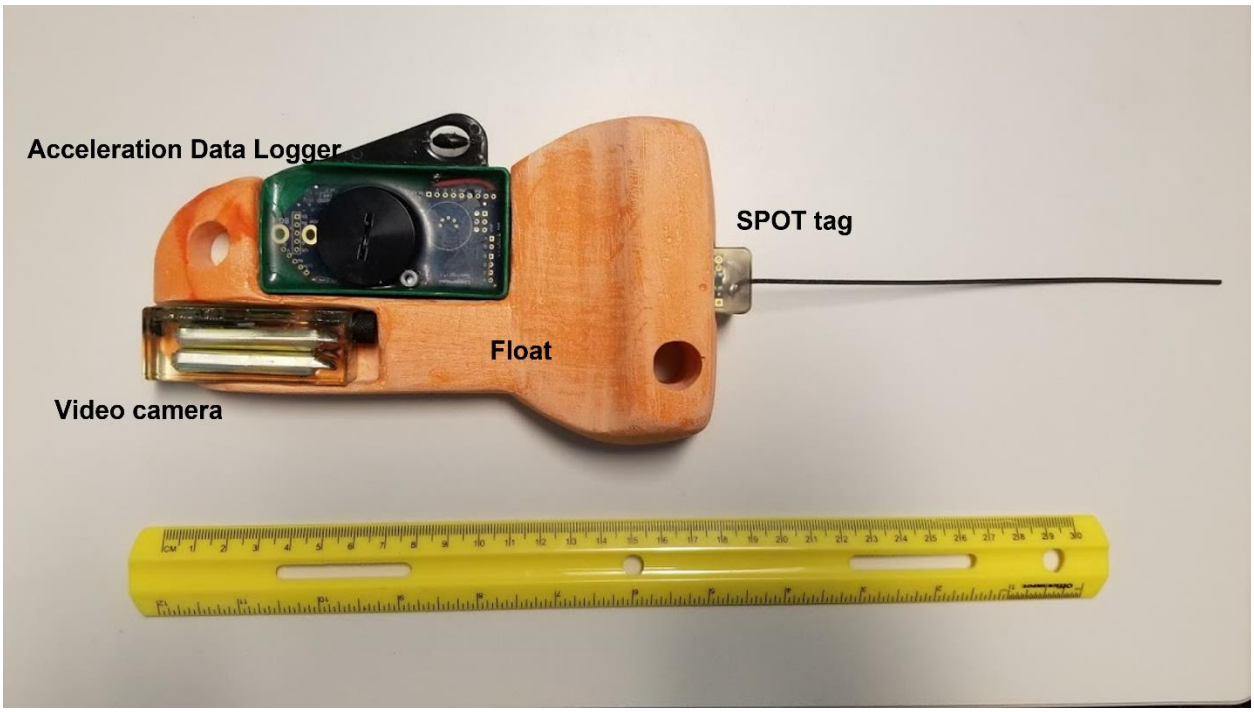

Supplemental figure S1. Custom designed tag package consisted of an acceleration data logger which also recorded depth, temperature, and light levels, and a small turbine-based fluid speed sensor all recording at 1 Hz (OpenTag 3.0, Loggerhead Instruments, Sarasota, FL, USA). The tag package also contained a miniaturized video camera (68 mm × 21 mm× 22 mm; Little Leonardo, Tokyo, Japan) and a Smart Position and Temperature tag (SPOT-363A; Wildlife Computers,Redland, WA, USA) to aid in package recovery.

Appendix B: Chapter III Supplemental Information

Supplemental Tables

Supplemental Table S1. P-values of pairwise comparisons of path tortuosity among blue marlin dive shapes from non-parametric Games-Howell post-hoc test

	V	W
U	0.0006	<0.001
V		<0.001

Supplemental Table S2. P-values of pairwise comparisons of path tortuosity among sailfish dive shapes from non-parametric Games-Howell post-hoc test.

	V	W	LA	LD
U	0.002	0.5	0.03	0.1
V		0.001	0.1	0.1
W			0.008	0.04
LA				0.8

Table S3. Blue marlin tortuosity GAMM results.

BLUE MARLIN						
Model	df	AIC	ΔAIC	Relative Liklihood	AICw	% Deviance Explained
s(Temperature by Dive Shape)	24.2	9.5	0.0	1.00E+00	1.00E+00	51.8
s(PC1 by Dive Shape)	23.5	75.3	65.7	5.37E-15	5.37E-15	48.3
s(Depth by Dive Shape)	23.3	127.2	117.6	2.85E-26	2.85E-26	45.3
s(% Oxygen Saturation by Dive Shape)	23.9	138.2	128.7	1.15E-28	1.15E-28	44.7
s(PC1) + s(PC2) + Dive Shape	23.7	140.1	130.5	4.52E-29	4.52E-29	44.6
s(Temperature) + Dive Shape	17.9	146.4	136.9	1.89E-30	1.89E-30	43.5
s(PC1) + s(PC2)	21.8	154.7	145.2	2.98E-32	2.98E-32	43.5
s(Temperature)	16	164.3	154.8	2.45E-34	2.45E-34	42.2
s(Depth) + Dive Shape	18.2	181.0	171.5	5.74E-38	5.74E-38	41.5
s(Depth)	16.3	190.8	181.2	4.48E-40	4.48E-40	40.6
s(PC1) + Dive Shape	16.8	195.5	186.0	4.17E-41	4.17E-41	40.4
s(PC1)	14.9	210.6	201.1	2.20E-44	2.20E-44	39.2
s(% Oxygen Saturation) + Dive Shape	15	229.0	219.5	2.21E-48	2.21E-48	37.9
s(% Oxygen Saturation)	8.9	254.8	245.3	5.44E-54	5.44E-54	35.4
Dive Shape	9.9	268.9	259.4	4.62E-57	4.62E-57	34.6
Intercept	7.9	282.1	272.6	6.46E-60	6.46E-60	33.4

Table S4. Sailfish tortuosity GAMM results.

SAILFISH						
Model	df	AIC	ΔAIC	Relative Liklihood	AICw	% Deviance Explained
s(PC1) + s(PC2) + Dive Shape	22.3	194.5	0.0	1.00E+00	8.69E-01	58.9
s(PC1) + s(PC2)	20.2	198.3	3.8	1.50E-01	1.30E-01	58.7
s(Temperature by Dive Shape)	18.7	209.9	15.4	4.60E-04	4.00E-04	58.1
s(PC1 by Dive Shape)	24.7	225.3	30.8	2.10E-07	1.83E-07	58
s(Temperature) + Dive Shape	16.0	242.4	47.9	4.03E-11	3.51E-11	56.8
s(Temperature)	11.8	251.0	56.5	5.34E-13	4.65E-13	56.2
s(PC1) + Dive Shape	14.3	253.0	58.5	2.02E-13	1.76E-13	56.3
s(PC1)	10.1	257.4	62.9	2.25E-14	1.96E-14	55.8
s(% Oxygen Saturation by Dive Shape)	15.5	260.2	65.7	5.54E-15	4.82E-15	56.1
s(% Oxygen Saturation) + Dive Shape	14.0	260.6	66.1	4.40E-15	3.82E-15	55.9
s(% Oxygen Saturation)	10.0	262.6	68.0	1.68E-15	1.46E-15	55.6
s(Depth by Dive Shape)	23.2	266.8	72.3	2.01E-16	1.74E-16	56.4
s(Depth) + Dive Shape	15.5	283.3	88.8	5.26E-20	4.57E-20	55.2
s(Depth)	11.0	285.9	91.4	1.42E-20	1.24E-20	54.8
Dive Shape	11.3	299.4	104.8	1.71E-23	1.49E-23	54.3
Intercept	7.2	300.9	106.4	7.97E-24	6.93E-24	53.9

Supplemental Figures

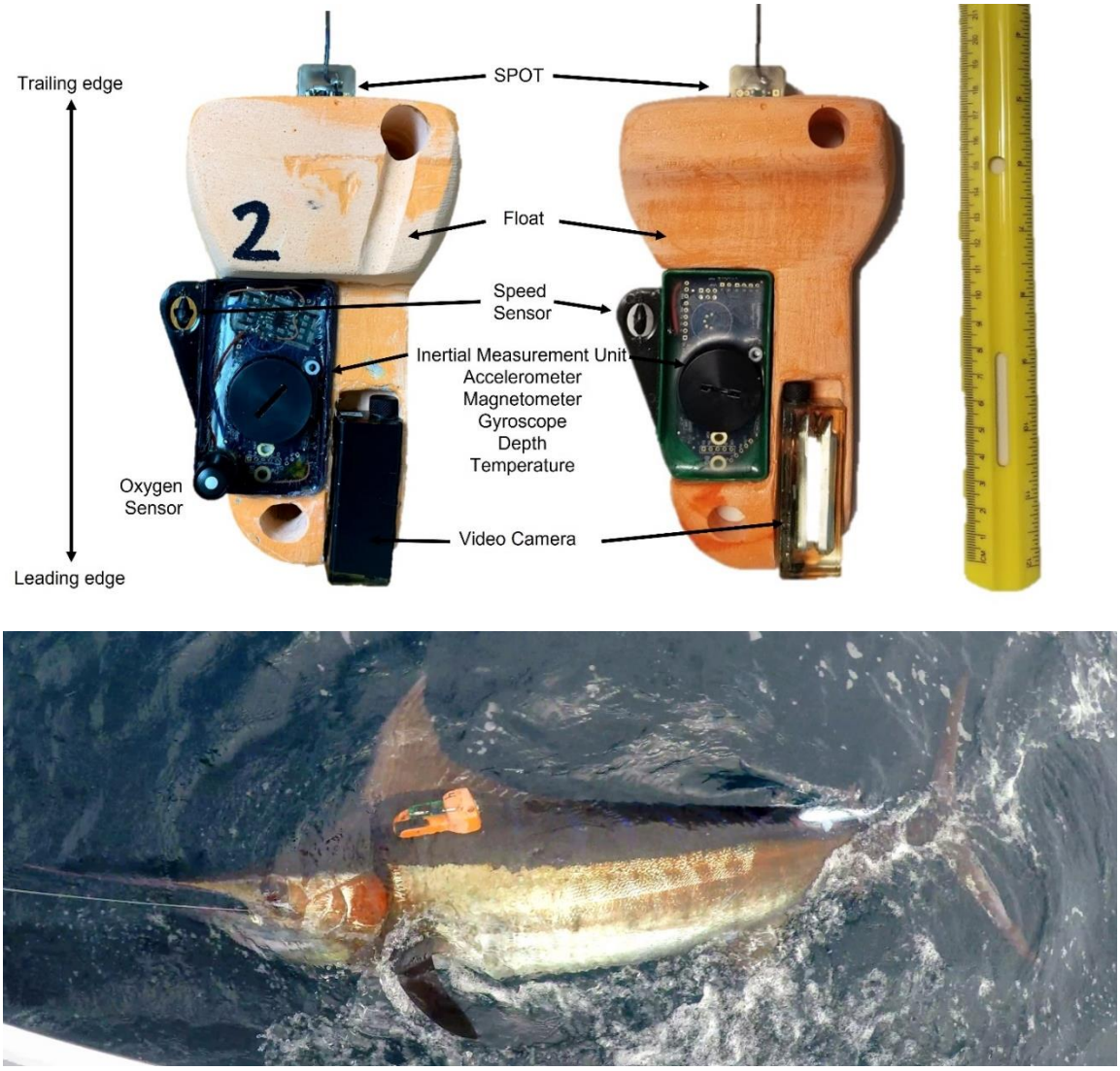

Supplemental Figure S1. Detailed view of the biologging tag package built to quantify blue marlin and sailfish fine scale behavior and habitat use with and without an oxygen sensor. The tag body (float) was constructed of a high-density mixture of microballoons and resin to achieve desired buoyancy. Tag dimensions were 18 × 7 cm at the leading edge, increasing to 18 × 10.5 cm at the trailing edge, with a weight of 335 g in air. The tag package consisted of a Smart Position and Temperature tag (SPOT-363A; Wildlife Computers, Redland, WA, USA) for package recovery, and an inertial measurement unit (IMU; OpenTag 3.0; Loggerhead Instruments, Sarasota, FL, USA). The IMU was comprised of a triaxial accelerometer, magnetometer, and gyroscope recording at 100 Hz, depth, temperature, and a small turbine-based fluid speed sensor recording at 1 Hz. A video camera was also housed in the tag package (DVL 2000M130; Little Leonardo, Tokyo, Japan). Finally, a subset of IMUs were equipped with a small (12 mm diameter × 20 mm long) oxygen sensor (Micro Probe; OxyGuard, Farum, Denmark) that recorded *in situ* dissolved oxygen (% saturation) of the water at 1 Hz. Below is an image of a blue marlin tagged with the tag package in the desired location and orientation.

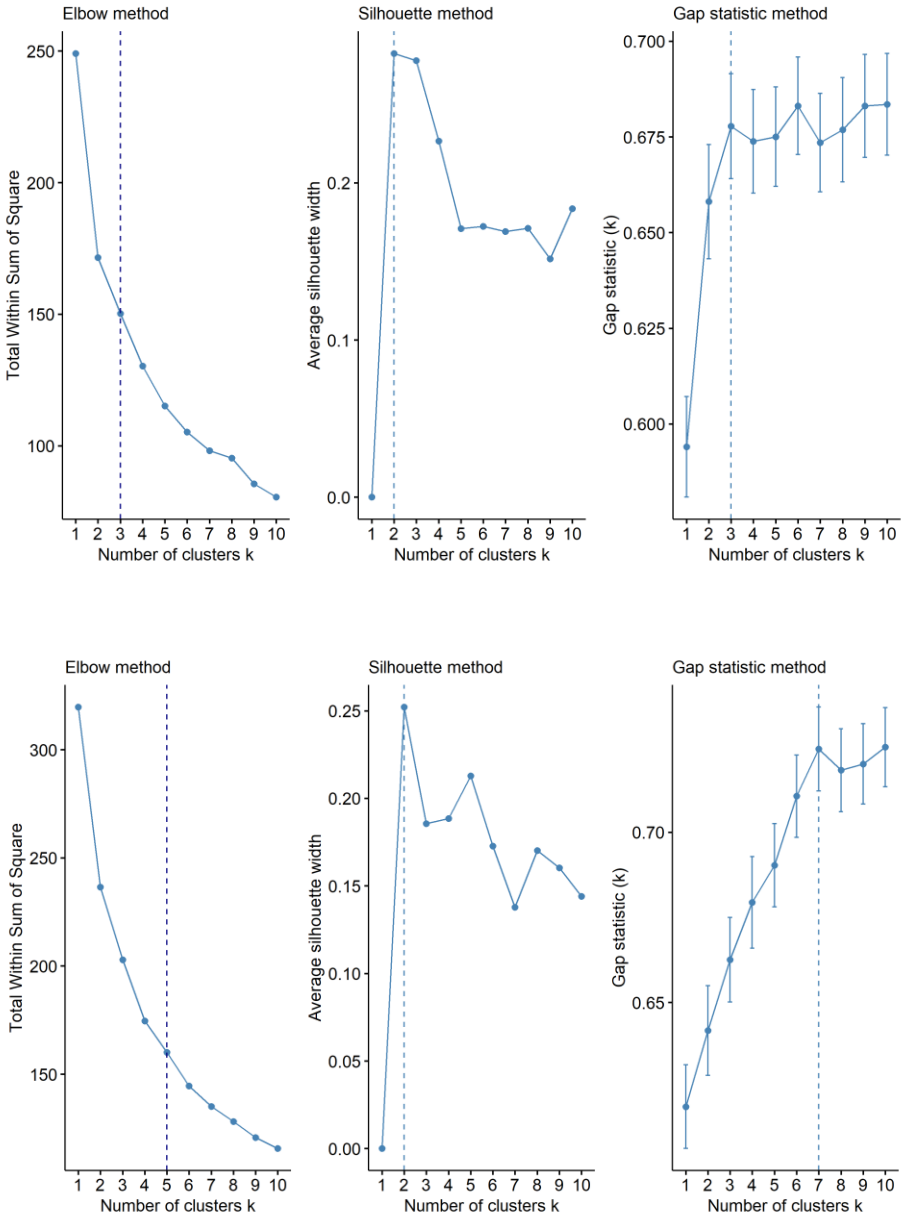

Supplemental Figure S2. Various methods used to determine the optimal number of dive shapes (i.e., clusters) for blue marlin (top) and sailfish (bottom). The elbow method, the silhouette method and the gap statistic method were compared and evaluated for biological realism and the number of clusters shared by the majority of methods was selected.

Appendix C: Chapter IV Supplemental Information

Supplemental Methods

1. Swim Speed and Drag

To calibrate the turbine speed sensor with water velocity, the completed tag package was placed into a 90-L Loligo swim tunnel respirometer with a flow-meter, resulting in a measured linear relationship of m/s = 0.022 * rotations/s + 0.25 ($r^2 = 0.99$, $p < 0.0001$; Fig. S1). It was found that the turbine requires a minimum flow speed of ~ 0.25 m/s to turn, therefore, after the calibration step any calculated speed of $\leq$ 0.25 m/s was set to 0.25 m/s to not underestimate.

While this calibration step in the flume was necessary, these are ideal conditions and may not be representative of the situation once it is attached to a fish. To ensure that the speed sensor in the flume accurately represents the velocity once it is attached to a fish, we compared the speed measured by the impeller to another established method of calculating speed via the vertical velocity of the fish (ms^{-1}) and the body pitch angle derived from the accelerometer, using body pitch angles of > 20° (Gleiss et al., 2011; Andrzejaczek et al., 2020). We regressed the vertical velocity (m/s) and body pitch angle method against the speed measured by the impeller attached to the tag. The blue line is the linear regression of the two, and the black line represents a 1:1 relationship. In general, the tag speed sensor matches the calculated speed method with some variability ($p < 0.001$, $r^2 = 0.7$, $y = 1.03x - 0.02$). The advantage of using the impeller is we are still able to obtain a speed measurement at low body pitch angles or at times when the fish is at a constant depth.

Finally, while there is little doubt that the tag had some effect on the drag of the sailfish, in the absence of swim tunnel experiments with and without a tag, we cannot say with certainty

exactly how much, and how this may have affected the sailfish's behavior. However, using cross-sectional area measurements from the largest section of a similarly sized sailfish (just posterior to the head; where the tag was placed) (Sagong et al., 2013) we calculated the drag acting on a body of that area using the equation $F_D = 0.5C\rho Av^2$, where C is the drag coefficient (0.24 [unitless]) (Sagong et al., 2013), ρ is the density of seawater at 27°C [1023 kg m^{-3}], A is the area of the object (cross-sectional area; 0.025 m^2), and ν is the velocity of the object (1 m/s). This resulted in a drag of 3.1 N acting on the sailfish. Because the tag was designed to be as hydrodynamic as possible, it is narrower at the leading edge (facing in the direction of travel) and gets thicker at the trailing edge (seen in figure 1 and figure S1). Using the cross-sectional area from the narrow end of the tag (0.001 m^2) and a drag coefficient of 0.6, we calculated an added drag of 0.3 N, or 9% of the drag on the sailfish. Using the largest portion of the tag for the cross-sectional area (0.0026 m^2), we calculated a drag of 0.79 N, or roughly 25% of the drag acting on the sailfish. While we cannot say exactly how this may have impacted behavior in the absence of behavioral data without a tag, Sagong et al. (2013) found that there was a 21.5% increase in the drag when they attached pectoral fins to their specimens. As such, a 9-25% increase from the tag does not appear to be a major increase, but there is undoubtedly some effect of tag attachment which may lead to an underestimation of metabolic rate estimates.

2. Proxy Species Selection & Metabolic Rate Calculation

Obtaining direct measurements of oxygen consumption at varying mass, swim speeds and activity levels is not currently feasible for sailfish. However, recent studies indicate that lifestyle, trophic level, and morphology are correlated with metabolic rate such that pelagic, upper trophic level fishes with similar morphology (e.g. high caudal fin aspect ratio, gill surface area) exhibit similar and elevated metabolic rates (Killen et al., 2010; Killen et al., 2016c; Bigman et al., 2021;

Norin and Speers-Roesch, 2021). As such, sailfish may have metabolic demands comparable to dolphinfish (Coryphaena hippurus; Brill, 1996), another subtropical epipelagic predator with comparable ecological interactions (Amezcua Gómez, 2007). Additionally, the gill surface area to body mass ratio is very similar between dolphinfish and the closely related striped marlin (*Kajikia audax*) (Wegner et al., 2010), indicating similar oxygen uptake capabilities between dolphinfish and istiophorid billfishes regardless of body size, further suggesting dolphinfish provide a suitable proxy for sailfish metabolic rate. Although sailfish possess cranial endothermy and warm their brain and retina with a specialized thermogenic organ that sits beneath the brain, the rest of the body is ectothermic and does not retain metabolic heat (Block, 1986). Therefore, we did not feel that a subtropical scombrid with endothermy, such as yellowfin tuna (*Thunnus albacares*), which warm their muscle, viscera and brain via vascular counter-current heat exchangers, were an acceptable proxy species for this study (Block and Finnerty, 1994). Although dolphinfish are smaller than the sailfish tagged in the present study, the effects of body size on swimming metabolic rates in fishes can be removed by using swim speed relative to body length (Beamish, 1978). More specifically, log swimming metabolic rates plotted against swim speed relative to body length produce similar straight lines independent of body size of the fish (Beamish, 1978). Owing to the lack of direct measurements of swimming metabolic rates for larger fishes with regional endothermy, data for dolphinfish was regarded as the best available information. Therefore, we took the equation of the line ($y = 0.1168x^2 – 0.6457x + 1.1994$) used to describe the relationship between the cost of transport ($mgO_2\ kg^{-1}\ m^{-1}$) and swim speed (U; BL s^{-1}) of dolphinfish in the control group (no oil exposure) of (Stieglitz et al., 2016) . We then converted cost of transport to mass-specific oxygen consumption ($\dot{M}O_2$, $mgO_2\ kg^{-1}\ h^{-1}$) by multiplying by both the mean fork length of dolphinfish in the control group (0.291 m) and 3600

s. Oxygen consumption (MO_2; $mgO_2\ kg^{-1}\ h^{-1}$) at various swim speeds was estimated using the equation $\log(MO_2) = [cU + \log(d)]$, where c and d are the slope and intercept of the logarithmic regression, and U is the swim speed (BLs^{-1}) after correcting for the BL of the sailfish (Figure S3). By correcting for the body length of the sailfish, the range of BLs^{-1} for the sailfish spans 0.08-0.63 BLs^{-1}, accounting for the majority of our observed speed data, and we linearly extrapolate to higher swim speeds (Figure S3). MO_2 was calculated continuously for every speed measurement throughout the 24 hours from the sailfish tag data, and we then took the inverse log of MO_2 and corrected for mass of the dolphinfish (M_D) in (Stieglitz et al., 2016) to obtain VO_2 ($mgO_2\ h^{-1}$). Oxygen consumption for the 40 kg sailfish was then calculated using the equation:

$$\mathrm{AMR_E} = VO_2 \left(\frac{M_S}{M_D}\right)^b$$

where AMR_E is the estimated active metabolic rate ($mgO_2\ h^{-1}$), VO_2 is the oxygen consumption at each swim speed ($mgO_2\ h^{-1}$), b is the mass scaling exponent, and M_S is the sailfish mass (kg). We corrected AMR_E for temperature by multiplying by Q_{10}^((T_2-T_1)/10) (Schmidt-Nielsen, 1997), where Q_{10} is the increase in standard metabolism with an increase in 10°C, T_1 is the temperature the dolphinfish were tested at in (Stieglitz et al., 2016), and T_2 was the continuous temperature experienced by the sailfish, with Q_{10} set to 1.83 (Clarke and Johnston, 1999; Killen et al., 2010). AMR_E was then made mass-specific to the estimated mass of the sailfish and corrected to units of $mgO_2\ kg^{-1}\ h^{-1}$.

3. Energy Expenditure and Prey Consumption

To estimate the amount of energy expended over the course of the 24-h period and during the predation event, we first converted the AMR_E from $mgO_2\ kg^{-1}\ h^{-1}$ to $kJ\ kg^{-1}\ h^{-1}$ by multiplying by the oxy caloric coefficient of 0.013 $kJ\ mgO_2^{-1}$. Because we sum across seconds, we then divide this by 3600 leaving $kJ\ kg^{-1}\ sec^{-1}$, and finally multiplied by the estimated mass of the

sailfish (40 kg), leaving an estimate of kJ burned sec^{-1} for the sailfish. Each value of kJ sec^{-1} was then summed across each period (the entire day or just the predation event; Table 2 of the main text) to determine energy expended. Finally, to estimate the daily amount of prey needed to maintain metabolic costs, we used the mean AMR_E of the 24 h period, converted it from mgO_2 kg^{-1} h^{-1} to kJ kg^{-1} h^{-1}, then to kJ. This value was then divided by the estimated energy content of the tuna (5.1 kJ), to arrive at 0.5 tuna d^{-1} to sustain daily AMR_E.

Supplemental Tables

Table S1. Mean ± SD of the normal distributions used when randomly sampling parameter values for b, c, d and dolphinfish mass (M_D) used in the 10,000 iterations when calculating the range of possible values of estimated active metabolic rate (AMR_E) of the sailfish.

Parameter	Value	Reference
b	0.79 ± 0.1	(Clarke and Johnston, 1999; Killen et al., 2010; Payne et al., 2015; Brodie et al., 2016)
c	0.9 ± 0.09	Estimated from regression of log(MO_2) ~ sailfish swim speed, back calculated from (Stieglitz et al., 2016)
d	2.6 ± 0.04	Estimated from regression of log(MO_2) ~ sailfish swim speed, back calculated from (Stieglitz et al., 2016)
M_D (g)	278 ± 23	(Stieglitz et al., 2016)

Table S2. Estimated metabolic rate for the 25th percentile, median and 75th percentile during the pursuit dive with and without applying a temperature correction to the calculations.

With Temperature Correction			Without Temperature Correction		
	AMR_E (mgO2/kg/h)	Energy Expenditure		AMR_E (mgO2/kg/h)	Energy Expenditure
25th percentile	361 ± 390	0.02	25th percentile	429 ± 514	0.03
Median	518 ± 586	0.04	Median	618 ± 773	0.05
75th percentile	748 ± 874	0.06	75th percentile	894 ± 1153	0.07

Table S3. Overall estimated metabolic rate for the 25th percentile, median and 75th percentile over the course of 24 hours with and without applying a temperature correction to the calculations.

With Temperature Correction			Without Temperature Correction		
	AMR_E (mgO2/kg/h)	Energy Expenditure		AMR_E (mgO2/kg/h)	Energy Expenditure
25th percentile	156 ± 48	1.9	25th percentile	157 ± 58	1.9
Median	219 ± 70	2.7	Median	220 ± 85	2.7
75th percentile	307 ± 102	3.8	75th percentile	308 ± 125	3.9

Supplemental Figures

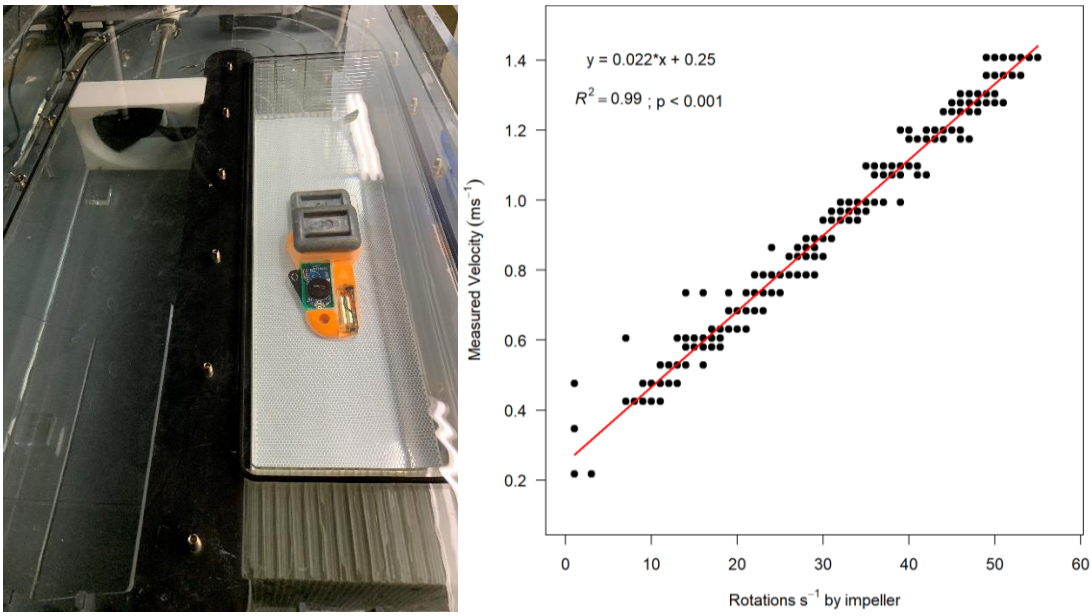

Figure S1. Completed biologging tag package in 90 L Loligo swim tunnel, and associated linear regression of swim speed calibration.

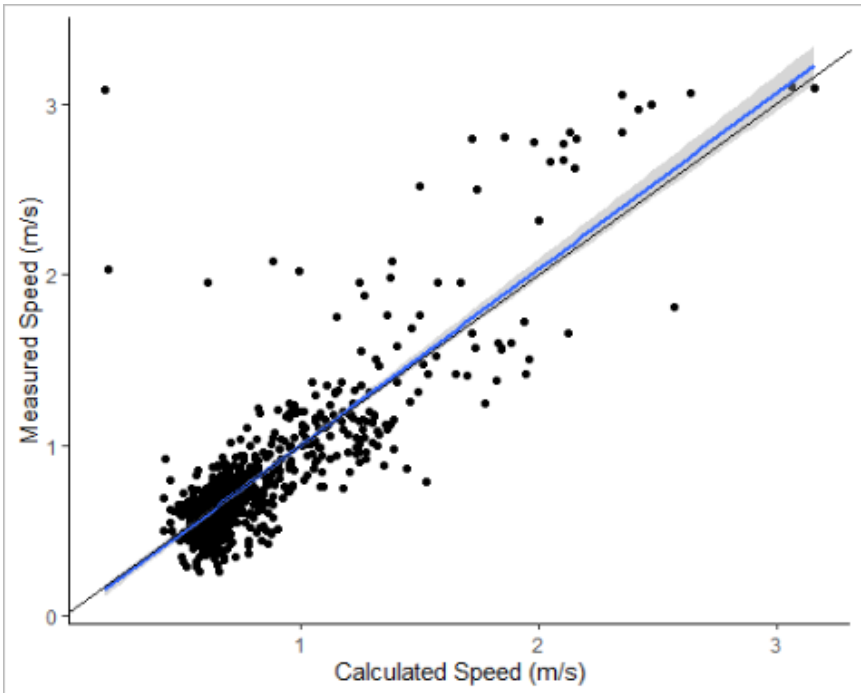

Figure S2. Linear regression (blue line) of the speed measured by the animal-borne impeller (Measured Speed (m/s)) and the calculated speed using the equation speed (m/s) = vertical velocity (m/s) / sin(φ), where φ is the body pitch. $p < 0.001$, $r^2 = 0.7$, $y = 1.03x - 0.02$. The black line represents a 1:1 relationship.

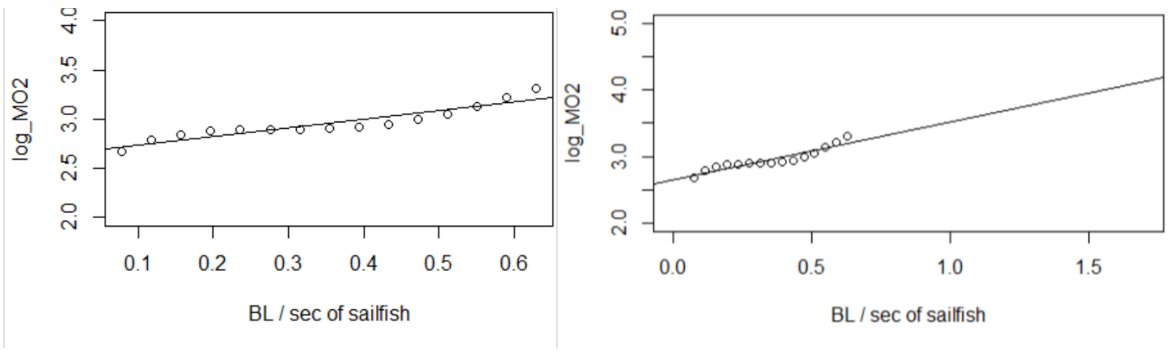

Figure S3. Logarithmic regression of dolphinfish (*Coryphaena hippurus*) oxygen consumption (MO_2), back-calculated from (Stieglitz et al., 2016) and swimming speed (body length [BL] s^{-1}), corrected for BL of the sailfish. Measured values correspond to those measured in (Stieglitz et al., 2016) (1-4 BLs^{-1} of dolphinfish = 0.08 – 0.63 BLs^{-1} of sailfish; left), and linearly extrapolated over the range of swimming speeds observed from the sailfish tagged in the present study (right).

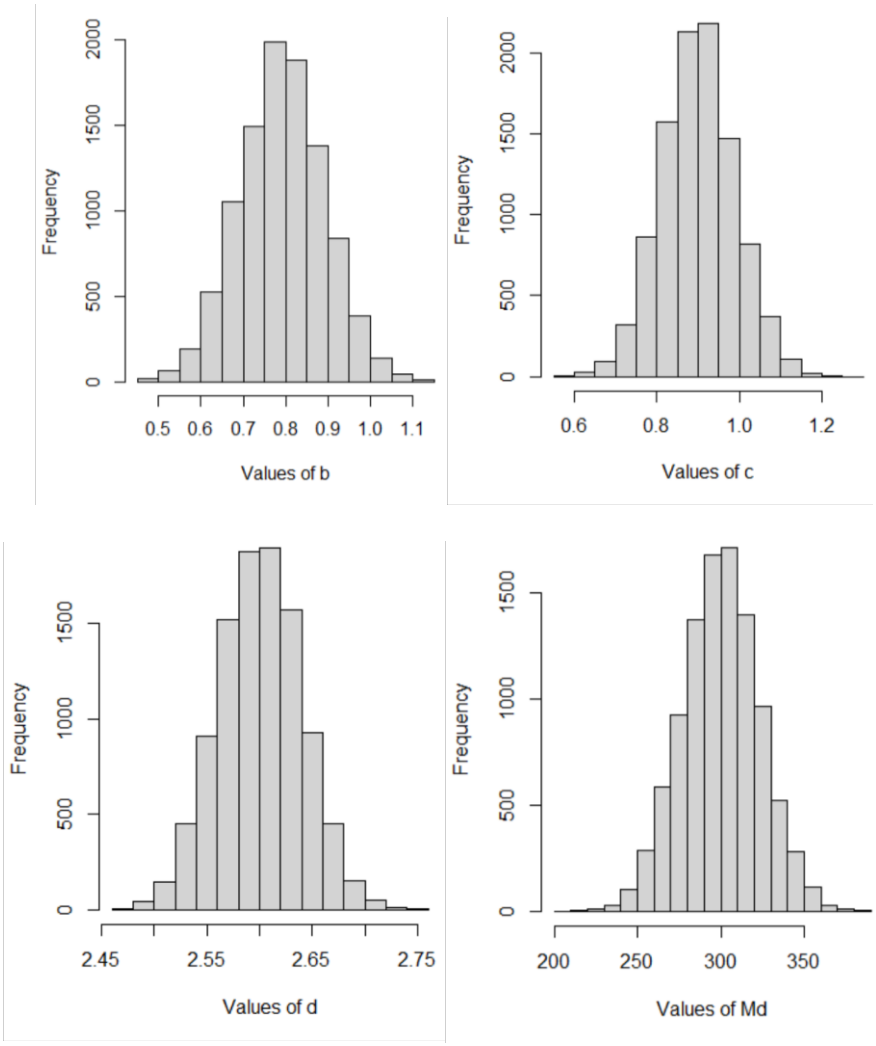

Figure S4. Histograms displaying the possible values of b, c, d and M_D used in the 10,000 iterations when calculating the estimated active metabolic rate (AMR_E) of the sailfish.

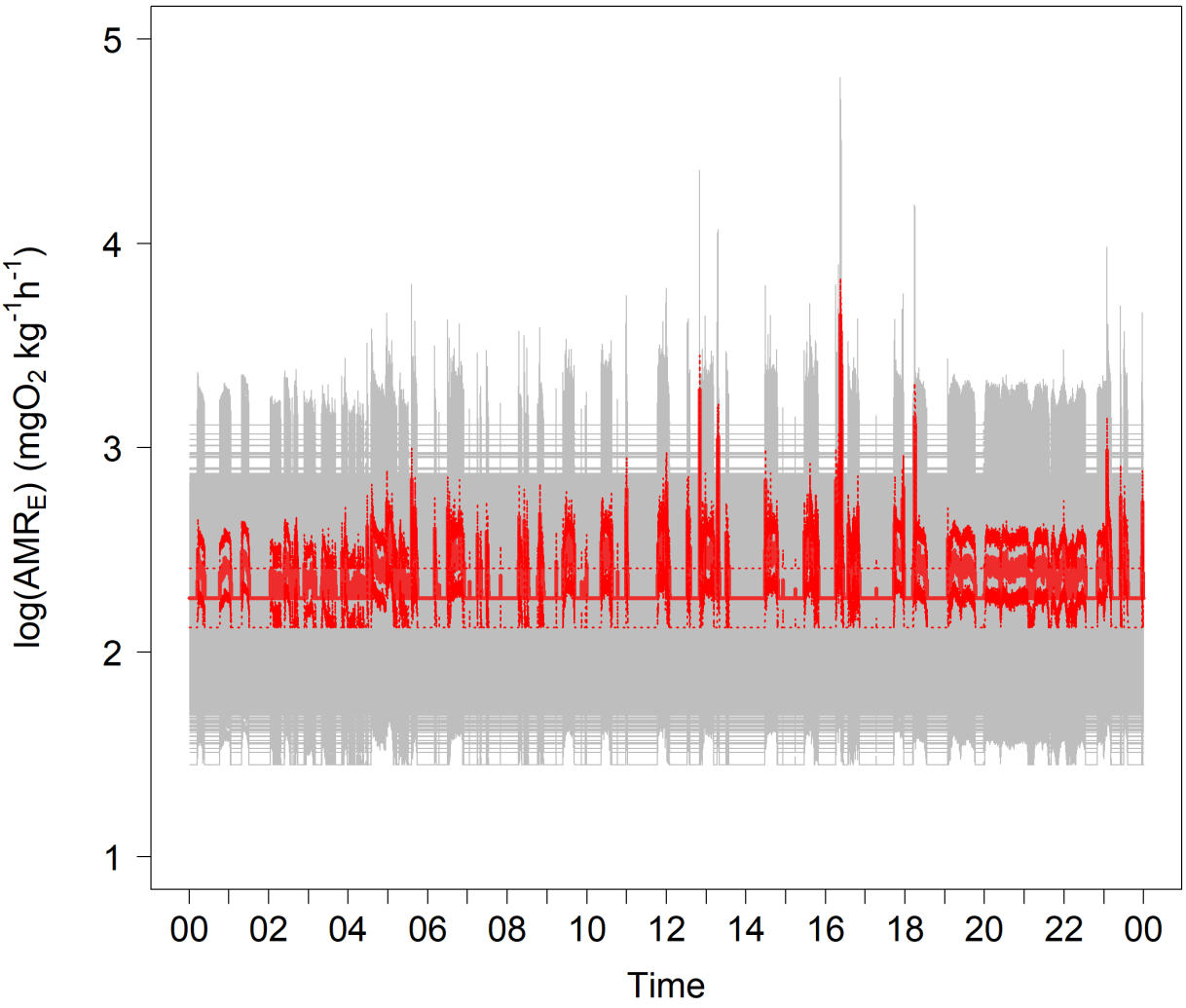

Figure S5. Output of the log transformed estimated active metabolic rate (AMR_E; mgO_2 kg^{-1} h^{-1}) from the 10,000 iterations over the 24 h period. AMR_E was calculated as the median of the 10,000 samples (solid red line), with the interquartile range (25 - 75%) taken to represent a range of probable AMR_E values (dotted red lines).

Appendix D: Chapter V Supplemental Information

Supplemental Tables

Table S1. Fixed effect estimates from a linear mixed effects model, testing if the number of time-series messages received was significantly different among species.

	Value	SE	DF	T	p
Intercept	409	27.8	3613	14.7	0.0
BUM	51.1	38.9	63	1.3	0.19
SFA	40.6	41.4	63	0.9	0.33

Table S2. Summary table of linear mixed effects models and multiple comparisons of means.

Model	df	AIC	delAIC	Estimate	Std Error
Mean Bottom Depth ~ Species + Individual + Date | Individual	6	21331	376		
BUM – BAM				6.8	1.5
SFA – BAM				8.7	1.6
SFA – BUM				1.9	1.6
Max Depth ~ Species + Individual + Date | Individual	6	29615	129		
BUM – BAM				20.7	4.6
SFA – BAM				27.3	4.8
SFA – BUM				6.6	4.8
Bottom Time ~ Species + Individual + Date | Individual	6	42132	267		
BUM – BAM				107	52
SFA – BAM				-64.9	53.5
SFA – BUM				-171.9	53
Bottom Distance ~ Species + Individual + Date | Individual	6	22740	138		
BUM – BAM				7.2	1.6
SFA – BAM				7.8	1.7
SFA – BUM				0.6	1.6
Number of Dives ~ Species + Individual + Date | Individual	6	23354	131		
BUM – BAM				1.1	2.3
SFA – BAM				14.9	2.5
SFA – BUM				13.8	2.5
Dive Duration ~ Species + Individual + Date | Individual	6	44463	28		
BUM – BAM				260.8	81.8
SFA – BAM				-9.3	84.2
SFA – BUM				-270.1	83.5

Supplemental Figures

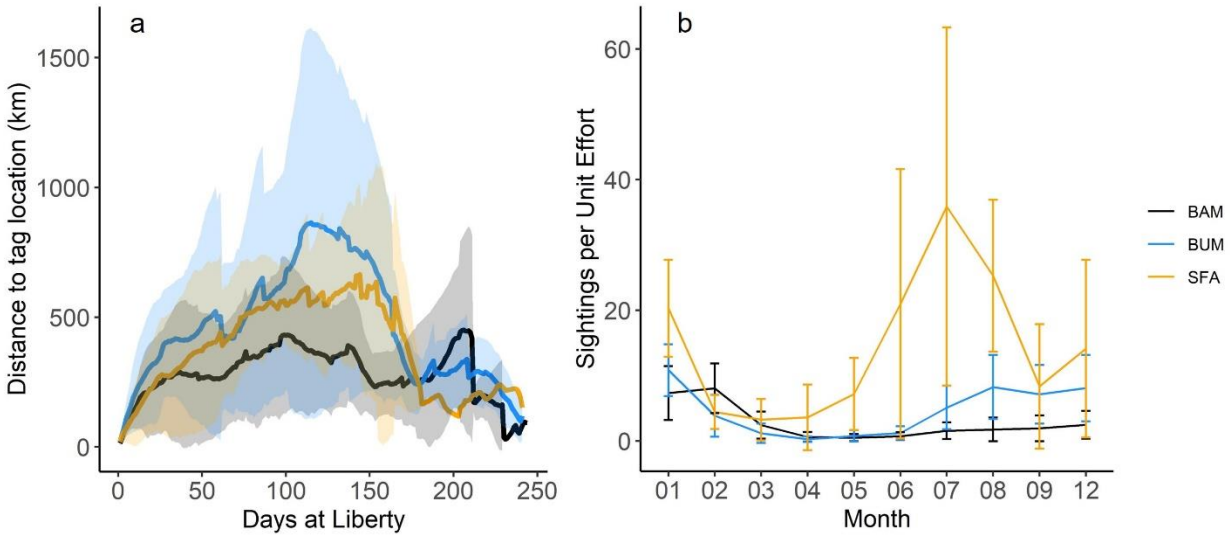

Figure S1. Mean and standard deviation (solid line and colored shading) distance from the tagging location (offshore Tropic Star Lodge; ~ 7.5 N, 78.2 W) compared to days at liberty (a) and the mean (± SD) sightings per unit effort (SPUE, see methods) by month at Tropic Star Lodge from 2010 – 2020 catch records (b) for black marlin (BAM), blue marlin (BUM) and sailfish (SFA). Note that Tropic Star Lodge closes October and much of November so these months were omitted from analysis.

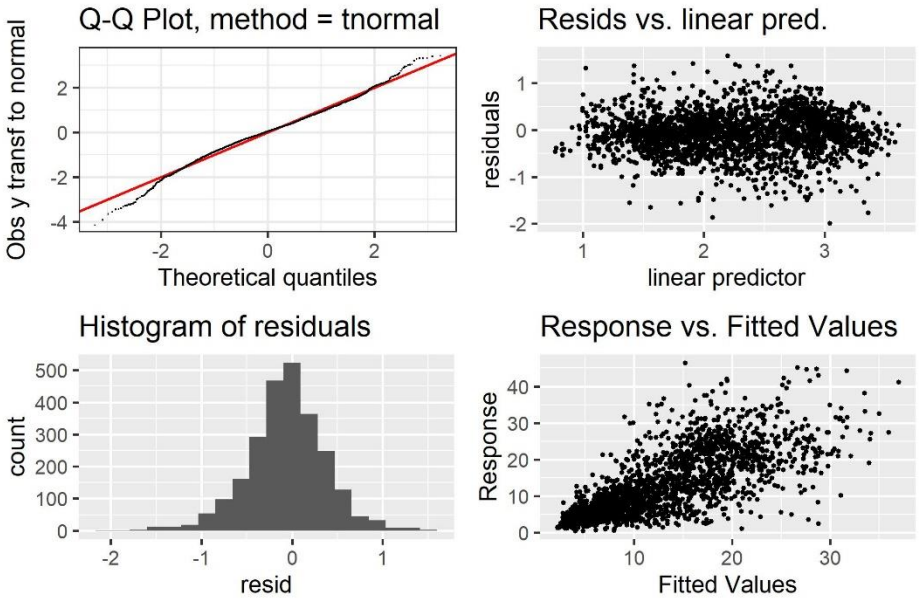

Figure S2. Fitted GAMM model diagnostics.

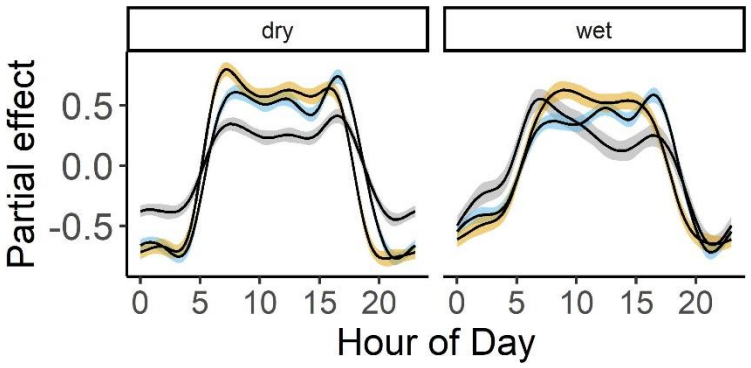

Figure S3. Mean depth GAMM response curves for the wet season and dry season for blue marlin (blue), black marlin (grey) and sailfish (orange).

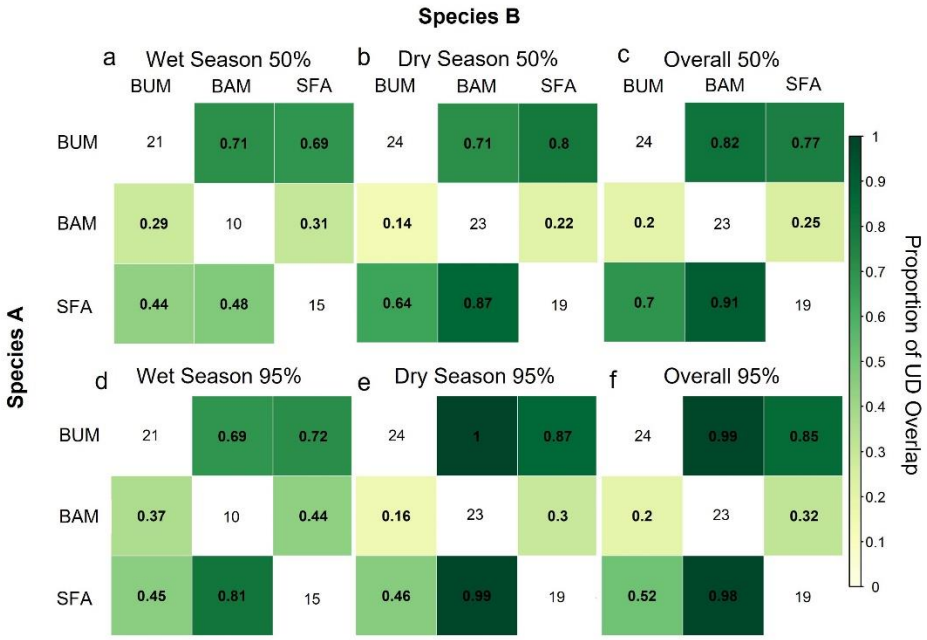

Figure S4. Proportion of utilization distribution (UD) overlap for black marlin (BAM), blue marlin (BUM) and sailfish (SFA) 50% and 95% 3D UDs for wet season, dry season, and overall. Sample size of fish used in each UD is listed on the diagonal. Two different overlap estimates are presented for each species comparison based on whether the total trophic niche of species A is being compared to species B, or vice versa (e.g. in (a), BUM overlaps 71% of BAM 50% UD, whereas BAM overlaps 29% of BUM 50% UD).

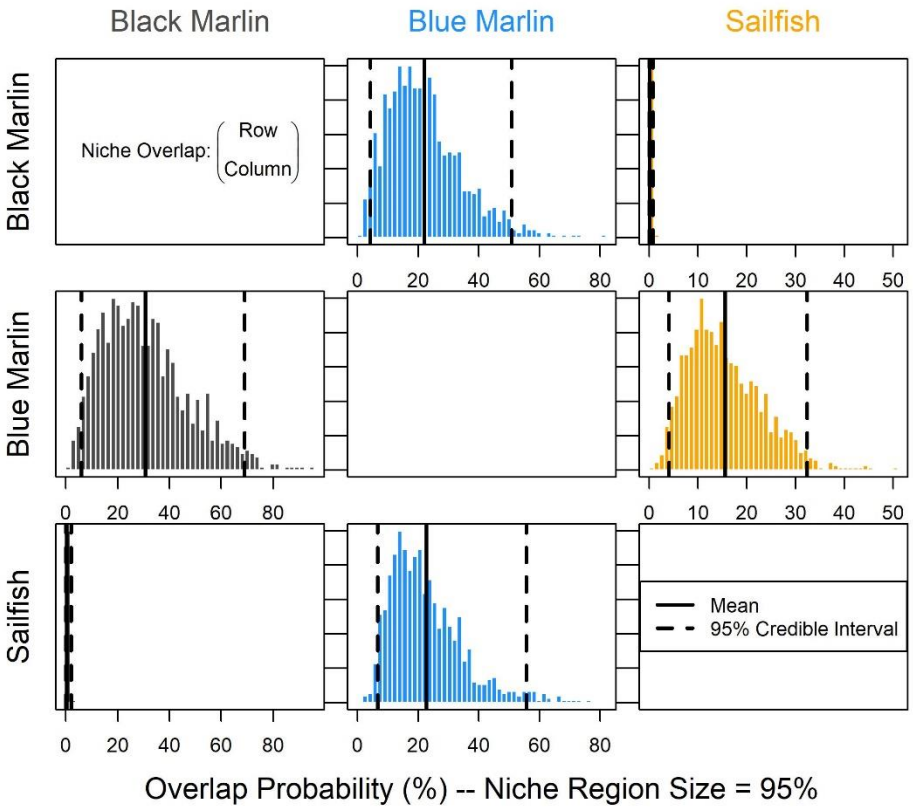

Figure S5. Posterior density distributions from Bayesian trophic niche overlap estimates for black marlin, blue marlin, and sailfish. Dashed lines represent 95% credible intervals and solid lines represent means overlap estimates.

Literature Cited

Abitia-Cardenas LA, Galvan-Magaña F, Rodriguez-Romero J. 1997. Food habits and energy values of prey of striped marlin, Tetrapturus audax, off the coast of Mexico. Fishery Bulletin:360-368.

Adachi T, Costa DP, Robinson PW, Peterson SH, Yamamichi M, Naito Y, Takahashi A. 2017. Searching for prey in a three-dimensional environment: hierarchical movements enhance foraging success in northern elephant seals. Functional Ecology 31:361-369.

Amezcua Gómez CA. 2007. Relaciones tróficas entre el pez vela (Istiophorus platypterus) y el dorado (Coryphaena hippurus) en la costa de los estados de Jalisco y Colima, México. In: Instituto Politécnico Nacional. Centro Interdisciplinario de Ciencias Marinas. p 110.

Anderson J, Spurgeon E, Stirling B, May JI, Rex P, Hyla B, McCullough S, Thompson M, Lowe C. 2022. High resolution acoustic telemetry reveals swim speeds and inferred field metabolic rates in juvenile white sharks (*Carcharodon carcharias*). PLoS ONE 17.

Andrzejaczek S, Gleiss AC, Lear KO, Pattiaratchi C, Chapple TK, Meekan MG. 2020. Depth-dependent dive kinematics suggest cost-efficient foraging strategies by tiger sharks. Royal Society open science 7:200789.

Andrzejaczek S, Gleiss AC, Lear KO, Pattiaratchi CB, Chapple T, Meekan M. 2019. Biologging tags reveal links between fine-scale horizontal and vertical movement behaviours in tiger sharks (Galeocerdo cuvier). Frontiers in Marine Science 6:229.

Arostegui MC, Gaube P, Woodworth-Jefcoats PA, Kobayashi DR, Braun CD. 2022. Anticyclonic eddies aggregate pelagic predators in a subtropical gyre. Nature 609:535-540.

Arthur PG, West TG, Brill RW, Schulte PM, Hochachka PW. 1992. Recovery metabolism of skipjack tuna (*Katsuwonus pelamis*) white muscle: rapid and parallel changes in lactate and phosphocreatine after exercise. Canadian Journal of Zoology 70:1230-1239.

Austin D, Bowen WD, McMillan JI, Iverson SJ. 2006. Linking movement, diving, and habitat to foraging success in a large marine predator. Ecology 87:3095-3108.

Bailleul F, Charrassin J-Bt, Ezraty R, Girard-Ardhuin F, McMahon CR, Field IC, Guinet C. 2007. Southern elephant seals from Kerguelen Islands confronted by Antarctic Sea ice. Changes in movements and in diving behaviour. Deep Sea Research Part II: Topical Studies in Oceanography 54:343-355.

Bakun A. 2022a. Adjusting intuitions as to the role of oxygen constraints in shaping the ecology and dynamics of ocean predator–prey systems. Environmental Biology of Fishes:1-13.

Bakun A. 2022b. Vertical ambush corridors: Intriguing multi-mechanism ecological structures embedded in the kinetic fluid architectures of ocean living resource production systems. Fish and Fisheries.

Baum JK, Worm B. 2009. Cascading top-down effects of changing oceanic predator abundances. Journal of Animal Ecology 78:699-714.

Beamish F. 1978. Swimming capacity. In 'Fish Physiology. Vol. VII'.(Eds WS Hoar and DJ Randall.) pp. 101–187. In: Academic Press: New York.

Beck CA, Bowen WD, McMillan JI, Iverson SJ. 2003. Sex differences in the diving behaviour of a size-dimorphic capital breeder: the grey seal. Animal Behaviour 66:777-789.

Bergman JN, Bennett JR, Binley AD, Cooke SJ, Fyson V, Hlina BL, Reid CH, Vala MA, Madliger CL. 2019. Scaling from individual physiological measures to population-level demographic change: case studies and future directions for conservation management. Biological Conservation 238:108242.

Bernal D, Brill RW, Dickson KA, Shiels HA. 2017. Sharing the water column: physiological mechanisms underlying species-specific habitat use in tunas. Reviews in Fish Biology and Fisheries 27:843-880.

Bernal D, Sepulveda C, Musyl M, Brill RW. 2010. The eco-physiology of swimming movement patterns of tunas, billfishes and large pelagic sharks. In: Domenici P, Kapoor BG, editors. Fish Locomotion: an eco-ethological perspective. Enfield, NH, USA: Science Publishers. pp 437-483.

Bertrand A, Ballon M, Chaigneau A. 2010. Acoustic observation of living organisms reveals the upper limit of the oxygen minimum zone. PLoS one 5:e10330.

Bertrand A, Barbieri MA, Gerlotto F, Leiva F, Córdova J. 2006. Determinism and plasticity of fish schooling behaviour as exemplified by the South Pacific jack mackerel Trachurus murphyi. Marine Ecology Progress Series 311:145-156.

Bestley S, Patterson TA, Hindell MA, Gunn JS. 2008. Feeding ecology of wild migratory tunas revealed by archival tag records of visceral warming. Journal of Animal Ecology 77:1223-1233.

Bianchi D, Galbraith ED, Carozza DA, Mislan K, Stock CA. 2013. Intensification of open-ocean oxygen depletion by vertically migrating animals. Nature Geoscience 6:545-548.

Bigman JS, M'Gonigle LK, Wegner NC, Dulvy NK. 2021. Respiratory capacity is twice as important as temperature in explaining patterns of metabolic rate across the vertebrate tree of life. Science Advances 7:eabe5163.

Blank JM, Farwell CJ, Morrissette JM, Schallert RJ, Block BA. 2007. Influence of swimming speed on metabolic rates of juvenile Pacific bluefin tuna and yellowfin tuna. Physiological and Biochemical Zoology 80:167-177.

Block B, Booth D, Carey F. 1992a. Depth and temperature of the blue marlin, Makaira nigricans, observed by acoustic telemetry. Marine Biology 114:175-183.

Block BA. 1986. Structure of the brain and eye heater tissue in marlins, sailfish, and spearfishes. Journal of Morphology 190:169-189.

Block BA. 2005. Physiological ecology in the 21st century: advancements in biologging science. Integrative and Comparative Biology 45:305-320.

Block BA, Booth D, Carey FG. 1992b. Direct measurement of swimming speeds and depth of blue marlin. Journal of Experimental Biology 166:267-284.

Block BA, Finnerty JR. 1994. Endothermy in fishes: a phylogenetic analysis of constraints, predispositions, and selection pressures. Environmental Biology of Fishes 40:283-302.

Botsford LW, Castilla JC, Peterson CH. 1997. The management of fisheries and marine ecosystems. Science 277:509-515.

Braun CD, Arostegui MC, Thorrold SR, Papastamatiou YP, Gaube P, Fontes J, Afonso P. 2022. The functional and ecological significance of deep diving by large marine predators. Annual Review of Marine Science 14:129-159.

Braun CD, Kaplan MB, Horodysky AZ, Llopiz JK. 2015. Satellite telemetry reveals physical processes driving billfish behavior. Animal Biotelemetry 3:2.

Brill RW. 1987. On the standard metabolic rates of tropical tunas, including the effect of body size and acute temperature change. Fisheries Bulletin 85:25-35.

Brill RW. 1996. Selective advantages conferred by the high performance physiology of tunas, billfishes, and dolphin fish. Comparative Biochemistry and Physiology Part A: Physiology 113:3-15.

Brill RW, Holts D, Chang R, Sullivan S, Dewar H, Carey F. 1993. Vertical and horizontal movements of striped marlin (*Tetrapturus audax*) near the Hawaiian Islands, determined by ultrasonic telemetry, with simultaneous measurement of oceanic currents. Marine Biology 117:567-574.

Brill RW, Lowe TE, Cousins KL. 1998. How water temperature really limits the vertical movements of tunas and billfishes–it's the heart stupid. In: International Congress on Biology of Fish. American Fisheries Society, Towson University. p 4.

Brill RW, Lutcavage ME. 2001. Understanding environmental influences on movements and depth distributions of tunas and billfishes can significantly improve population assessments. In: American Fisheries Society Symposium: American Fisheries Society. pp 179-198.

Brodie S, Taylor MD, Smith JA, Suthers IM, Gray CA, Payne NL. 2016. Improving consumption rate estimates by incorporating wild activity into a bioenergetics model. Ecology and Evolution 6:2262-2274.

Brown JH, Gillooly JF, Allen AP, Savage VM, West GB. 2004. Toward a metabolic theory of ecology. Ecology 85:1771-1789.

Browning NE, Cockcroft VG, Worthy GA. 2014. Resource partitioning among South African delphinids. Journal of Experimental Marine Biology and Ecology 457:15-21.

Bubley WJ, Galuardi B, Dukes AW, Jenkins WE. 2020. Incorporating depth into habitat use descriptions for sailfish Istiophorus platypterus and habitat overlap with other billfishes in the western North Atlantic. Marine Ecology Progress Series 638:137-148.

Bushnell PG, Brill RW. 1991. Responses of swimming skipjack (Katsuwonus pelamis) and yellowfin (Thunnus albacares) tunas to acute hypoxia, and a model of their cardiorespiratory function. Physiological Zoology 64:787-811.

Byrne ME, Cortés E, Vaudo JJ, Harvey GCM, Sampson M, Wetherbee BM, Shivji M. 2017. Satellite telemetry reveals higher fishing mortality rates than previously estimated, suggesting overfishing of an apex marine predator. Proceedings of the Royal Society B: Biological Sciences 284:20170658.

Carey F, Scharold J, Kalmijn AJ. 1990. Movements of blue sharks (Prionace glauca) in depth and course. Marine biology 106:329-342.

Carlisle AB, Kochevar RE, Arostegui MC, Ganong JE, Castleton M, Schratwieser J, Block BA. 2017. Influence of temperature and oxygen on the distribution of blue marlin (Makaira nigricans) in the Central Pacific. Fisheries Oceanography 26:34-48.

Carroll G, Brodie S, Whitlock R, Ganong J, Bograd SJ, Hazen E, Block BA. 2021. Flexible use of a dynamic energy landscape buffers a marine predator against extreme climate variability. Proceedings of the Royal Society B 288:20210671.

Carter MID, Bennett KA, Embling CB, Hosegood PJ, Russell DJ. 2016. Navigating uncertain waters: a critical review of inferring foraging behaviour from location and dive data in pinnipeds. Movement Ecology 4:1-20.

Cherel Y, Le Corre M, Jaquemet S, Menard F, Richard P, Weimerskirch H. 2008. Resource partitioning within a tropical seabird community: new information from stable isotopes. Mar Ecol Prog Ser 366:281-291.

Chiang W-C, Musyl MK, Sun C-L, DiNardo G, Hung H-M, Lin H-C, Chen S-C, Yeh S-Z, Chen W-Y, Kuo C-L. 2015. Seasonal movements and diving behaviour of black marlin (Istiompax indica) in the northwestern Pacific Ocean. Fisheries Research 166:92-102.

Chittka L, Skorupski P, Raine NE. 2009. Speed–accuracy tradeoffs in animal decision making. Trends in ecology & evolution 24:400-407.

Clarke A, Johnston NM. 1999. Scaling of metabolic rate with body mass and temperature in teleost fish. Journal of animal ecology 68:893-905.

Coffey DM, Holland KN. 2015. First autonomous recording of in situ dissolved oxygen from free-ranging fish. Animal Biotelemetry 3:47.

Collette B, Carpenter K, Polidoro B, Juan-Jordá M, Boustany A, Die DJ, Elfes C, Fox W, Graves J, Harrison L. 2011. High value and long life—double jeopardy for tunas and billfishes. Science 333:291-292.

Collette B, Graves J. 2019. Tunas and billfishes of the world. Johns Hopkins University Press.

Collette BB, Aadland C. 1996. Revision of the frigate tunas (Scombridae, Auxis), with descriptions of two new subspecies from the eastern Pacific. Fishery Bulletin.

Collette BB, Di Natale A, Fox W, Juan Jorda M, Pohlot B, Schratwieser J, Graves J. 2022. *Istiompax indica*. The IUCN Red List of Threatened Species 2022: e.T170312A46646193. . In.

Combes S, Salcedo M, Pandit M, Iwasaki J. 2013. Capture success and efficiency of dragonflies pursuing different types of prey. Integrative and comparative biology 53:787-798.

Cooke S, Schramm H. 2007. Catch-and-release science and its application to conservation and management of recreational fisheries. Fisheries Management and Ecology 14:73-79.

Correa SB, Winemiller KO. 2014. Niche partitioning among frugivorous fishes in response to fluctuating resources in the Amazonian floodplain forest. Ecology 95:210-224.

Cremers J, Klugkist I. 2018. One direction? A tutorial for circular data analysis using R with examples in cognitive psychology. Frontiers in psychology 9:2040.

Croxall J, Prince P, Reid K. 1997. Dietary segregation of krill-eating South Georgia seabirds. Journal of Zoology 242:531-556.

D'Croz L, O'Dea A. 2007. Variability in upwelling along the Pacific shelf of Panama and implications for the distribution of nutrients and chlorophyll. Estuarine, Coastal and Shelf Science 73:325-340.

Dale JJ, Brodie S, Carlisle AB, Castleton M, Hazen EL, Bograd SJ, Block BA. 2022. Global habitat loss of a highly migratory predator, the blue marlin (Makaira nigricans). Diversity and Distributions 28:2020-2034.

Davie PS. 1990. Pacific marlins: anatomy and physiology. Massey University, Palmerston North, New Zealand.

Derenbach J, Astheimer H, Hansen H, Leach H. 1979. Vertical microscale distribution of phytoplankton in relation to the thermocline. Marine Ecology Progress Series 1:187-193.

Dickson KA. 1995. Unique adaptations of the metabolic biochemistry of tunas and billfishes for life in the pelagic environment. Environmental Biology of Fishes 42:65-97.

Dobson G, Wood S, Daxboeck C, Perry S. 1986. Intracellular buffering and oxygen transport in the Pacific blue marlin (*Makaira nigricans*): adaptations to high-speed swimming. Physiological zoology 59:150-156.

Domeier ML, Speare P. 2012. Dispersal of adult black marlin (Istiompax indica) from a Great Barrier Reef spawning aggregation. PLoS One 7:e31629.

Domenici P. 2001. The scaling of locomotor performance in predator–prey encounters: from fish to killer whales. Comparative Biochemistry and Physiology Part A: Molecular & Integrative Physiology 131:169-182.

Domenici P, Wilson A, Kurvers R, Marras S, Herbert-Read JE, Steffensen J, Krause S, Viblanc P, Couillaud P, Krause J. 2014. How sailfish use their bills to capture schooling prey. Proceedings of the Royal Society B: Biological Sciences 281:20140444.

Donaldson MR, Arlinghaus R, Hanson KC, Cooke SJ. 2008. Enhancing catch-and-release science with biotelemetry. Fish and Fisheries 9:79-105.

Dröge E, Creel S, Becker MS, M'soka J. 2017. Spatial and temporal avoidance of risk within a large carnivore guild. Ecology and evolution 7:189-199.

Dulvy NK, Baum JK, Clarke S, Compagno LJ, Cortés E, Domingo A, Fordham S, Fowler S, Francis MP, Gibson C. 2008. You can swim but you can't hide: the global status and conservation of oceanic pelagic sharks and rays. Aquatic Conservation: Marine and Freshwater Ecosystems 18:459-482.

Dulvy NK, Fowler SL, Musick JA, Cavanagh RD, Kyne PM, Harrison LR, Carlson JK, Davidson LN, Fordham SV, Francis MP. 2014. Extinction risk and conservation of the world's sharks and rays. elife 3:e00590.

Duong T. 2007. ks: Kernel density estimation and kernel discriminant analysis for multivariate data in R. Journal of Statistical Software 21:1-16.

Ehrhardt NM, Fitchett MD. 2006. On the seasonal dynamic characteristics of the sailfish, Istiophorus platypterus, in the eastern Pacific off Central America. Bulletin of Marine Science 79:589-606.

Elliott J, Davison W. 1975. Energy equivalents of oxygen consumption in animal energetics. Oecologia 19:195-201.

Estes JA, Heithaus M, McCauley DJ, Rasher DB, Worm B. 2016. Megafaunal impacts on structure and function of ocean ecosystems. Annual Review of Environment and Resources 41:83-116.

Evans R, McLain D, Bauer R. 1981. Atlantic Skipjack Tuna: Influences of Mean Environmental Conditions on Their Vulnerability to Surface Fishing Gear. Marine Fisheries Review 43:1-11.

Ferretti F, Worm B, Britten GL, Heithaus MR, Lotze HK. 2010. Patterns and ecosystem consequences of shark declines in the ocean. Ecology letters 13:1055-1071.

Fiedler PC. 2010. Comparison of objective descriptions of the thermocline. Limnology and Oceanography: Methods 8:313-325.

Fiedler PC, Lavín MF. 2017. Oceanographic conditions of the eastern tropical Pacific. In: Coral reefs of the eastern tropical Pacific. Springer. pp 59-83.

Fortune SM, Ferguson SH, Trites AW, Hudson JM, Baumgartner MF. 2020. Bowhead whales use two foraging strategies in response to fine-scale differences in zooplankton vertical distribution. Scientific reports 10:1-18.

Freitas C, Lydersen C, Fedak MA, Kovacs KM. 2008. A simple new algorithm to filter marine mammal Argos locations. Marine Mammal Science 24:315-325.

Fritsches K, Litherland L, Thomas N, Shand J. 2003a. Cone visual pigments and retinal mosaics in the striped marlin. Journal of fish biology 63:1347-1351.

Fritsches KA, Brill RW, Warrant EJ. 2005. Warm eyes provide superior vision in swordfishes. Current Biology 15:55-58.

Fritsches KA, Marshall NJ, Warrant EJ. 2003b. Retinal specializations in the blue marlin: eyes designed for sensitivity to low light levels. Marine and Freshwater Research 54:333-341.

Froese R, Pauly D. 2010. FishBase. In: Fisheries Centre, University of British Columbia.

Gabaldon J, Turner EL, Johnson-Roberson M, Barton K, Johnson M, Anderson EJ, Shorter KA. 2019. Integration, calibration, and experimental verification of a speed sensor for swimming animals. IEEE Sensors Journal 19:3616-3625.

Gallo N, Levin L. 2016. Fish ecology and evolution in the world's oxygen minimum zones and implications of ocean deoxygenation. Advances in marine biology 74:117-198.

Ghirlanda S, Frasnelli E, Vallortigara G. 2009. Intraspecific competition and coordination in the evolution of lateralization. Philosophical Transactions of the Royal Society B: Biological Sciences 364:861-866.

Gleiss AC, Norman B, Wilson RP. 2011. Moved by that sinking feeling: variable diving geometry underlies movement strategies in whale sharks. Functional Ecology 25:595-607.

Gleiss AC, Schallert RJ, Dale JJ, Wilson SG, Block BA. 2019. Direct measurement of swimming and diving kinematics of giant Atlantic bluefin tuna (Thunnus thynnus). Royal Society open science 6:190203.

Gleiss AC, Wright S, Liebsch N, Wilson RP, Norman B. 2013. Contrasting diel patterns in vertical movement and locomotor activity of whale sharks at Ningaloo Reef. Marine Biology 160:2981-2992.

Graves JE, Horodysky AZ. 2008. Does hook choice matter? Effects of three circle hook models on postrelease survival of white marlin. North American Journal of Fisheries Management 28:471-480.

Halsey L, Bost C-A, Handrich Y. 2007. A thorough and quantified method for classifying seabird diving behaviour. Polar Biology 30:991-1004.

Haulsee DE, Blondin HE, Logan RK, Crowder LB. 2022. Where do the billfish go? Using recreational catch data to relate local and basin scale environmental conditions to billfish occurrence in the Eastern Tropical Pacific. Fisheries Oceanography 31:135-148.

Hazen EL, Abrahms B, Brodie S, Carroll G, Jacox MG, Savoca MS, Scales KL, Sydeman WJ, Bograd SJ. 2019. Marine top predators as climate and ecosystem sentinels. Frontiers in Ecology and the Environment 17:565-574.

Hazen EL, Jorgensen S, Rykaczewski RR, Bograd SJ, Foley DG, Jonsen ID, Shaffer SA, Dunne JP, Costa DP, Crowder LB. 2013. Predicted habitat shifts of Pacific top predators in a changing climate. Nature Climate Change 3:234.

Hazen EL, Scales KL, Maxwell SM, Briscoe DK, Welch H, Bograd SJ, Bailey H, Benson SR, Eguchi T, Dewar H. 2018. A dynamic ocean management tool to reduce bycatch and support sustainable fisheries. Science advances 4:eaar3001.

Heithaus MR, Wirsing A, Dill L. 2012. The ecological importance of intact top-predator populations: a synthesis of 15 years of research in a seagrass ecosystem. Marine and Freshwater Research 63:1039-1050.

Herbert-Read JE, Romanczuk P, Krause S, Strömbom D, Couillaud P, Domenici P, Kurvers RH, Marras S, Steffensen JF, Wilson AD. 2016. Proto-cooperation: group hunting sailfish improve hunting success by alternating attacks on grouping prey. Proceedings of the Royal Society B: Biological Sciences 283:20161671.

Hilborn R, Branch TA, Ernst B, Magnusson A, Minte-Vera CV, Scheuerell MD, Valero JL. 2003. State of the world's fisheries. Annual review of Environment and Resources 28:359-399.

Hinke JT, Polito MJ, Goebel ME, Jarvis S, Reiss CS, Thorrold SR, Trivelpiece WZ, Watters GM. 2015. Spatial and isotopic niche partitioning during winter in chinstrap and Adélie penguins from the South Shetland Islands. Ecosphere 6:1-32.

Holland KN, Brill R, Chang RK. 1990. Horizontal and vertical movements of Pacific blue marlin captured and released using sportfishing gear. Fishery Bulletin 88:397.

Holland KN, Brill RW, Chang RK, Sibert JR, Fournier DA. 1992. Physiological and behavioural thermoregulation in bigeye tuna (Thunnus obesus). Nature 358:410-412.

Holland SM, Ditton RB, Graefe AR. 1998. An ecotourism perspective on billfish fisheries. Journal of Sustainable Tourism 6:97-116.

Hoolihan JP, Luo J, Abascal FJ, Campana SE, De Metrio G, Dewar H, Domeier ML, Howey LA, Lutcavage ME, Musyl MK. 2011a. Evaluating post-release behaviour modification in large pelagic fish deployed with pop-up satellite archival tags. ICES Journal of Marine Science 68:880-889.

Hoolihan JP, Luo J, Goodyear C, Orbesen ES, Prince ED. 2011b. Vertical habitat use of sailfish (*Istiophorus platypterus*) in the Atlantic and eastern Pacific, derived from pop-up satellite archival tag data. Fisheries Oceanography 20:192-205.

Hooten MB, Johnson DS, McClintock BT, Morales JM. 2017. Animal movement: statistical models for telemetry data. CRC press.

Horodysky AZ, Cooke SJ, Brill RW. 2015. Physiology in the service of fisheries science: why thinking mechanistically matters. Reviews in Fish Biology and Fisheries 25:425-447.

IATTC. 2018. Tunas, billfishes and other pelagic species in the Eastern Pacific Ocean in 2017. Inter-American Tropical Tuna Commission 93-01:78-85.

Idrisi N, Capo TR, Luthy S, Serafy JE. 2003. Behavior, Oxygen Consumption and Survival of Stressed Juvenile Sailfish (*Istiophorus platypterus*) in Captivity. Marine and Freshwater Behavior and Physiology 36:51-57.

Jackson AL, Inger R, Parnell AC, Bearhop S. 2011. Comparing isotopic niche widths among and within communities: SIBER–Stable Isotope Bayesian Ellipses in R. Journal of Animal Ecology 80:595-602.

Jackson JB, Kirby MX, Berger WH, Bjorndal KA, Botsford LW, Bourque BJ, Bradbury RH, Cooke R, Erlandson J, Estes JA. 2001. Historical overfishing and the recent collapse of coastal ecosystems. Science 293:629-637.

Johnson GD. 1986. Scombroid phylogeny: an alternative hypothesis. Bulletin of marine science 39:1-41.

Jolley Jr JW, Irby Jr EW. 1979. Survival of tagged and released Atlantic sailfish (*Istiophorus platypterus*: Istiophoridae) determined with acoustical telemetry. Bulletin of Marine Science 29:155-169.

Juan-Jordá MJ, Murua H, Arrizabalaga H, Merino G, Pacoureau N, Dulvy NK. 2022. Seventy years of tunas, billfishes, and sharks as sentinels of global ocean health. Science 378:eabj0211.

Karanth KU, Srivathsa A, Vasudev D, Puri M, Parameshwaran R, Kumar NS. 2017. Spatio-temporal interactions facilitate large carnivore sympatry across a resource gradient. In: Proc. R. Soc. B: The Royal Society. p 20161860.

Karstensen J, Stramma L, Visbeck M. 2008. Oxygen minimum zones in the eastern tropical Atlantic and Pacific oceans. Progress in Oceanography 77:331-350.

Kassambara A, Mundt F. 2017. Package 'factoextra'. Extract and visualize the results of multivariate data analyses 76.

Keeling RF, Körtzinger A, Gruber N. 2010. Ocean deoxygenation in a warming world. Annu. Rev. Mar. Sci 2:199-229.

Keppeler FW, Montaña CG, Winemiller KO. 2020. The relationship between trophic level and body size in fishes depends on functional traits. Ecological Monographs 90:e01415.

Kerstetter DW, Bayse SM, Fenton JL, Graves JE. 2011. Sailfish habitat utilization and vertical movements in the southern Gulf of Mexico and Florida Straits. Marine and Coastal Fisheries 3:353-365.

Killen SS, Adriaenssens B, Marras S, Claireaux G, Cooke S. 2016a. Context dependency of trait repeatability and its relevance for management and conservation of fish populations. Conservation Physiology 4.

Killen SS, Atkinson D, Glazier DS. 2010. The intraspecific scaling of metabolic rate with body mass in fishes depends on lifestyle and temperature. Ecology letters 13:184-193.

Killen SS, Glazier DS, Rezende EL, Clark TD, Atkinson D, Willener AS, Halsey LG. 2016b. Ecological influences and morphological correlates of resting and maximal metabolic rates across teleost fish species. The American Naturalist 187:592-606.

Killen SS, Glazier DS, Rezende EL, Clark TD, Atkinson D, Willener AS, Halsey LG, Kearney M, Bronstein JL. 2016c. Ecological Influences and Morphological Correlates of Resting and Maximal Metabolic Rates across Teleost Fish Species. The American Naturalist 187:592-606.

Kitagawa T, Nakata H, Kimura S, Itoh T, Tsuji S, Nitta A. 2000. Effect of ambient temperature on the vertical distribution and movement of Pacific bluefin tuna Thunnus thynnus orientalis. Marine Ecology Progress Series 206:251-260.

Kitchell JF, Kaplan IC, Cox SP, Martell SJ, Essington TE, Boggs CH, Walters CJ. 2004. Ecological and economic components of alternative fishing methods to reduce by-catch of marlin in a tropical pelagic ecosystem. Bulletin of Marine Science 74:607-619.

Klimley PA, Beavers SC, Curtis TH, Jorgensen SJ. 2002. Movements and swimming behavior of three species of sharks in La Jolla Canyon, California. Environmental biology of fishes 63:117-135.

Krebs CJ, Boutin S, Boonstra R, Sinclair A, Smith J, Dale MR, Martin K, Turkington R. 1995. Impact of food and predation on the snowshoe hare cycle. Science 269:1112-1115.

Kurvers RH, Krause S, Viblanc PE, Herbert-Read JE, Zaslansky P, Domenici P, Marras S, Steffensen JF, Svendsen MB, Wilson AD. 2017. The evolution of lateralization in group hunting sailfish. Current Biology 27:521-526.

Laffoley D, Baxter JM. 2019. Ocean deoxygenation: Everyone's problem - Causes, impacts, consequences and solutions. Full report. Gland, Switzerland: IUCN. 580 p.

Lam CH, Galuardi B, Mendillo A, Chandler E, Lutcavage ME. 2016. Sailfish migrations connect productive coastal areas in the West Atlantic Ocean. Scientific reports 6:1-14.

Lam CH, Kiefer DA, Domeier ML. 2015. Habitat characterization for striped marlin in the Pacific Ocean. Fisheries Research 166:80-91.

Lane F. 1941. How fast do fish swim. Country Life (London) 90:534-535.

Layman CA, Arrington DA, Montaña CG, Post DM. 2007. Can stable isotope ratios provide for community-wide measures of trophic structure? Ecology 88:42-48.

Lear KO, Whitney NM, Morris JJ, Gleiss AC. 2021. Temporal niche partitioning as a novel mechanism promoting co-existence of sympatric predators in marine systems. Proceedings of the Royal Society B 288:20210816.

Lennox RJ, Alós J, Arlinghaus R, Horodysky A, Klefoth T, Monk CT, Cooke SJ. 2017. What makes fish vulnerable to capture by hooks? A conceptual framework and a review of key determinants. Fish and Fisheries 18:986-1010.

Leung S, Mislan KAS, Muhling B, Brill R. 2019. The significance of ocean deoxygenation for open ocean tunas and billfishes. In: Laffoley D, Baxter JM, editors. Ocean deoxygenation: Everyone's problem - Causes, impacts, consequences and solutions. Gland, Switzerland: IUCN. pp 277 - 308.

Lewin W-C, Arlinghaus R, Mehner T. 2006. Documented and potential biological impacts of recreational fishing: insights for management and conservation. Reviews in Fisheries Science 14:305-367.

Logan RK, Luongo SM, Vaudo JJ, Wetherbee BM, Shivji MS. 2023. Hunting behavior of a solitary sailfish Istiophorus platypterus and estimated energy gain after prey capture. Scientific Reports 13:1484.

Logan RK, Vaudo JJ, Lowe CG, Wetherbee BM, Shivji MS. 2022. High-resolution post-release behaviour and recovery periods of two highly prized recreational sportfish: the blue marlin and sailfish. ICES Journal of Marine Science 79:2055-2068.

Luo J, Ortner PB, Forcucci D, Cummings SR. 2000. Diel vertical migration of zooplankton and mesopelagic fish in the Arabian Sea. Deep Sea Research Part II: Topical Studies in Oceanography 47:1451-1473.

Luque SP. 2007. Diving behaviour analysis in R. R news 7:8-14.

Madigan DJ, Richardson AJ, Carlisle AB, Weber SB, Brown J, Hussey NE. 2021. Water column structure defines vertical habitat of twelve pelagic predators in the South Atlantic. ICES Journal of Marine Science 78:867-883.

Marín-Enríquez E, Abitia-Cárdenas LA, Moreno-Sánchez XG, Ramírez-Pérez JS. 2019. Historical analysis of blue marlin (*Makaira nigricans* Lacepède, 1802) catches by the pelagic longline fleet in the eastern Pacific Ocean. Marine and Freshwater Research 71:532-541.

Marras S, Noda T, Steffensen JF, Svendsen MB, Krause J, Wilson AD, Kurvers RH, Herbert-Read J, Boswell KM, Domenici P. 2015. Not so fast: swimming behavior of sailfish during predator–prey interactions using high-speed video and accelerometry. Integrative and comparative biology 55:719-727.

Matich P, Ault JS, Boucek RE, Bryan DR, Gastrich KR, Harvey CL, Heithaus MR, Kiszka JJ, Paz V, Rehage JS. 2017. Ecological niche partitioning within a large predator guild in a nutrient-limited estuary. Limnology and Oceanography 62:934-953.

Matich P, Heithaus MR, Layman CA. 2010. Size-based variation in intertissue comparisons of stable carbon and nitrogen isotopic signatures of bull sharks (Carcharhinus leucas) and tiger sharks (Galeocerdo cuvier). Canadian Journal of Fisheries and Aquatic Sciences 67:877-885.

McCauley DJ, Young HS, Dunbar RB, Estes JA, Semmens BX, Micheli F. 2012. Assessing the effects of large mobile predators on ecosystem connectivity. Ecological Applications 22:1711-1717.

McGhee KE, Pintor LM, Bell AM. 2013. Reciprocal behavioral plasticity and behavioral types during predator-prey interactions. The American Naturalist 182:704-717.

McKenzie DJ, Axelsson M, Chabot D, Claireaux G, Cooke SJ, Corner RA, De Boeck G, Domenici P, Guerreiro PM, Hamer B. 2016. Conservation physiology of marine fishes: state of the art and prospects for policy. Conservation physiology 4.

Metz MC, Smith DW, Vucetich JA, Stahler DR, Peterson RO. 2012. Seasonal patterns of predation for gray wolves in the multi-prey system of Yellowstone National Park. Journal of Animal Ecology 81:553-563.

Miyabe N, Bayliff WH. 1987. A review of the Japanese longline fishery for tunas and billfishes in the eastern Pacific Ocean, 1971-1980. Inter-American Tropical Tuna Commission Bulletin 19:1-163.

Musyl MK, Moyes CD, Brill RW, Mourato BL, West A, McNaughton LM, Chiang W-C, Sun C-L. 2015. Postrelease mortality in istiophorid billfish. Canadian Journal of Fisheries and Aquatic Sciences 72:538-556.

Myers AE, Hays GC. 2006. Do leatherback turtles Dermochelys coriacea forage during the breeding season? A combination of data-logging devices provide new insights. Marine Ecology Progress Series 322:259-267.

Myers RA, Worm B. 2003. Rapid worldwide depletion of predatory fish communities. Nature 423:280.

Mysterud A, Ims RA. 1998. Functional responses in habitat use: Availability influences relative use in trade-off situations. Ecology 79:1435-1441.

Nakamura I. 1985. Billfishes of the world. An annotated and illustrated catalogue of marlins, sailfishes, spearfishes and swordfishes known to date. FAO species catalogue; FAO Fisheries Synopsis 5.

Nakamura I, Goto Y, Sato K. 2015. Ocean sunfish rewarm at the surface after deep excursions to forage for siphonophores. Journal of Animal Ecology 84:590-603.

Nakamura I, Watanabe YY, Papastamatiou YP, Sato K, Meyer CG. 2011. Yo-yo vertical movements suggest a foraging strategy for tiger sharks Galeocerdo cuvier. Marine Ecology Progress Series 424:237-246.

Nathan R, Getz WM, Revilla E, Holyoak M, Kadmon R, Saltz D, Smouse PE. 2008. A movement ecology paradigm for unifying organismal movement research. Proceedings of the National Academy of Sciences 105:19052-19059.

Norin T, Speers-Roesch B. 2021. Metabolism. In: Currie S, Evans DH, editors. The Physiology of Fishes. Boca Raton, FL: CRC Press. pp 129 - 141.

Orbesen ES, Hoolihan JP, Serafy JE, Snodgrass D, Peel E, Prince E. 2008. Transboundary movement of Atlantic istiophorid billfishes among international and US domestic management areas inferred from mark-recapture studies.

Pacoureau N, Rigby CL, Kyne PM, Sherley RB, Winker H, Carlson JK, Fordham SV, Barreto R, Fernando D, Francis MP. 2021. Half a century of global decline in oceanic sharks and rays. Nature 589:567-571.

Papastamatiou YP, Friedlander AM, Caselle JE, Lowe CG. 2010. Long-term movement patterns and trophic ecology of blacktip reef sharks (Carcharhinus melanopterus) at Palmyra Atoll. J Exp Mar Bio Ecol 386:94-102.

Papastamatiou YP, Meyer CG, Watanabe YY, Heithaus MR. 2018. Animal-borne video cameras and their use to study shark ecology and conservation. Shark Research: Emerging Technologies and Applications for the Field and Laboratory:83-91.

Parmesan C. 2006. Ecological and evolutionary responses to recent climate change. Annu. Rev. Ecol. Evol. Syst. 37:637-669.

Pauly D, Christensen V, Dalsgaard J, Froese R, Torres Jr F. 1998. Fishing down marine food webs. Science 279:860-863.

Payne NL, Snelling EP, Fitzpatrick R, Seymour J, Courtney R, Barnett A, Watanabe YY, Sims DW, Squire Jr L, Semmens JM. 2015. A new method for resolving uncertainty of energy requirements in large water breathers: the ‘mega-flume’seagoing swim-tunnel respirometer. Methods in Ecology and Evolution 6:668-677.

Payne NL, Taylor MD, Watanabe YY, Semmens JM. 2014. From physiology to physics: are we recognizing the flexibility of biologging tools? Journal of Experimental Biology 217:317-322.

Pepperell J, Davis T. 1999. Post-release behaviour of black marlin, Makaira indica, caught off the Great Barrier Reef with sportfishing gear. Marine Biology 135:369-380.

Petchey OL, McPhearson PT, Casey TM, Morin PJ. 1999. Environmental warming alters food-web structure and ecosystem function. Nature 402:69-72.

Pewsey A, Neuhäuser M, Ruxton GD. 2013. Circular statistics in R. Oxford University Press.

Pianka ER. 1974. Niche overlap and diffuse competition. Proceedings of the National Academy of Sciences 71:2141-2145.

Pinheiro J, Bates D, DebRoy S, Sarkar D, Heisterkamp S, Van Willigen B, Maintainer R. 2017. Package ‘nlme’. Linear and nonlinear mixed effects models, version 3.

Pinheiro J, Bates D, DebRoy S, Sarkar D, Team RC. 2007. Linear and nonlinear mixed effects models. 3:1-89.

Pinsky ML, Worm B, Fogarty MJ, Sarmiento JL, Levin SA. 2013. Marine taxa track local climate velocities. Science 341:1239-1242.

Pohlot BG, Ehrhardt N. 2018. An analysis of sailfish daily activity in the Eastern Pacific Ocean using satellite tagging and recreational fisheries data. ICES Journal of Marine Science 75:871-879.

Poloczanska ES, Brown CJ, Sydeman WJ, Kiessling W, Schoeman DS, Moore PJ, Brander K, Bruno JF, Buckley LB, Burrows MT. 2013. Global imprint of climate change on marine life. Nature Climate Change 3:919.

Pörtner HO, Knust R. 2007. Climate change affects marine fishes through the oxygen limitation of thermal tolerance. science 315:95-97.

Prince ED, Goodyear CP. 2006. Hypoxia-based habitat compression of tropical pelagic fishes. Fisheries Oceanography 15:451-464.

Prince ED, Luo J, Phillip Goodyear C, Hoolihan JP, Snodgrass D, Orbesen ES, Serafy JE, Ortiz M, Schirripa MJ. 2010. Ocean scale hypoxia-based habitat compression of Atlantic istiophorid billfishes. Fisheries Oceanography 19:448-462.

Prince ED, Ortiz M, VENIzELOS A. 2002. A comparison of circle hook and" J" hook performance in recreational catch-and-release fisheries for billfish. In: American Fisheries Society Symposium: American Fisheries Society. pp 66-79.

Pyke GH, Pulliam HR, Charnov EL. 1977. Optimal foraging: a selective review of theory and tests. The quarterly review of biology 52:137-154.

Queiroz N, Humphries NE, Mucientes G, Hammerschlag N, Lima FP, Scales KL, Miller PI, Sousa LL, Seabra R, Sims DW. 2016. Ocean-wide tracking of pelagic sharks reveals extent of overlap with longline fishing hotspots. Proceedings of the National Academy of Sciences 113:1582-1587.

R Core Team. 2019. R: A language and environment for statistical computing. In. Vienna, Austria: R Foundation for Statistical Computing.

Rogers LJ. 2002. Advantages and disadvantages of lateralization. Comparative vertebrate lateralization:126-153.

Rohner CA, Bealey R, Fulanda BM, Prebble CE, Williams SM, Pierce SJ. 2022. Vertical habitat use by black and striped marlin in the Western Indian Ocean. Marine Ecology Progress Series 690:165-183.

Rollins E, Hospital J. 2019. Economic contributions of pelagic fishing tournaments in Hawaii, 2018. In: Center PIFS, Editor.: NOAA.

Ropert-Coudert Y, Kato A, Chiaradia A. 2009. Impact of small-scale environmental perturbations on local marine food resources: a case study of a predator, the little penguin. Proceedings of the Royal Society B: Biological Sciences 276:4105-4109.

Rosas-Luis R, Navarro J, Loor-Andrade P, Forero MG. 2017. Feeding ecology and trophic relationships of pelagic sharks and billfishes coexisting in the central eastern Pacific Ocean. Marine Ecology Progress Series 573:191-201.

Rubalcaba JG, Verberk WC, Hendriks AJ, Saris B, Woods HA. 2020. Oxygen limitation may affect the temperature and size dependence of metabolism in aquatic ectotherms. Proceedings of the National Academy of Sciences 117:31963-31968.

Sagong W, Jeon W-P, Choi H. 2013. Hydrodynamic characteristics of the sailfish (Istiophorus platypterus) and swordfish (Xiphias gladius) in gliding postures at their cruise speeds. PloS one 8:e81323.

Sakamoto KQ, Sato K, Ishizuka M, Watanuki Y, Takahashi A, Daunt F, Wanless S. 2009. Can ethograms be automatically generated using body acceleration data from free-ranging birds? PLoS one 4.

Schaefer KM, Fuller DW, Block BA. 2011. Movements, behavior, and habitat utilization of yellowfin tuna (Thunnus albacares) in the Pacific Ocean off Baja California, Mexico, determined from archival tag data analyses, including unscented Kalman filtering. Fisheries Research 112:22-37.

Scheffer M, Carpenter S, de Young B. 2005. Cascading effects of overfishing marine systems. Trends in ecology & evolution 20:579-581.

Schlenker LS, Latour RJ, Brill RW, Graves JE. 2016. Physiological stress and post-release mortality of white marlin (Kajikia albida) caught in the United States recreational fishery. Conservation Physiology 4.

Schmidt-Nielsen K. 1997. Animal physiology: adaptation and environment. Cambridge university press.

Schoener TW. 1974. Resource Partitioning in Ecological Communities: Research on how similar species divide resources helps reveal the natural regulation of species diversity. Science 185:27-39.

Seibel BA. 2011. Critical oxygen levels and metabolic suppression in oceanic oxygen minimum zones. Journal of Experimental Biology 214:326-336.

Seminoff JA, Jones TT, Marshall GJ. 2006. Underwater behaviour of green turtles monitored with video-time-depth recorders: what's missing from dive profiles? Marine Ecology Progress Series 322:269-280.

Sepulveda C, Graham J, Bernal D. 2007. Aerobic metabolic rates of swimming juvenile mako sharks, Isurus oxyrinchus. Marine Biology 152:1087-1094.

Sepulveda C, Kohin S, Chan C, Vetter R, Graham J. 2004. Movement patterns, depth preferences, and stomach temperatures of free-swimming juvenile mako sharks, Isurus oxyrinchus, in the Southern California Bight. Marine Biology 145:191-199.

Sepulveda CA, Aalbers SA, Heberer C, Kohin S, Dewar H. 2018. Movements and behaviors of swordfish Xiphias gladius in the United States pacific leatherback conservation area. Fisheries Oceanography 27:381-394.

Sequeira AM, Rodríguez J, Eguíluz VM, Harcourt R, Hindell M, Sims DW, Duarte CM, Costa DP, Fernández-Gracia J, Ferreira L. 2018. Convergence of marine megafauna movement patterns in coastal and open oceans. Proceedings of the National Academy of Sciences 115:3072-3077.

Sergio F, Caro T, Brown D, Clucas B, Hunter J, Ketchum J, McHugh K, Hiraldo F. 2008. Top predators as conservation tools: ecological rationale, assumptions, and efficacy. Annual review of ecology, evolution, and systematics 39:1-19.

Shepard EL, Wilson RP, Halsey LG, Quintana F, Laich AG, Gleiss AC, Liebsch N, Myers AE, Norman B. 2008. Derivation of body motion via appropriate smoothing of acceleration data. Aquatic Biology 4:235-241.

Sibert J, Hampton J, Kleiber P, Maunder M. 2006. Biomass, size, and trophic status of top predators in the Pacific Ocean. science 314:1773-1776.

Simpfendorfer CA, Olsen EM, Heupel MR, Moland E. 2012. Three-dimensional kernel utilization distributions improve estimates of space use in aquatic animals. Canadian Journal of Fisheries and Aquatic Sciences 69:565-572.

Sinclair AR, Mduma S, Brashares JS. 2003. Patterns of predation in a diverse predator–prey system. Nature 425:288-290.

Steffensen JF, Lomholt JP. 1983. Energetic cost of active branchial ventilation in the sharksucker, Echeneis naucrates. Journal of Experimental Biology 103:185-192.

Stephens DW, Krebs JR. 1986. Foraging theory. Princeton University Press.

Stevens ED, Neill WH. 1978. Body temperature relations of tunas, especially skipjack. In: Hoar WS, Randall DJ, editors. Fish Physiology. New York: Academic Press. pp 315-359.

Stewart JD, Smith TT, Marshall G, Abernathy K, Fonseca-Ponce IA, Froman N, Stevens GM. 2019. Novel applications of animal-borne Crittercams reveal thermocline feeding in two species of manta ray. Marine Ecology Progress Series 632:145-158.

Stieglitz JD, Mager EM, Hoenig RH, Benetti DD, Grosell M. 2016. Impacts of Deepwater Horizon crude oil exposure on adult mahi-mahi (Coryphaena hippurus) swim performance. Environmental Toxicology and Chemistry 35:2613-2622.

Stock CA, John JG, Rykaczewski RR, Asch RG, Cheung WW, Dunne JP, Friedland KD, Lam VW, Sarmiento JL, Watson RA. 2017. Reconciling fisheries catch and ocean productivity. Proceedings of the National Academy of Sciences 114:E1441-E1449.

Stramma L, Prince ED, Schmidtko S, Luo J, Hoolihan JP, Visbeck M, Wallace DW, Brandt P, Körtzinger A. 2012. Expansion of oxygen minimum zones may reduce available habitat for tropical pelagic fishes. Nature Climate Change 2:33.

Svendsen MB, Domenici P, Marras S, Krause J, Boswell KM, Rodriguez-Pinto I, Wilson AD, Kurvers RH, Viblanc PE, Finger JS. 2016. Maximum swimming speeds of sailfish and three other large marine predatory fish species based on muscle contraction time and stride length: a myth revisited. Biology open 5:1415-1419.

Swanson HK, Lysy M, Power M, Stasko AD, Johnson JD, Reist JD. 2015. A new probabilistic method for quantifying n-dimensional ecological niches and niche overlap. Ecology 96:318-324.

Swingland IR, Greenwood PJ. 1983. Ecology of animal movement. Clarendon Press.

Thompson D, Hammond P, Nicholas K, Fedak MA. 1991. Movements, diving and foraging behaviour of grey seals (Halichoerus grypus). Journal of Zoology 224:223-232.

Tibshirani R, Walther G, Hastie T. 2001. Estimating the number of clusters in a data set via the gap statistic. Journal of the Royal Statistical Society: Series B (Statistical Methodology) 63:411-423.

Torres Rojas Y, Hernandez Herrera A, Ortega-Garcia S, Domeier M. 2013. Stable isotope differences between blue marlin (Makaira nigricans) and striped marlin (Kajikia audax) in the southern Gulf of California, Mexico. Bulletin of Marine Science 89:421-436.

Vanak AT, Fortin D, Thaker M, Ogden M, Owen C, Greatwood S, Slotow R. 2013. Moving to stay in place: behavioral mechanisms for coexistence of African large carnivores. Ecology 94:2619-2631.

Varghese SP, Somvanshi V, Dalvi RS. 2014. Diet composition, feeding niche partitioning and trophic organisation of large pelagic predatory fishes in the eastern Arabian Sea. Hydrobiologia 736:99-114.

Vaudo J, Byrne M, Wetherbee BM, Harvey G, Mendillo Jr A, Shivji M. 2018. Horizontal and vertical movements of white marlin, Kajikia albida, tagged off the Yucatán Peninsula. ICES Journal of Marine Science 75:844-857.

Vaudo JJ, Wetherbee BM, Wood AD, Weng K, Howey-Jordan LA, Harvey GM, Shivji MS. 2016. Vertical movements of shortfin mako sharks Isurus oxyrinchus in the western North Atlantic Ocean are strongly influenced by temperature. Marine Ecology Progress Series 547:163-175.

Wares PG, Sakagawa GT. 1974. Some Morphometrics of Billfishes From the Eastern Pacific Ocean. In: Shomura RS, Williams F, editors. Proceedings of the International Billfish Symposium. Kailua-Kona, Hawaii: NOAA Technical Report. pp 107-120.

Watanabe YY, Goldbogen JA. 2021. Too big to study? The biologging approach to understanding the behavioural energetics of ocean giants. Journal of Experimental Biology 224:jeb202747.

Watanabe YY, Nakamura I, Chiang W-C. 2021. Behavioural thermoregulation linked to foraging in blue sharks. Marine biology 168:1-10.

Watanabe YY, Takahashi A. 2013. Linking animal-borne video to accelerometers reveals prey capture variability. Proceedings of the National Academy of Sciences 110:2199-2204.

Wegner NC, Sepulveda CA, Bull KB, Graham JB. 2010. Gill morphometrics in relation to gas transfer and ram ventilation in high-energy demand teleosts: Scombrids and billfishes. Journal of Morphology 271:36-49.

Weihs D. 1973. Optimal fish cruising speed. Nature 245:48-50.

Wells R, Davie P. 1985. Oxygen binding by the blood and hematological effects of capture stress in two big game-fish: mako shark and striped marlin. Comparative biochemistry and physiology. A, Comparative physiology 81:643-646.

Westrelin S, Cucherousset J, Roy R, Tissot L, Santoul F, Argillier C. 2022. Habitat partitioning among three predatory fish in a temperate reservoir. Ecology of Freshwater Fish 31:129-142.

White CF, Moxley J, Jorgensen S. 2017. gRumble. In. https://github.com/MBayOtolith/gRumble.

Whitford M, Klimley AP. 2019. An overview of behavioral, physiological, and environmental sensors used in animal biotelemetry and biologging studies. Animal Biotelemetry 7:1-24.

Whitlock RE, Hazen EL, Walli A, Farwell C, Bograd SJ, Foley DG, Castleton M, Block BA. 2015. Direct quantification of energy intake in an apex marine predator suggests physiology is a key driver of migrations. Science Advances 1:e1400270.

Whitmore BM, White CF, Gleiss AC, Whitney NM. 2016. A float-release package for recovering data-loggers from wild sharks. Journal of experimental marine biology and ecology 475:49-53.

Whitney NM, Pratt Jr HL, Pratt TC, Carrier JC. 2010. Identifying shark mating behaviour using three-dimensional acceleration loggers. Endangered Species Research 10:71-82.

Whitney NM, White CF, Gleiss AC, Schwieterman GD, Anderson P, Hueter RE, Skomal GB. 2016. A novel method for determining post-release mortality, behavior, and recovery period using acceleration data loggers. Fisheries Research 183:210-221.

Williams HJ, Holton MD, Shepard EL, Largey N, Norman B, Ryan PG, Duriez O, Scantlebury M, Quintana F, Magowan EA. 2017a. Identification of animal movement patterns using tri-axial magnetometry. Movement ecology 5:6.

Williams SM, Holmes BJ, Tracey SR, Pepperell JG, Domeier ML, Bennett MB. 2017b. Environmental influences and ontogenetic differences in vertical habitat use of black marlin (Istiompax indica) in the southwestern Pacific. Royal Society open science 4:170694.

Williams SM, Pepperell JG, Bennett M, Ovenden JR. 2018. Misidentification of istiophorid billfishes by fisheries observers raises uncertainty over stock status. Journal of fish biology 93:415-419.

Wilson AM, Hubel TY, Wilshin SD, Lowe JC, Lorenc M, Dewhirst OP, Bartlam-Brooks HL, Diack R, Bennitt E, Golabek KA. 2018. Biomechanics of predator–prey arms race in lion, zebra, cheetah and impala. Nature 554:183-188.

Wilson AM, Lowe J, Roskilly K, Hudson PE, Golabek K, McNutt J. 2013a. Locomotion dynamics of hunting in wild cheetahs. Nature 498:185-189.

Wilson R, Griffiths I, Legg P, Friswell M, Bidder O, Halsey L, Lambertucci SA, Shepard E. 2013b. Turn costs change the value of animal search paths. Ecology letters 16:1145-1150.

Wilson RP, Shepard E, Liebsch N. 2008. Prying into the intimate details of animal lives: use of a daily diary on animals. Endangered species research 4:123-137.

Wilson RP, White CR, Quintana F, Halsey LG, Liebsch N, Martin GR, Butler PJ. 2006. Moving towards acceleration for estimates of activity-specific metabolic rate in free-living animals: the case of the cormorant. Journal of Animal Ecology 75:1081-1090.

Wood S. 2015. Package 'mgcv'. R package version 1:29.

Woodson CB, Litvin SY. 2015. Ocean fronts drive marine fishery production and biogeochemical cycling. Proceedings of the National Academy of Sciences 112:1710-1715.

Xie S-P, Xu H, Kessler WS, Nonaka M. 2005. Air–sea interaction over the eastern Pacific warm pool: Gap winds, thermocline dome, and atmospheric convection. Journal of Climate 18:5-20.

Yasuda T, Nagano N, Kitano H. 2018. Diel vertical migration of chub mackerel: preliminary evidence from a biologging study. Marine Ecology Progress Series 598:147-151.

Yoda K, Sato K, Niizuma Y, Kurita M, Bost C, Le Maho Y, Naito Y. 1999. Precise monitoring of porpoising behaviour of Adélie penguins determined using acceleration data loggers. Journal of Experimental Biology 202:3121-3126.

Zuur A, Ieno E, Walker N, Saveliev A, Smith G. 2009. Mixed Effects Models and Extensions in Ecology with R. New York, USA: Springer.